UNIVERSITY OF CALIFORNIA

Santa Barbara

Influences of coastal fog on the physiology and distribution of Bishop pine on Santa Cruz Island, California

A dissertation submitted in partial satisfaction of the

requirements for the degree Doctor of Philosophy

in Geography

by

Sara Alexa Baguskas

Committee in charge:

Professor Christopher J. Still, Chair

Professor Jennifer Y. King, co-Chair

Professor Carla M. D'Antonio

Dr. Craig D. Allen

September 2014

The dissertation of Sara Alexa Baguskas is approved.

_____

Jennifer Y. King

_____

Carla M. D'Antonio

_____

Craig D. Allen

_____

Christopher J. Still, Committee Chair

September 2014

Influences of coastal fog on the physiology and distribution of

Bishop pine on Santa Cruz Island, California

ACKNOWLEDGEMENTS

I would like to thank my committee for contributing their time and energy in support of the success of this research. First, my primary advisor, Christopher Still, provided a consistent voice of encouragement since day 1. His inquisitive and considerate nature fostered my *exploration* of the natural world. Jennifer King, my co-advisor, set an example of excellence of how to thoughtfully navigate the scientific process as a critical thinker. As a true student advocate, she attended all of my research presentations and provided timely comments on pieces of writing. Carla D'Antonio's aptitude for thinking and communicating ideas clearly influenced my growth as a scientist at each stage in my graduate career. As a U.S.G.S. researcher, Craig Allen provided a refreshing and unique perspective to my scientific inquiry. I would also like to thank Bodo Bookhagen for contributing his expertise to the development of my remote sensing skills, an area of research that was unfamiliar to me at the beginning.

Conducting research is not a one-person job. I have had the pleasure to work with many volunteers who accompanied me out to Santa Cruz Island for field sampling (including my mother!) and shared their excitement over the natural wonders of the island. In particular, Ryan Perroy assisted with collecting essential field data for the remote sensing component of my research. I would like to thank Aaron Ramirez for leading field sampling efforts for the pressure-volume curve dataset on the island, and enduring many hours of post-collection processing in the laboratory with me. The support of Lyndal Laughrin, Brian Guererro, and the Island Packers Co. made conducting field work on the island possible. Field research

was also supported by the University of California Natural Reserve System-Santa Cruz Island, The Nature Conservancy, and Channel Islands National Park.

This work could not have been completed without the generous funding through the Kearney Foundation for Soil Science Grant, Mildred E. Mathias Graduate Research Grant, Olivia Long Converse Graduate Fellowship, Decagon Devices Instrumentation Grant, the Save the Redwoods League, and the Department of Geography Dangermond Travel Scholarship. I greatly appreciate the support from the Department of Geography and Department of Environmental Studies as a Teaching Assistant and Instructor. These teaching positions provided not only financial support, but also the opportunity for me to develop my love and appreciation for teaching.

Intellectual support from Mariah Carbone, Douglas T. Fischer, A. Park Williams, and Bharat Rastogi greatly enhanced my learning process. In addition, I had the opportunity to mentor stellar undergraduates, Sabrina Wuu, Jared Nohra, and Kayla Smietanka, on independent research projects related to fog-plant interactions, all of which contributed intellectually to this body of work. My involvement in the Tuesday night Plant Ecology seminar, weekly Biogeosciences group meetings, and King-Chadwick-Still lab meetings at UCSB prepared me well for a scientific career beyond graduate school. Thank you for all of your honest feedback along the way.

Lastly, thank you to Seth Peterson for his unwavering support as a peer and partner.
And my folks, Eugene and Barbara Baguskas, for reminding me that I am on a journey.

VITA OF SARA ALEXA BAGUSKAS
September 2014

Education

2014	PhD in Geography, University of California, Santa Barbara (expected)
2005	BA in Biology, Lewis & Clark College, Portland, Oregon

Research Experience

2014	*Research Associate Specialist*, Physiological response of trees vs. shrubs to changes in seasonal water availability in a rain-snow transition zone in the southern Sierra Nevada, CA. Mentor: Max Moritz, UC-Berkeley
2009-2014	*Dissertation research,* Influence of coastal fog on the physiology and distribution of Bishop pine on Santa Cruz Island, California. Mentors: Dr. Christopher J. Still and Jennifer Y. King
2008	*Biological technician* Botanical surveys in Colorado Plateau, Moab, UT. Mentors: Mary Moran (USGS) and Dr. Jayne Belnap (USGS)
2006	*National Park Intern*, Island Oak habitat restoration, Santa Rosa Island, CA. Mentor: Sarah Chaney (Channel Islands National Park)
2005-2006	*Biological technician*, Biological soil crust research, USGS, Moab, Utah. Mentor: Dr. Jayne Belnap (USGS)
2004	*Undergraduate research assistant*, Pollination biology, Rocky Mountain Biological Laboratory (RMBL), Gothic, CO. Mentor: Dr. Rebecca Irwin (Dartmouth College)
2003	*NSF-Research Experience Undergraduate Fellow,* Pollination Biology, RMBL. Mentors: Dr. Allison Brody (Univ. of Vermont) and Dr. Paulette Bierzychudek (Lewis & Clark College)

Teaching Experience (all at UCSB)

Instructor: California's Channel Islands (ES111/GEOG 149) 2014, 2013

***Teaching Assistant*:**

Intro to Environmental Ecology (ES100)	2013, 2013
Biotechnology, Food, and Agriculture (ES166BT)	2012
Biogeography (GEOG167)	2010, 2008
Biogeochemistry (GEOG 195)	2009
California's Channel Islands (ES111/GEOG 149)	2009
Land, Water, and Life (GEOG 3B)	2008

***Guest lecturer (developed original material)*:**

Environmental Ecology (ES100): *Urban Ecology: Can cities be ecosystems too?*
Santa Barbara County Agrifood System (ES 157): *Intro to plant water relations*

Publications

Baguskas SA, Peterson SH, Bookhagen B, Still CJ (2014) Evaluating spatial patterns of drought-induced tree mortality in a coastal California pine forest. *Forest Ecology & Management* **315**: 43-53.

Manuscripts in review

Baguskas SA, Still CJ, Ramirez A, D'Antonio CM, King JY (in review). Coastal fog during seasonal drought: Impact on the water relations of adult and sapling trees in a California pine forest. *Oecologia*.

Manuscripts in prep

Baguskas, SA, Still CJ, Fischer DT, King JY. (in prep). Impact of fog-drip versus fog immersion on the physiology of Bishop pine saplings.

Fellowships and Research Grants

USDA-NIFA Postdoctoral Fellowship	2015
Dangermond Travel Scholarship, UC-Santa Barbara	2012
Grant. A. Harris Research Instruments Fellowship, Decagon Devices Inc.	2011
Kearney Foundation of Soil Science Graduate Fellowship	2010-12
Olivia Long Converse Fellowship, UC-Santa Barbara	2009
Mildred E. Mathias Graduate Research Grant, UC-Natural Reserve System	2008
Education Award, Student Conservation Association, Americorps	2007
Student Academic Affairs Board Research Grant, LC-College	2004

Academic Awards

Excellence in Teaching Award, Dept. of Geography, UC-Santa Barbara	2013
David Martinsen Prize, Biology Departmental Award, LC-College	2005

Presentations, Workshops, Professional Meetings

2014 October	(talk) *Impact of fog-drip versus fog immersion on physiological function of Bishop pines*, MEDECOS XIII, Olmué, Chile
2013 December	(poster) *Impact of fog-drip versus fog immersion on physiological function of Bishop pines* American Geophysical Union Annual Meeting, San Francisco, CA
2013 August	(talk) *Summertime fog and its impact on the water relations of adult and sapling trees in a coastal pine forest*, Ecological Society of America Meeting, Minneapolis, MN
2013 February	(poster) *Fog and its influence on the water relations of a California coastal pine forest*, University of California Natural Reserve System Conference, UCSB

2012 October	(talk) *Fog and its influence on the water relations of a California coastal pine forest,* 8th California Islands Symposia, Ventura, CA
2012 January	(talk) *Tree mortality, drought stress, and water relations in a California coastal pine forest,* Annual California Native Plant Society (CNPS), San Diego, CA
2010 December	(poster) *Understanding the spatial patterns of tree mortality in a coastal pine forest in California,* American Geophysical Union Annual Meeting, San Francisco, CA
2010 June	(poster) *Understanding the spatial and temporal variability of tree mortality in a coastal pine forest in California,* MntClim 2010 Conference, HJ Andrews Experimental Forest, Blue River, OR
2010 February	(poster) *Understanding the spatial and temporal variability of tree mortality in a coastal pine forest in California,* Southern California Botanist Graduate Symposium, San Jose, CA
2009 August	(attendee) Ecological Society of America Meeting, Albuquerque, New Mexico

Synergistic Activities

2014 February	Presenter at a USGS Fog Webinar where I led a discussion on fog collector design and utility
2013 May	Invited participant to first interdisciplinary meeting on the topic of coastal fog to discuss knowledge gaps and direction for future research (organizer: Alicia Torregrosa, USGS researcher, Menlo Park, CA)
2014 June	Invited participant to meeting, 'Coastal Fog as a System,' to help identify interdisciplinary challenges related to studying coastal fog and impacts on terrestrial and aquatic ecosystems (organizer: Dr. Kathleen Weathers, research scientist, Cary Institute for Ecosystem Studies)
2010-2012	Mentor for McNair Scholar Program at UCSB, which provides opportunities for underrepresented undergraduate students to gain research experience.
2009-present	Participant in weekly meetings of a Biogeosciences Group and Plant Ecology Seminar at UCSB

Special Courses

Summer 2010	Stable Isotope Course, University of Utah
Summer 2009	Radiocarbon Short Course, University of California-Irvine

ABSTRACT

Influences of coastal fog on the physiology and distribution of

Bishop pine on Santa Cruz Island, California

by

Sara Alexa Baguskas

In my dissertation research, I investigated how coastal fog influences the water relations and distribution of Bishop pine (*Pinus muricata* D. Don), a drought sensitive species restricted to the fog belt of coastal California and offshore islands. I will discuss three related projects motivated by the following research questions: *1) Can the current spatial pattern of Bishop pine mortality on Santa Cruz Island be explained by important environmental and biological controls on plant available water? 2) How do summertime fog water inputs affect the water status of Bishop pines? Do adult and sapling trees respond to fog differently?* and *3) What is the relative importance of fog-drip and fog immersion to the physiological function of Bishop pine saplings?* I addressed these questions by using a variety of approaches ranging from remote sensing techniques to field-based plant physiology. The outcomes of these studies provide evidence that coastal fog is an essential element to augmenting plant available water during the dry season and that its occurrence supports the southern extent of its range on Santa Cruz Island. Moreover, this work advances our ability to make mechanistically-based predictions of how foggy coastal forests may respond to a warmer, drier climate.

TABLE OF CONTENTS

Chapter I. Introduction

While plant species that exist in water-limited areas, such as the southwest corner of the United States, have adaptations to deal with especially dry periods, climate change poses a significant threat to water resources in these already drought-prone environments. A testament to the ecological consequences of more frequent and intense droughts predicted for the future is widespread drought-induced tree mortality, which has impacted numerous forests around the world (Allen et al. 2010). Understanding the vulnerability and/or resilience of dominant plant species to water stress in present day is fundamental to developing accurate predictions of how ecosystem structure and function may be affected by future changes in climate.

Water crises that develop during drought periods in California (e.g., 1987-1991, 2007-2009, 2012-2014) are exacerbated by the onset of the seasonal dry period (June-September), which occurs several months (~2-3) after the last winter rain. Yet, coastal California is somewhat buffered from these stressful conditions due to the occurrence of coastal fog. Coastal fog is formed when warm subsiding air interacts with cool air over the ocean. Water vapor condenses around nuclei, such as salt spray, forming low marine stratus clouds. Coastal fog is defined when these low stratus clouds are advected onshore and intercepted by land. While projections of how the fog regime may change in the future are highly uncertain, recent studies provide evidence that fog frequency along the California coast fog may decline (Johnstone and Dawson 2010). However, patterns of summer coastal fog formation have been shown to differ between northern and southern California (Iacobellis and Cayan 2013, Swartz et al. 2014); therefore, any changes in the fog regime is not likely to be uniform along California's coastline. As projections of how the fog regime

may change in the future are refined, it is critical to also assess how potential changes in fog patterns may impact the hydrologic and ecological function of fog-influenced ecosystems.

There are several direct and indirect mechanisms by which fog can augment plant-available water during the dry season. At the intersection of the low-stratus coastal clouds and land, fog water droplets deposit on plant canopies and drip to the ground, increasing shallow soil moisture. Shading effects alone can dampen heat loading and reduce potential evapotranspiration. Leaf-wetting from fog immersion (even without drip) can rehydrate leaves directly via foliar uptake and/or by suppressing transpiration rates, both of which reduce plant demand for soil water. Despite the long history of fog-related research on plants, it still remains unclear the mechanisms, magnitude, and direction by which coastal fog impacts the water and carbon relations of most plants in foggy ecosystems.

The objective of my dissertation research was to determine how coastal fog influences the water relations and range dynamics of Bishop pine (*Pinus muricata* D. Don), a drought sensitive species restricted to the fog belt of coastal California and offshore islands. The distribution of Bishop pine was more widespread when conditions were cooler and wetter in the late-Pleistocene (Raven and Axelrod 1967), but now it is restricted to the foggy coastline. Today, Santa Cruz Island (SCI) supports the largest populations of Bishop pine at the warmer, drier southern extent of its range; therefore, SCI provides an ideal study system for elucidating how changes in moisture availability, which are driven by soil water dry-down and fog, control physiological function, mortality risk, and the range dynamics of the species as a whole.

Specifically, I investigated the effects of coastal fog on the physiology and distribution of Bishop pine trees during seasonal and episodic drought on SCI by

implementing three approaches that spanned landscape to leaf-level scales. First, I evaluated spatial patterns and underlying environmental drivers of drought-induced tree mortality on SCI at a landscape scale using aerial photograph interpretation and remote sensing techniques. Second, I conducted a field-based ecophysiological study to advance our mechanistic understanding of how fog water inputs during the dry season impact water relations of adult and sapling trees. Third, I narrowed the research focus to leaf-level interactions with fog to assess the relative importance of fog-drip and foliar absorption on the carbon relations of sapling trees relative to plants that receive drip or no fog at all. I organized the dissertation into these three parts, which I describe below.

The first component of my dissertation focused on evaluating the effects of an extreme drought in southern California that occurred between 2007 and 2009 on spatial patterns of Bishop pine mortality on SCI. While anecdotal evidence supports that these drought-induced mortality events had occurred in the past, this was the first attempt to quantify the spatial extent and underlying environmental drivers of Bishop pine mortality events. Using aerial photograph interpretation, remote sensing techniques, and a decision tree analysis, I demonstrated that drought-induced Bishop pine mortality was more prevalent in the less foggy areas of the largest Bishop pine stand on SCI. In addition, this study provides evidence that smaller trees were more vulnerable to drought stress than larger trees. Because the persistence of Bishop pine (and other) tree species in the future relies on the longevity of saplings, our ability to predict the response of species to potential changes in the fog regime in California and other foggy places hinges on understanding the basic relationship between fog-water input and the physiological function of these tree species across age classes.

The objective of the second component of this dissertation was to examine how the water relations and tolerance of Bishop pines from two distinct age classes (adults and saplings) were affected by both seasonal dry period as well as coastal fog water inputs. To address these objectives, I conducted a field study during summer (June-September) 2010 and summer 2011 to quantify ecophysiological response variables of adult and sapling trees at two sites along a coastal-inland moisture gradient. To quantify fog water inputs in terms of potential plant-available water, fog-drip and shallow soil moisture (0-10 cm) were measured after fog events in 2011. I found that sapling trees were more vulnerable to experiencing water stress during the dry season than adult trees. While fog water inputs that increase shallow soil moisture had a positive effect on the water status of both age classes, the effect was stronger for sapling than adult trees. The results of this field study support that fog-drip to the soil is an important way fog water becomes available to plants; however, recent studies provide convincing evidence that foliar absorption of fog water is also possible (Simonin et al. 2009; Limm et al. 2010). For Bishop pine, it remains unclear if foliar uptake of fog water is possible. Yet, identifying the specific mechanisms by which Bishop pine use fog water is necessary for evaluating if and how the water and carbon balance of this, and other coastal forest species, may be affected by potential future changes in the coastal fog regime (Johnstone and Dawson 2010).

The final component of my dissertation research assessed the relative importance of fog-drip versus fog immersion on the carbon and water relations of Bishop pines. I conducted a controlled, manipulative study where fifteen potted Bishop pine saplings were randomly assigned one of three treatments during a three-week dry-down period: 1) fog-drip and fog-immersion, 2) fog immersion alone, and 3) no fog water inputs. To detect changes

in soil moisture across treatment, volumetric soil moisture was measured at 2 and 10 cm depth. The plant response variables measured were photosynthetic capacity and maximum gas exchange rates of sapling trees. The results from this study support that fog-drip is the primary mechanism by which Bishop pine saplings benefit from fog during otherwise dry periods; however, foliar wetting from fog events is enough to increase photosynthetic rates of Bishop pines. This study provides convincing evidence that foliar absorption is a probable mechanism of fog water use by Bishop pines.

The outcomes of this dissertation research advance our basic understanding of how coastal fog affects the physiological function and mortality risk of Bishop pine during otherwise dry times of year. Moreover, the results of this work have important implications for projecting how climate change, and potential changes in the fog regime (Johnstone and Dawson 2010), may impact the water and carbon budgets of coastal fog-influences forests in the future.

References

Allen, C.D., Macalady, A.K., Chenchouni, H., Bachelet, D., McDowell, N., Vennetier, M., Kitzberger, T., Rigling, A., Breshears, D.D., Hogg, E.H. (Ted), Gonzalez, P., Fensham, R., Zhang, Z., Castro, J., Demidova, N., Lim, J.H., Allard, G., Running, S.W., Semerei, A., Cobb, N., 2010. A global overview of drought and heat-induced tree mortality reveals emerging climate change risks for forests. For. Ecol. Manage. 259, 660–684. doi:10.1016/j.foreco.2009.09.001

Iacobellis, S.F., Cayan, D.R., 2013. The variability of California summertime marine stratus: Impacts on surface air temperatures. J. Geophys. Res. Atmos. 118, 9105–9122. doi:10.1002/jgrd.50652

Johnstone, J.A, Dawson, T.E., 2010. Climatic context and ecological implications of summer fog decline in the coast redwood region. Proc. Natl. Acad. Sci. U. S. A. 107, 4533–8. doi:10.1073/pnas.0915062107

Limm, E.B., Simonin, K.A, Bothman, A.G., Dawson, T.E., 2009. Foliar water uptake: a common water acquisition strategy for plants of the redwood forest. Oecologia 161, 449–59. doi:10.1007/s00442-009-1400-3

Raven, PH, Axelrod DI (1978) Origin and relationships of the California flora. Univ of California Press.

Schwartz, R., Gershunov, A., Iacobellis, S.F., Cayan, D.R., 2014. North American west coast summer low cloudiness: Broadscale variability associated with sea surface temperature. Geophys. Res. Lett. 41, 1–8. doi:10.1002/2014GL059825.

Simonin, K.A, Santiago, L.S., Dawson, T.E., 2009. Fog interception by Sequoia sempervirens (D. Don) crowns decouples physiology from soil water deficit. Plant. Cell Environ. 32, 882–92. doi:10.1111/j.1365-3040.2009.01967.x

Chapter II. Evaluating spatial patterns of drought-induced tree mortality in a coastal California pine forest

1. Introduction

Across the western United States, widespread increases in tree mortality rates have been observed in recent decades (van Mantgem *et al.*, 2009). Many experimental, observational, and modeling studies attribute tree mortality to drought stress in response to regional warming (Anderegg, *et al.*, 2012; Allen *et al.*, 2010; Williams, *et al.*, 2010; Adams *et al.*, 2009; Breshears *et al.*, 2005; Allen and Breshears, 1998). To date, the geographical scope of studies of tree mortality in the American West has been limited to continental, montane climates (Hanson and Weltzin, 2000). Much less is known about the extent and frequency of drought-induced mortality events in coastal forests.

The maritime influence on weather and climate in coastal forests is assumed to buffer coastal ecosystems from extreme climate fluctuations, and therefore help maintain a stable distribution of species over time. However, we observed extensive mortality of a coastal pine species, Bishop pine (*Pinus muricata,* D.Don), following a brief, yet intense, drought period at the southern extent of its range in California, where they are at the climatic margin that can support the species (Williams *et al.*, 2008; Fischer *et al.*, 2009).

Throughout the Pliocene and Pleistocene, when the California climate was considered to be more mesic compared to today, with year-round precipitation, Bishop pine, and closely related Monterey pine (*P.radiata*), were more widely and evenly distributed along the California coast (Raven and Axelrod, 1978). Bishop pine populations are currently

restricted to a small number of stands scattered along the fog-belt of coastal California and northern Baja California (Lanner, 1999). The reduction of suitable habitat for Bishop pine (and similar coastal forests) since the late Pleistocene is attributed to the onset of xeric Mediterranean climate conditions (warmer temperatures, and reduced seasonal precipitation, occurring predominantly during the winter). However, summer precipitation from fog drip, and potentially foliar uptake of fog water (Limm *et al.*, 2009, 2010), is thought to enable Bishop Pines to persist along the coast and offshore islands (Raven and Axelrod, 1978).

Fog water inputs to a forest, and its effects on the water relations of trees, are spatially heterogeneous because deposition of fog water and shading effects of fog are controlled by a variety of factors that range from the landscape to canopy scale. Fog is commonly defined as a low-stratus cloud that intercepts land. The mechanisms by which fog ameliorates the water stress of trees largely depend on their relative position to the fog layer. Shading effects, which reduce evapotranspiration, will benefit trees that are below the fog layer (Fischer *et al.*, 2009). Plants immersed in the fog layer benefit from direct water inputs because fog droplets deposit on leaves and drip to the ground increasing shallow soil moisture (Carbone *et al.*, 2012; Fischer *et al.*, 2009; Corbin *et al.*, 2005; Dawson, 1998; Ingraham and Matthews, 1995; Harr, 1982; Azevedo and Morgan, 1974; Vogelmann, 1973). Moreover, vegetation type, and canopy structure of a forest, has been shown to strongly influence fog water deposition (Ponette-Gonzalez *et al.*, 2010; Hutley *et al.*, 1997). For instance, direct fog water inputs decrease from the windward edge of the forest to its interior (Weathers *et al.*, 1995), negatively impacting the water status of trees that receive less fog-water inputs in the interior (Ewing *et al.*, 2009). Such edge effects can also impact recruitment rate of trees, and ultimately forest structure (Barbosa *et al.*, 2010; del-Val *et al.*,

2006). In short, the effect of fog on the growth and persistence of tree species in fog-influenced ecosystems is strongly mediated by the spatial heterogeneity of the landscape, namely topographic variation and forest structure (Uehara and Kume, 2012; Gutierrez *et al.*, 2008; Cavelier *et al.*, 1996; Vogelmann, 1973). Since the influence of summer cloud shading and fog drip/immersion on the moisture regime of forested ecosystems vary spatially, it is reasonable to hypothesize that the risk of drought-induced mortality in a fog-influenced forest would follow suit.

The proportion of dead Bishop pines that followed the recent drought event increased from the coast inland, and mortality was more severe at the margins of the stand. These spatial patterns seemed to coincide with modeled water deficit, which included the influence of fog on the water budget of the ecosystem. Specifically, Fischer *et al.* (2009) found that the combined effects of fog drip and cloud shading can reduce summertime drought stress up to 56% in Bishop pine stands, and inland locations are particularly sensitive to reduced cloud shading and increased evapotranspiration compared to more coastal areas. While observations and water deficit models may infer that fog inundation and cloud shading are key climate variables explaining spatial patterns of tree mortality in this coastal forest, it is unlikely that a single environmental variable, such as fog frequency, can entirely explain the spatial patterns of tree mortality.

A suite of physical factors, such as landscape features (e.g., soil thickness and type, slope, aspect, elevation, topography, and drainage networks), can generate stress gradients across the landscape (Gitlin *et al*., 2006) and may explain the distribution of water stress in trees and tree mortality just as well as spatial patterns of climate (Koepke *et al.*, 2010, Olge *et al.*, 2000). In addition to landscape factors, biotic factors, such as tree size, may help

predict mortality within a forest stand (Floyd *et al.*, 2009). While trees at different life stages (for which size can be proxy) may make different physiological adjustments to avoid or tolerate water stress, in general, it has been argued that larger trees with an extensive rooting distribution should be more capable of accessing stable water resources even during dry periods compared to smaller trees, and therefore be less sensitive to drought conditions (Cavender-Bares and Bazzaz, 2000; Dawson, 1996; Donovan and Ehleringer, 1994). In particular, water status of larger, adult Bishop pines is less affected by the summer dry period compared to smaller, sapling trees, which become water stressed by late-summer (S. Baguskas, *unpublished data*). Understanding how interacting environmental factors explain the spatial patterns of mortality will improve our ability to assess the vulnerability of coastal forests to drought-induced mortality in the future.

Remote sensing is a powerful tool for quantifying the spatial extent of tree mortality, which is often the first step towards elucidating patterns and processes underlying a mortality event, such as drought stress (Allen *et al.*, 2010; Williams *et al.*, 2010; Macomber and Woodcock, 1994), bark beetle infestation (Edburg *et al.*, 2012; Wulder *et al.*, 2006), and the potential impacts on regional carbon budgets (Huang and Anderegg, 2012). While many studies have quantified the spatial extent of tree mortality at regional and landscape scales using moderate-spatial (>30-m ground resolution) resolution remote sensing data (e.g., Meigs *et al.*, 2011; Anderson *et al.*¸2010; Fraser and Latifovic, 2005), a growing number of studies have used high-spatial (< 5-m ground resolution) resolution remote sensing data to examine tree mortality at finer spatial scales in order to detect mortality of individual trees (or clusters) within a stand (e.g., Stone *et al.*, 2012: Dennison *et al.*, 2010; Hicke and Logan, 2009; Chambers *et al.*, 2007; Guo *et al.*, 2007; Coops *et al.*, 2006; Clark *et al.*, 2004).

Developing a way to possibly make large scale estimates and predictions of tree mortality based on remotely sensed data can help land managers, who are tasked with making decisions about species and land conservation in the future, respond to a future expected to become warmer and drier.

Our research addresses the following questions: 1) What is the spatial distribution of tree mortality observed during the 2007-2009 drought period? 2) What is the correlative relationship between environmental variables, such as climate, landscape features, and tree size, and the spatial distribution of tree mortality? 3) Where is tree mortality likely to occur on the landscape during periods of drought stress?

3. Methods

3.1. Study Site

This study was conducted in the westernmost and most extensive (3.6 km^2) Bishop pine stand on Santa Cruz Island (SCI, 34^o N, 119^o 45' W), which is the largest of the northern islands in Channel Islands National Park (~250 km^2 , 38 km E-W extension) located approximately 40 km south of Santa Barbara, CA (Figure 2.1.). The Mediterranean climate along the California coast and islands offshore is characterized by cool, rainy winters and warm, rain-free (yet foggy) summers. While rainfall is highly variable both inter- and intra-annually, on average about 80% of rain falls on SCI between December and March (Fischer *et al.*, 2009). We observed mortality of Bishop pines during water year 2006-07 and 2008-09, when fewer than 25 cm of rain fell (median rainfall is 43 cm) (Figure 2.1A). In 2009, we observed peak mortality of Bishop pine trees in the field based on the

high number of tree canopies with red foliage, and we found that no other plant species exhibited a mortality response like the Bishop pines did.

The Bishop pine stand that we studied exists on complex and rugged terrain ranging from sea level to just over 400 m in elevation. Bishop pines are almost entirely restricted to the wetter, cooler north-facing slopes. There are only a few scattered clusters of trees that exist on the drier south-facing slopes, and those tend to occur in drainages. Steep ridges rise from the Santa Cruz Island fault that runs E-W through the central part of the island. There is a stark ecological and geographical difference between the northern and southern sections of the island. The northern half of the island is composed of Santa Cruz Island volcanics and is sparsely vegetated compared to the southern half, which is mostly metamorphic in origin and supports most of the vegetation (Junak *et al*., 1995). The habitat for woody vegetation is considered to be more suitable at the center of the largest Bishop pine stand where the canopies are continuous relative to the margins of the stand where pines are intermixed with more drought-tolerant coastal chaparral angiosperm plant species, such as Manzanita (*Arctostaphylos insularis, A. tomentosa*), Ceanothus (*Ceanothus arboreus, C.megacarpus subsp. insularis*), and Scrub Oak (*Quercus pacifica, Q. dumosa*).

3.2. Datasets

We used a variety of data sources to quantify the spatial variability and extent of tree mortality across the Bishop pine stand (Table 2.1A). We included in our analysis Digital Orthophoto Quarter Quads (DOQQ), which are true color aerial photographs at 1-m spatial resolution, collected by the United States Geological Survey, from 2005 (pre-drought) and 2009 (post-drought). In order for us to accurately identify dead and live trees on a pixel-by-

pixel basis, source images first needed to be georeferenced (i.e., aligned), with one another. The 2005 DOQQ was georeferenced to the 2009 DOQQ using 90 ground control points (GCPs) with root mean square error (RMSE) of 1.25 m. GCPs were selected from temporally invariant targets, such as road intersections. In conjunction with the DOQQ images, we used spectral information of different land cover types from an Airborne Visible Infrared Imaging Spectrometer (AVIRIS, 224 bands, 2.3 m) image collected by the Jet Propulsion Lab prior to the mortality event (7 August 2007). For the AVIRIS image, a geometric look-up table was applied to remove some of the geometric distortion for approximate georeferencing. We further improved the registration by georeferencing the AVIRIS image to the 2009 DOQQ using unambiguous reference points, such as road edges and distinct plant canopies (105 GCPs, 1.07 m RMSE).

Environmental variables used to explain the spatial patterns of tree mortality were derived from remotely sensed data (Table 2.1). These layers were already georeferenced. To evaluate the strength of the relationship between summertime cloud shading/fog immersion and tree mortality, we compared mortality to average summertime cloudcover frequency (Figure 2.2a). Average summertime cloudcover frequency was calculated from composite MODIS (Moderate Resolution Imaging Spectroradiometer) images at 250 m collected daily at 10:30 am PST from July to September between 2000 to 2006 (Williams, 2009; Fischer *et al.*, 2009). The 10:30 am PST overpass time of the Terra satellite captures the lingering fog from a heavy nighttime event, as the fog layer is often present until noon on SCI (Fischer *et al*., 2009; Carbone *et al.*, 2012). For each MODIS pixel, a quality control classification was assigned for one of three conditions: clear sky, partial cloud cover, or total cloud cover. We determined the average fraction of days each month (i.e., frequency) when the pixels

covering our study sites were classified as partially or totally cloudy using these quality classifications (Williams, 2009). In the summer, low-level marine stratus clouds are the most common cloud types on the California coast (Iacobellis and Cayan, 2013). Cloud frequency should be closely related to fog frequency, though information on elevation is required to determine whether the clouds were overhead (shading effect) or at the ground (i.e., fog immersion).

Four topographic layers (elevation, solar radiation, slope, and aspect) were included as explanatory variables. These variables exert control on the water budget of an ecosystem, such as the amount of solar radiation received by a surface (Dubayah, 1994). Topographic variables were derived from a digital elevation model (DEM) generated from a dense Light Detection and Ranging (LiDAR) point cloud collected by the USGS in January 2012. LiDAR return signals were classified into bare-earth and vegetation points and we created a regularly spaced grid at 1 m spatial resolution. The resulting DEM (Figure 2.2b) has been verified in the field and found to be very robust (cf. Perroy et al., 2010; Perroy et al., 2012). Field-based validation points were similar in 2010 and 2012, though the density of return signals was greater in 2010. From the DEM, we calculated average daytime solar radiation at the surface (i.e., insolation) for the summertime months (1 June – 30 September) at 14-day intervals using standard GIS techniques (Hetrick, *et al.*, 1993) (Figure 2.2c). The primary spatial variations in modeled cloud-free solar insolation for these calculations are driven by slope, aspect, and elevation. Slope and aspect (Figure 2.2e and 3f, respectively) were calculated from the DEM using standard algorithms. Aspect was rotated by 180 degrees to avoid discontinuity on north-facing slopes, where Bishop pines are most common (i.e. aspects of 1 degree and 359 degrees are not different ecologically but are very different

numerically). Therefore, north-facing slopes are 180 degrees, south-facing slopes are 360 degrees, west-facing slopes are 90 degrees, and east-facing slopes are 270 degrees. We used the average value for solar insolation, elevation, slope, and aspect within a 3-m radius from each tree point.

Attributes measuring the surface shape (i.e., the geomorphology of the landscape) can help characterize how topography controls and integrates hydrologic processes on a range of timescales (Monger and Bestelmeyer, 2006; Sorensen *et al.*, 2006; Moore *et al.*, 1991), and therefore strongly influences the spatial distribution of soil moisture and groundwater. We included a topographic wetness index (TWI), which describes the amount of water that potentially accumulates in every given pixel (Moore *et al.*, 1991) (Figure 2.2g). This index was calculated as (ln(upslope catchment area/slope)). We calculated the maximum values within a 4.5 m radius of each tree point to best represent the potential water accumulated at the rooting zone of the tree, which we estimated to expand at least 1 -2 meters beyond the tree canopy. We also included an estimate of the curvature (concavity and convexity) of the landscape, which affects the flow path of water (Gessler *et al.*, 2000; Ali *et al*., 2010) (Figure 2.2h). Curvature is the second derivative of the DEM. We calculated the average value of curvature within a 3 m radius of each tree point.

Lastly, we included a data layer of vegetation height, which we calculated from the classified lidar point cloud by analyzing the bare earth DEM and canopy-height DEM (Figure 2.2d). Because the point of live and dead trees identified in the DOQQ may not necessarily capture the apex of the canopy in the lidar DEM, we calculated the maximum height for vegetation within the 3-m radius of each tree point to more accurately represent the height of each tree.

3.3. Map of tree mortality

We identified dead trees manually in the 2009 DOQQ as areas of red pixels within the Bishop pine stand (Figure 2.3a). By combining this base image with the 2005 DOQQ (pre-drought), we were able to identify trees that died due to the drought period by identifying trees with red canopies in 2009 and green canopies in 2005 (Figure 2.3b). We validated our remotely sensed map of mortality by measuring distances between dead tree canopies in the field and corresponding nearest dead tree canopies identified in the map. We collected location data of dead (n=80) trees in the field using a differential GPS unit (Trimble Geoexplorer 6000 rover) in July 2010 with accuracy of < 15 cm. We aimed to sample areas with low and high density of tree mortality.

3.4 Random Forest analysis

We used the Random Forest (RF) decision tree algorithm (Breiman, 2001) implemented in R (R Development Core Team 2010 version 2.12.2) to identify environmental variables that best explain the distribution of dead trees, relative to live trees, across the Bishop pine stand. The RF sample population was composed of 1740 trees, of which 869 were identified as live, and 871 as dead, *a priori*. For each of these live and dead tree points, we extracted values from the environmental variable raster datasets (Table 2.1), and these values were used as input to the RF analysis.

Decision trees and RF are used to uncover complex hierarchical relationships between response variables and diverse environmental variables in multivariate data sets (Michelson

et al., 1994; Moore *et al.,* 1991). Non-linear and non-additive relationships are learned from the data rather than explicitly modeling them (Michaelsen et al. 1994, Bi and Chung 2011). Further, they are non-parametric models, which means that variable normality and independence assumptions need not be met (Michaelsen et al. 1994, Bi and Chung 2011). Decision trees use threshold values of predictor variables to separate the response variable into more and more homogeneous groups, in our case live and dead tree populations. The RF approach aggregates the results from hundreds of individual decision trees to provide more robust predictions. Specifically, different decision trees are generated for the same data set by 1) using a sub-sample of the predictor variables at any given node (or split, based on threshold value) in the tree, and 2) using sub-samples of the response variable for training and testing each decision tree. Furthermore, values of each predictor variable are varied by +/- 10 percent and the resulting effect on classification accuracy is used to quantify variable importance through the Mean Decrease in Accuracy (MDA) score (range of 0 to 1) (Breiman, 2001). The greater the MDA score, the more important the variable is in separating live and dead tree populations. While the RF analysis ranks the importance of variables, it does not indicate the nature of the relationships between explanatory variables and the dependent variable. In order to identify and illustrate the nature of these relationships, we compared the histograms of live and dead tree populations for each of these variables, and conducted a Mann-Whitney U test (R version 2.12.2) to test for significant differences between median values at the $p<0.01$ level.

We acknowledge that some of the environmental variables used in our analysis are interdependent, e.g., slope correlates positively with solar insolation and elevation is correlated with cloudiness (Table 2.2A). However, the use of correlated variables in RF

analyses biases neither the classification output (because RF is non-parametric) nor the measure of variable importance (Bi and Chung 2011; Peterson *et al.,* 2012).

3.5. Predictive map of tree mortality

We created a predictive map of tree mortality using the RF results and the maps of environmental variables. Specifically, we used the R function 'yaimpute' (R version 2.12.2), which takes the 500 decision trees generated by the RF and applies them to the environmental variables. The algorithm then averages the 500 resulting predictor maps to make one final map. Areas where trees are more likely to die following drought are indicated by values closer to one, whereas trees in areas closer to zero are more likely to live. To better understand what environmental conditions characterize areas of low and high mortality during drought, we compared and contrasted average values of environmental variables at five sites that fall along a coastal inland elevation gradient established by Fischer *et al.* (2007). We examined mortality risk at these sites for two reasons: 1) sites varied in their levels of probability of mortality, and 2) field data on fog-water inputs were available for these locations providing an opportunity for us to relate our remotely sensed data of environmental factors with field observations related to potential moisture availability.

4. Results

4.1.Spatial pattern of tree mortality

We were able to accurately identify mortality of nearly 900 Bishop pine trees at 1-m spatial resolution (Figure 2.3b and 3c). To more clearly represent the spatial distribution of dead tree clusters across the stand, we generated a map of dead tree density (Figure 2.3d). While there are many isolated patches of dead trees in various locations within the stand, we found the highest density of dead trees to be in the eastern, more inland margin. We assessed the accuracy of our remote sensing approach with field validation points, and found that 30% of the remotely sensed dead trees were within 10 m of the ground points (n=80), and 33% of the dead trees were between 10 and 20 m (Figure 2.2A). In addition, visual inspection of the proximity of remotely sensed dead trees to field-based points revealed good agreement between the two datasets.

4.2. Relationship between environmental variables and tree mortality

The variables included in our RF analysis formed interacting, hierarchical relationships to distinguish dead (n=871) from live (n=869) tree populations within the stand. These variables, however, had different levels of importance (Table 2.3). Cloud frequency and elevation received a high rank by the RF analysis (Table 2.3, MDA: clouds = 0.84, elevation = 0.79), which suggests that the position of trees relative to the summertime stratus cloud layer is important for reducing the likelihood of mortality. Bishop pines on SCI grow along an elevation gradient that increases from the coast inland, and along this gradient, summertime cloud cover frequency decreases (Figure 2.3A, a). We found most of the dead trees were clustered at the upper limits of the elevation range within the stand (~360-400 m), where cloud frequency was lowest (Figure 2.3A, b), coinciding with where we observed the greatest tree mortality. Live trees spanned a broader range of elevation and cloud

frequencies (Figure 2.3A, c). In particular, most Bishop pines that died were located at or above 350 m elevation (Figure 2.4a, median = 351 m) and where cloud frequency was less than 27% (Figure 2.4b, median = 0.26) compared to live trees that were more frequently found below 300 m (Figure 2.4a, median = 279 m) in cloudier parts of the stand (Figure 2.4b, median = 0.30).

Vegetation height was found to be of roughly equal importance to cloud cover and elevation in separating live and dead trees (Table 2.3, MDA: veg. height = 0.81). Dead trees were significantly shorter than live trees (Figure 2.4c; median dead = 7.4 m, median live = 9.0 m, $p<0.001$). We did not find a correlation between tree height and any of the environmental factors used in our analysis; however, the spatial distribution of vegetation height indicates that taller trees dominate ridges in the southwest portion of the stand where tree mortality was minimal (Figure 2.2d).

The remaining topographic variables (solar insolation, slope, and aspect) contributed to distinguishing live and dead tree populations, yet were ranked lower than cloud frequency, elevation, and vegetation height (Table 2.3). Nonetheless, the degree of spread and skewness in the histograms revealed subtle, but interesting differences between groups. The absolute difference in median solar insolation values between live and dead tree populations was negligible; however, live trees were normally distributed over the entire range of solar insolation values, whereas dead trees occurred more often in areas of higher solar insolation (Figure 2.4d; median dead =19.5 MJ m^{-2}, median live = 18.5 MJ m^{-2}, $p<0.001$). Additionally, dead trees were found on more shallow slopes compared to live trees (Figure 2.4e; median dead = 25^{o}, median live = 30^{o}). Most Bishop pines (dead or live) grew on northeast-facing slopes, yet live trees were slightly more

restricted to north-facing slopes compared to dead trees (Figure 2.4f; median dead= 194 degrees, live = 203 degrees).

Geomorphic variables that characterize the hydrologic environment (TWI and curvature) received the lowest MDA rank relative to other variables in the RF analysis (Table 2.3). Both live and dead trees tended to grow in partially channelized areas of the landscape as indicated by larger, positive values of TWI (Figure 2.4g). The negative curvature values for most of the trees indicate that they also grow in areas with convergent flow lines (Figure 2.4h). Certainly Bishop pines grow on ridges as well, but these results suggest growing in drainages where more water accumulates is important for tree growth, especially during dry years.

Of the three environmental variables with the highest importance (clouds, elevation, and vegetation height), clouds and vegetation height showed linear relationships with probability of mortality (correlations of 0.54 and 0.48 respectively). Elevation was not linearly correlated with mortality, though the high importance value of elevation suggests a non-linear or hierarchical relationship.

4.3. Accuracy Assessment for Random Forest analysis

An accuracy assessment of the RF analysis allows us to evaluate how well the RF algorithm classified live and dead trees based on the reference map we generated from the DOQQ. The accuracy of RF analysis is evaluated using a confusion matrix from which the Producer's, User's, and overall accuracy are derived (Table 2.2). Producer's accuracy refers to the probability that a certain land-cover category, e.g., dead trees, in the reference map was classified as such by the RF algorithm (Congalton, 1991). For

example, the Producer's accuracy of dead trees was 77% because 674 pixels were modeled as 'dead' by the RF algorithm out of the total 871 identified as dead in our reference map. On the other hand, the User's accuracy refers to the probability that a pixel modeled as 'dead' is accurately modeled as dead by the RF algorithm (Congalton, 1991). For example, the User's accuracy for dead trees is 78% because 674 pixels were correctly modeled as dead out of the 863 total pixels modeled as such by the RF algorithm. The Producer's and User's accuracy results for live trees were similar to that of dead trees. Overall, the classification accuracy was high with a score of 78% (kappa 0.55). The kappa statistic incorporates misclassification information, so is a more robust measure of accuracy than overall classification accuracy (Congalton, 1991).

4.4. Predictive map of tree mortality

The predictive map identifies where trees were most vulnerable to drought-induced mortality across the Bishop pine stand given the RF results (Figure 2.5). We present these results in terms of probability of mortality, where values closer to one indicate a greater probability of dying through a drought period. We found that the probability of mortality in the Bishop pine stand ranged from 30-75% and that trees growing in eastern and western margins of the stand were at greater risk of mortality (shades of red/brown) compared to the central and southwest portions of the stand (shades of blue) (Figure 2.5).

We compared the probability of mortality and environmental conditions at five sites that fell along a coastal-to-inland elevation gradient for which we also had fog-water input data collected in the field (Fischer *et al.*, 2007) (Table 2.3). The sites represent the

mid-to-high values of the mortality probability scale (54-70%), and for each area we present the average values of the environmental predictor variables (Table 2.3). Sites were generally characterized by steep (30-34°), north-facing slopes with moderate solar insolation (17.6-18.9 MJ m^{-2}). Sites tended to be located in drainages (~ -0.02 – 0.13 m m^{-2}) and where water accumulates (TWI, 7.9-9.1). There was greater variability in other environmental predictive variables across sites.

Site 1 is located at the western margin of the forest stand relatively close to the coast. Mortality risk is highest at this site (Table 2.3; probability of mortality = 70%). Of the five sites, site 1 has the highest cloud frequency (32 %), yet the lowest average fog water input over the summer (597 ml). This is likely attributed to its position below the cloud layer (elevation 141 m). Trees are shorter (5.4 m tall) than at most other sites. Site 2 is slightly higher in elevation (201 m). While less cloudy (28%) than site 1, it receives more fog-drip (938 ml) (Table 2.3). Trees are relatively tall (9.7 m) here and mortality risk low (56 %). Site 3 is at higher elevation (423 m), with the highest solar insolation (18.9 MJ m^{-2}) of all the sites. This site has moderate values of cloud cover frequency (26%), fog-drip (1300 ml), vegetation height (7.8 m), and risk of mortality (63%) relative to other sites. Site 4 is located at the far eastern margin of the Bishop pine stand, close in elevation to site 3 (390 m). Probability of mortality (64 %) is also similar to that at site 3. While cloud frequency is low (24 %), fog-drip (~1900 ml) exceeded that collected at most other sites. Like site 1, vegetation was relatively short (6 m). Site 5 is located in the southwest portion of the stand at moderate elevation (275 m) where cloud frequency is high (31 %) and receives the most fog-drip (3205 ml). Trees are tall (11 m) and grow on northwest facing slopes (131°).

5. Discussion

Spatial patterns of tree mortality

We accurately identified approximately 900 dead Bishop pine tree clusters in the largest Bishop pine stand on SCI. While we are confident that the high-spatial resolution of the 2009 DOQQ captured larger trees with red canopies when the photo was acquired (Figure 2.3b), we believe that we under-sampled smaller trees (saplings) that we know died during the 2007-2009 drought period, based on field observations. For example, the DOQQ could not have captured smaller trees growing beneath the canopy of larger trees (Meentemeyer *et al.*, 2008), or simply canopies too small to be detected at 1-m spatial resolution, e.g., sub-meter diameter or seedlings. Furthermore, we observe that there were smaller trees that died, or were very close to dead tree canopies, based on the vegetation height data derived from the LiDAR dataset (Figure 2.4c), which has much higher precision compared to an aerial photo.

The discrepancy between field-validation points and the remotely sensed trees (Figure 2.2A) was likely attributed to the temporal disconnect between when we identified dead trees remotely (June 2009) and when we collected validation points (July 2010). Because many dead trees that expressed red needles in 2009 had lost their needles by July 2010, we could not identify in the field exactly which trees we identified in our remotely sensed map of mortality. Despite these shortcomings, the techniques used to identify dead trees were robust, and feel that we captured the majority of the trees that died in response to drought.

Environmental controls on tree mortality

Our study demonstrates that there is an inverse relationship between drought-induced mortality of Bishop pines and the occurrence of summertime clouds along a coastal inland elevation gradient on SCI. The spatial clustering of dead trees in the eastern, and more inland, margin of the stand is consistent with predictions from previous research. Fischer *et al.* (2009) characterized this area as marginal habitat for Bishop pine based on higher modeled soil water deficit, which incorporated the cloud frequency variables used in our analysis, as well as fog water volumes collected from the field. The occurrence of fog is spatially heterogeneous, thus the strength of its impact on reducing water stress and supporting tree growth depends on how it interacts with other landscape and forest elements, such as canopy height.

The vegetation height dataset derived from the 1-m LiDAR DEM provided us with a unique opportunity to address how characteristics of vegetation interact with climatic and landscape variables. We found that larger trees (>8 m tall) that occurred in cloudier, and thus foggier, areas (~30% summertime cloud frequency, Figure 2.2a and 3d) had high survivorship following drought. This agrees with previous research that showed Bishop pines had higher summertime growth rates in the cloudier portion of the stand compared to trees that grow further inland and at higher elevation (Carbone *et al*, 2012). The positive relationship between fog frequency, tree size, and survivability could be explained by the fact that larger trees having a greater capacity to intercept fog and generate fog drip to the soil, which can significantly offset the effects of drought stress and support growth even during low rainfall years (Fischer *et al.* 2009; Carbone *et al.*, 2012). Therefore, fogginess may confer a fitness advantage over trees that grow in the less foggy, and more xeric parts

of the stand (del-Val *et al.*¸2006), which has important implications for the local distribution of trees that persist at the water-limited extent of the species range.

Environmental heterogeneity and probability of mortality

The occurrence of low-stratus clouds in the summertime is not the only factor important to the survival of Bishop pine trees during drought. Complex and subtle interactions between climate, topography, and vegetation can have large effects on plant-available water, and the suitability of habitat for growth and survival. We observed that the three main distinguishing factors between sites with the highest and lowest mortality risk (Table 2.3; site 1 and site 5, respectively) were elevation, volume of fog-drip, and vegetation height (Table 2.3). Because cloudiness was equally high at both sites (~31-32%), the large difference in fog water input is attributed to where the low-stratus clouds are intercepted by land. Based on a climatology of cloud base heights from the Santa Barbara airport, interception of low-stratus clouds is 40% more likely at sites between 240-280 m than at lower elevation (B. Rastogi, pers. comm). Therefore, topographic relief is necessary for cloudiness to translate to direct fog water inputs, which influences plant-available water (Fischer *et al.*, 2007). In addition, trees were twice as tall at site 5 than site 1 (Table 2.3).

The probability of mortality was similarly low between sites 2 and 5. While these sites supported the tallest trees, they were dissimilar with respect to other environmental variables. Unlike site 5, site 2 is located at the mouth of a large drainage in the central valley on SCI, which supports cool, wet conditions compared to sites located in more exposed areas. Because ridges rise steeply from the valley floor, this site is also located on a steep,

north-facing slope, which explains why solar insolation was low compared to other sites (Table 2.3).

The similarity in probability of mortality at sites 3 and 4 (63 and 64 %, respectively) coincide with many of the environmental factors that characterize these sites. Located on ridges at the upper limit of the elevation range for Bishop pines on the island (~ 400 m) where cloud frequency was relatively low (24-26 %) suggests that the evaporative losses may dominate at these sites. The distinguishing factor between these sites, other than measured fog-drip, is vegetation height. Trees are taller at site 3, therefore may have greater access to groundwater, which could compensate for lower fog-water inputs. Conversely, trees at site 4 are shorter, but grow on steeper slopes and are less exposed, thus buffered from drying effects.

The results of our study indicate that microhabitat conditions in the Bishop pine stand on SCI are critical for determining the survival and persistence of trees during exceptionally warm, dry periods. However, just as environmental conditions can vary widely across a forested ecosystem, many studies have demonstrated that variation in physiological adjustments of trees to stressful conditions, and differential growth patterns, are strong predictors of spatial patterns of mortality in forests (McDowell *et al.*, 2008; Suarez *et al.*, 2004; Wycoff and Clark, 2002; Olge *et al*., 2000; Pederson, 1998; Cregg, 1994). While we did not explicitly test for variation in physiological responses or growth of Bishop pine trees in response to drought, we did find mortality risk varied among trees of different size classes. The probability of mortality was greater for shorter trees, even if the height difference was only 1-2 m (Figure 2.4d). One possible explanation for this pattern could be that smaller trees have limited access to stable water reserves deeper in the soil, thus are at a

disadvantage during drought periods compared to larger trees that have a greater root:shoot ratio (Suarez *et al.*, 2004). Another interpretation of this pattern may be related to how drought has historically affected population dynamics (i.e., tree age and size structure) in the Bishop pine stand.

The most recent drought period (2007-09) was not an isolated event. Periodic droughts have affected the local distribution of Bishop pine on SCI in the past (Walter and Taha, 2000). The last major drought occurred between years 1986 and 1991, and killed off large swaths of Bishop pines across the island, particularly at the margins of the Bishop pine stands (Walter and Taha, 2000; Lyndal Laughrin, *pers. comm.*). Our results support the idea that survivorship of Bishop pine trees is compromised at the stand margins during drought (Figure 2.3). However, regeneration of the pine population in these areas has not ceased (Fischer *et al.*, 2009). The net effect of these drought cycles are even-aged cohorts dominating the stand margins. Therefore, the majority of trees we observed die after the most recent drought likely emerged following the previous drought that ended in 1991; thus, they were younger and had a shorter stature than the trees more resilient to drought stress that dominate the central and southwest parts of the stand.

Implications for management

Analyzing high-spatial resolution (1 m) aerial imagery and LiDAR remotely sensed data of tree mortality can provide more precise spatial information about the growing conditions of individual trees, or small tree clusters, and provide a more efficient approach to forest inventory (Maggi and Meentemeyer, 2002; Hicke *et al.*, 2012). Specifically, the color infrared DOQQ used in our study clearly showed red-attack trees allowing us to

delineate dead tree canopies. DOQQ imagery is available at no cost and collected 2-3 times per decade for any given local in the United States; therefore, acquiring and analyzing imagery that bookends a mortality event is feasible, allowing for a cost-effective method of inventorying forest damage. In contrast, LiDAR data is expensive and not readily available but the utility of deriving vegetation height and landscape variables was clearly demonstrated in this project.

We found RF to be a power statistical tool for analyzing a large multivariate dataset that ranked a suite of environmental variables used to predict tree mortality. This approach can be used in a variety of forest management applications that require analysis of large datasets where there may be correlation among the predictors and hierarchical and/or non-linear relationships between predictor and response variables.

This study supports the idea that low-stratus summertime clouds are important to survival of Bishop pines during drought periods at the most southern and water-limited extent of its range. However, the distribution of this species is restricted to the narrow fog-belt of California, despite the fact that precipitation is much higher further north, so fog must play a role in the more northern parts of the range as well. There is a great amount of uncertainty surrounding how the spatial and temporal variability of fog may change in the future; however, evidence suggests that fog frequency may decline in parts of the California coastline (Johnstone and Dawson, 2010), which would have negative effects on the distribution of Bishop pines and other fog-dependent species.

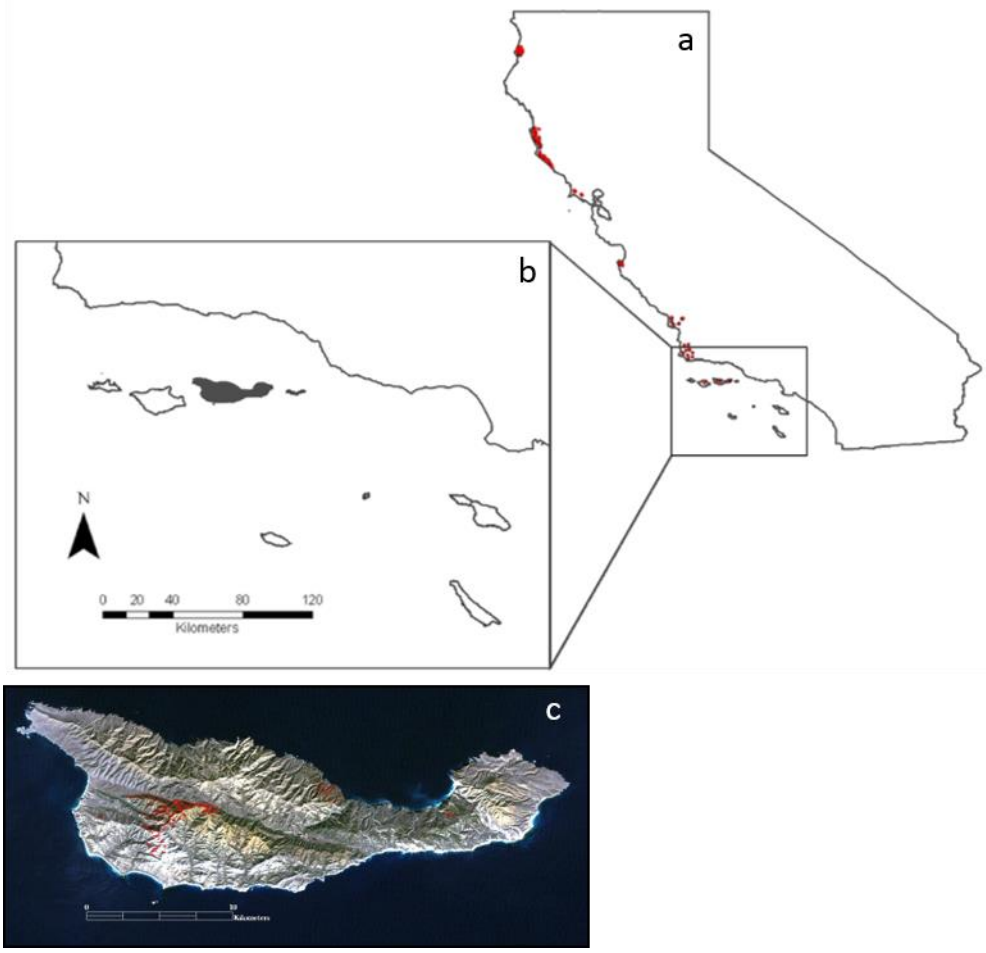

Figure 2.1. (a) Study area is located on Santa Cruz Island (SCI, 34º N, 119º 45' W), about 40 km off the coast of Santa Barbara in south-central California, and it supports the southernmost extent of Bishop pine trees in the United States. Other populations in California indicated by red marks along the coastline (Lanner, 1999); (b) SCI (shaded in gray) is the largest of the islands in Channel Islands National Park; (c) Bishop pine stands on SCI are delineated with a red outline. Our study area is the westernmost and largest stand of trees.

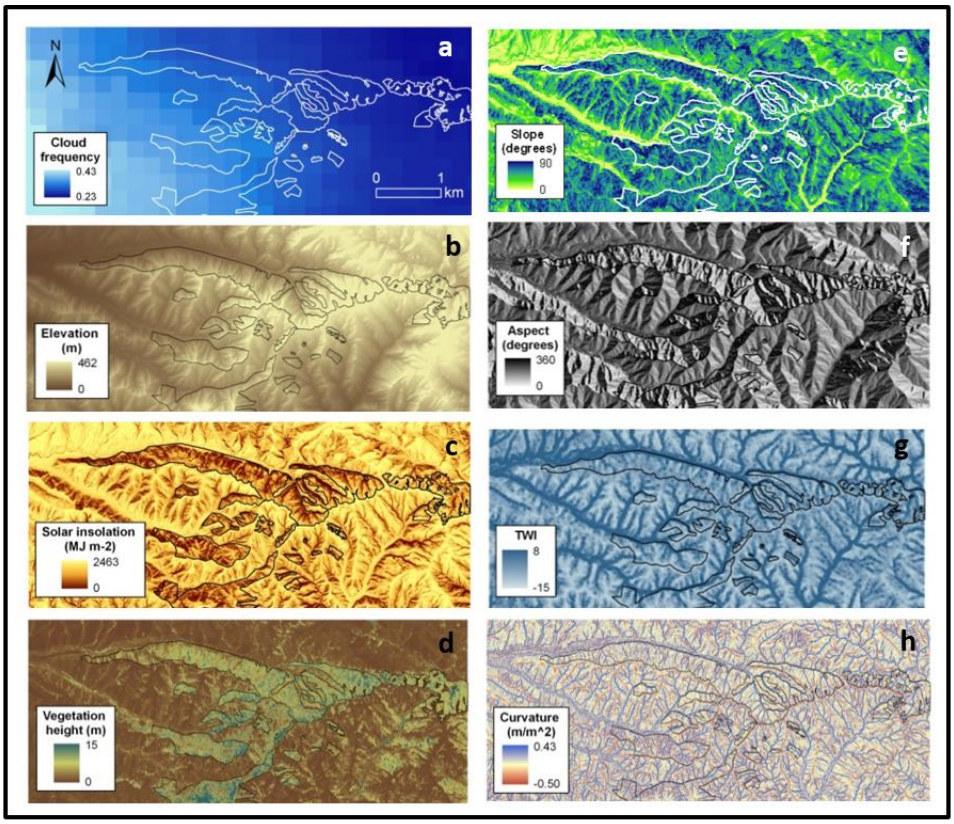

Figure 2.2. Environmental layers used in the Random Forest analyses. The Bishop pine stand perimeter is delineated in each layer with a white or black line. Layers include: a) summertime cloud frequency, b) elevation (m), c) solar insolation (MJ m^{-2}), d) vegetation height (m), e) slope (degrees), f) aspect (degrees), g) topographic wetness index (TWI), and h) curvature (m m^{-2}).

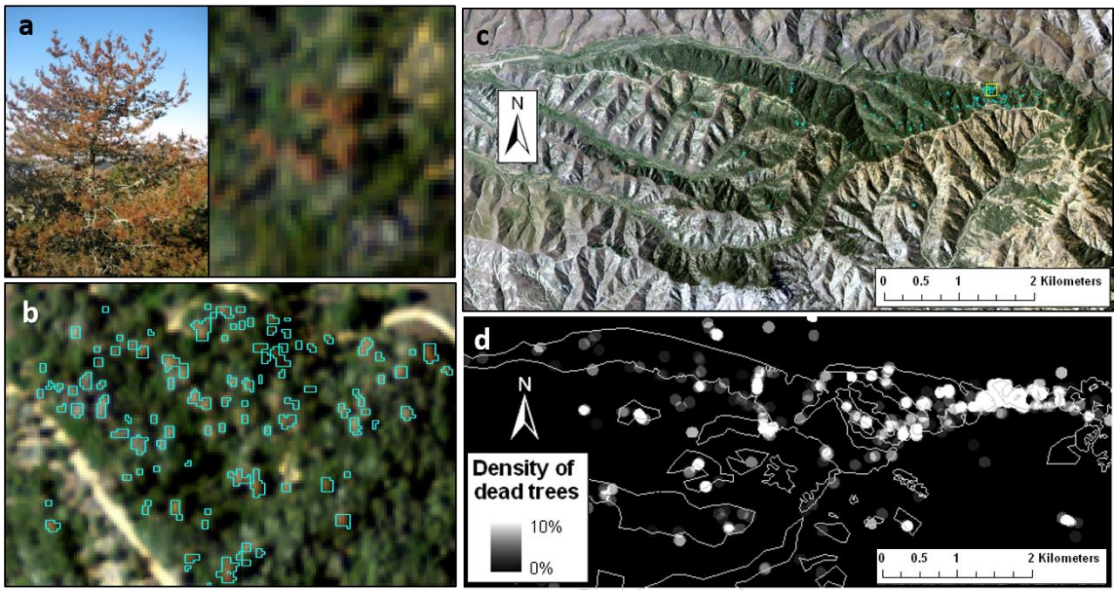

Figure 2.3. (a) Photograph of a single dead Bishop pine in the field and associated red tree canopies observed in the 2009 true color aerial photo (Digital Ortho Quarter Quad from the U.S.G.S); (b) zoomed in an area highlighted by yellow box in (c) of high tree mortality in the 2009 DOQQ showing individual dead canopies delineated by cyan colored polygons; (c) showing the entire extent of westernmost Bishop pine stand where dead tree canopies (n=871) are indicated by cyan polygons; (d) density map of dead tree canopies where white circles represent average number of dead tree canopy pixels within a 30 m radius of each dead tree. There are only circles where there is a value for tree density. Higher densities of dead trees are represented by the brighter circles. The highest density of dead tree pixels is 10%, which represents about 5-10 dead tree canopies depending on the canopy size. Stand boundaries are given by the polygons (white lines).

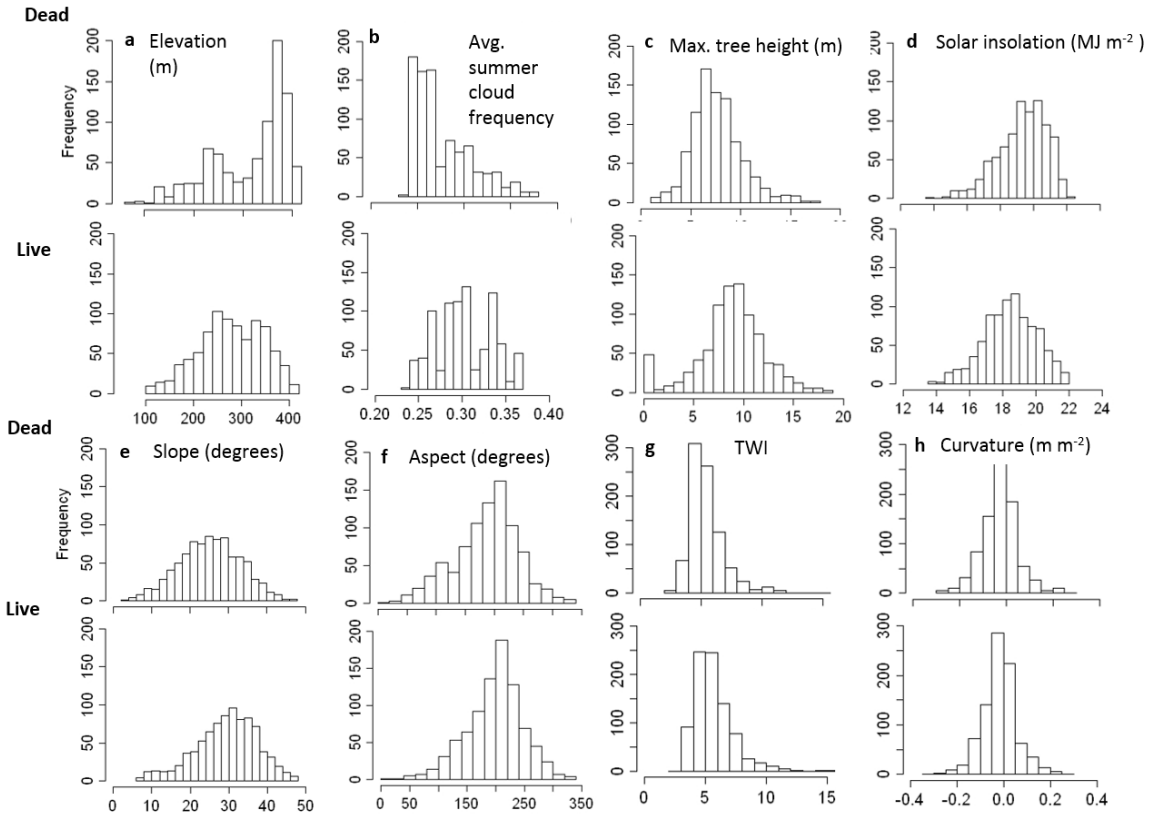

Figure 2.4. Histogram of variables for dead (above dashed line) and live (below dashed line) tree populations. Differences between median values for live and dead tree populations differed significantly at the $p<0.01$ level, and values are reported in text. To interpret aspect, north-facing =180°, south-facing=360°, west-facing= 90°, and east-facing =270°.

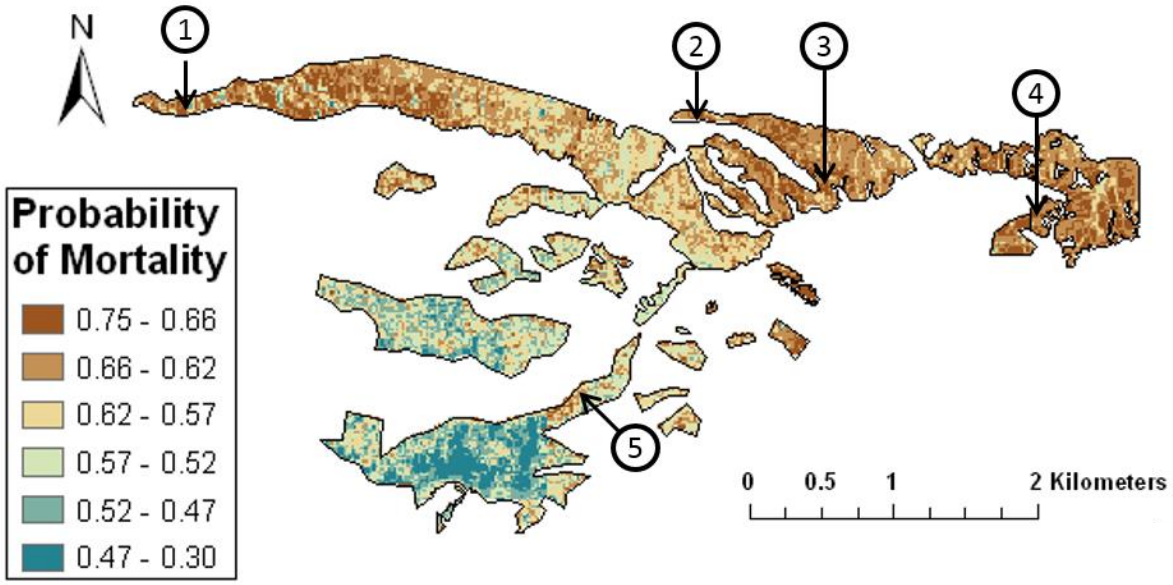

Figure 2.5. Predictive map of tree mortality following drought for our study area (see Figure 1.1c for reference). Bishop pine stand is delineated with a black line, and other land surface types are masked out. Red-colored areas represent areas where probability of mortality following drought is high (closer to one) compared to blue-colored areas (closer to 0). Numbered areas (1-5) are described in the text with respect to how probability of mortality relates to environmental conditions and tree height, and are included in Table 1.5.

Table 2.1. Potential explanatory variables used in the Random Forest analyses. The Mean Decrease in Accuracy (MDA) value ranks the variables based on how well they separate live and dead tree populations in the RF analysis. The larger the MDA value, the higher ranked the variable, i.e., the greater explanatory power.

Type	Variable	abbreviation	Data source	Spatial scale	Units	MDA
Climatic	Summertime (June-Sept.) cloud cover frequency	clouds	MODIS	250 m	percent	0.84
Topographic	Elevation	elevation	LiDAR DEM	1 m	m	0.79
	Daily integrated summertime (June-Sept.) solar insolation	solar insolation			MJ m^{-2}	0.72
	Slope	slope			degrees	0.70
	Aspect	aspect			degrees	0.63
Geomorphic	Topographic Wetness Index	twi			--	0.36
	Topographic Curvature	curvature			m/m^{-2}	0.28
Biotic	Vegetation Height	veg. height			m	0.81

Table 2.2. Average accuracy assessment of 500 decision classification trees in Random Forest analysis.

		Reference			
		Dead	**Live**	**Total**	**User's**
Modeled	**Dead**	674	189	863	0.78
	Live	197	680	877	0.78
	Total	871	869	1740	
	Producer's	0.77	0.78		
	Overall accuracy	0.78			
	Kappa	0.55			

Table 2.3. Average probability of tree mortality and environmental variables for the ten sites indicated in Figure 8. Sample locations were determined based on field sites for which we had data on fog-water inputs. The area of each site was approximately 20 m^2.

Site	Probability of mortality (%)	Avg. summer fog-drip (ml)*	Cloud cover frequency	Elevation (m)	Vegetation height (m)	Solar insolation (MJ m^{-2})	Aspect** (degrees)	Slope (degrees)	Curvature (m m^{-2})	TWI
1	70	597	0.32	141	5.4	17.8	208	32	0.041	8.1
2	56	938	0.28	201	9.7	17.6	186	31	-0.033	8.7
3	63	1300	0.26	423	7.8	18.9	115	30	0.076	9.2
4	64	1889	0.24	390	6.0	18.0	176	34	0.128	9.1
5	54	3205	0.31	275	11.1	18.3	131	33	-0.021	7.9

*Fog-drip (ml) data was collected in the field at weather stations (Fischer *et al.*, 2007) from May-September in 2004. We calculated average volume of fog-water inputs over these summer months.
**Aspect: north-facing =180°, south-facing=360°, west-facing= 90°, and east-facing =270°.

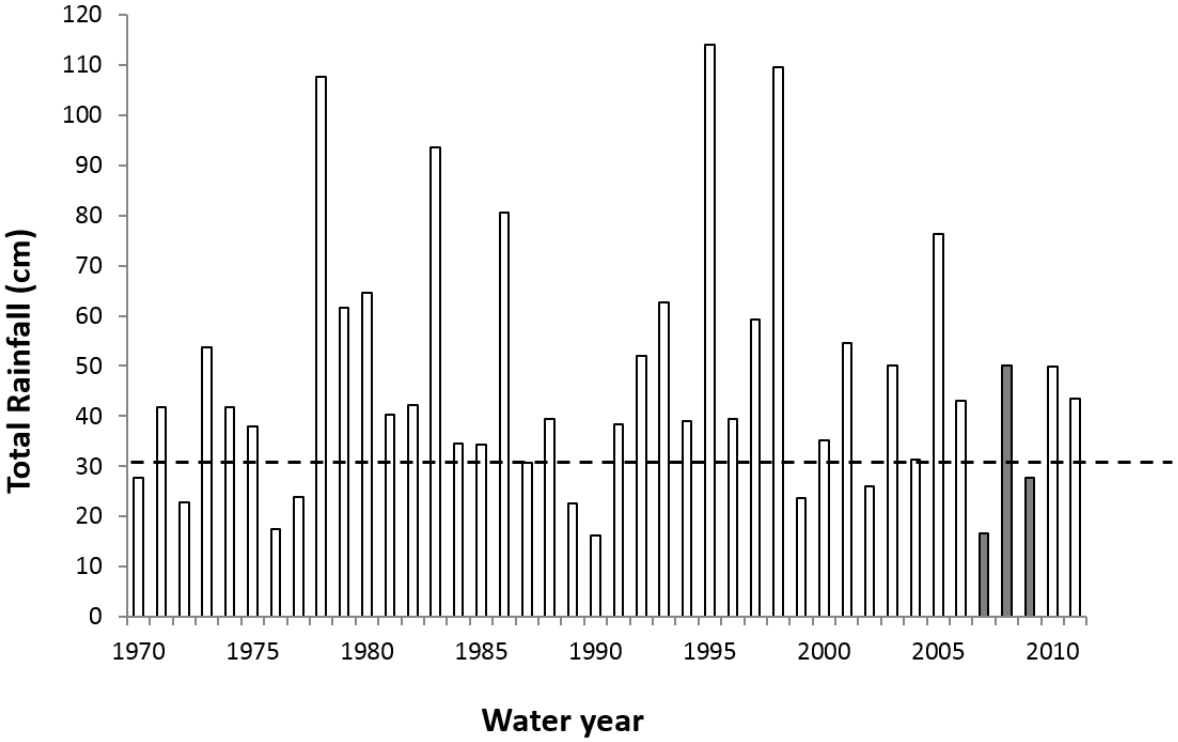

Figure 2.1A. Total rainfall (cm) by water year on Santa Cruz Island from 1970 to 2011. Dashed line is the long term median value (43 cm), and is based on rainfall recorded since 1904. Bars highlighted in gray are years during which the most recent Bishop pine mortality event was observed (2007-2009). There was a severe mortality event in the late 1980s, also during a drought period (1987-1990), which ended in 1991.

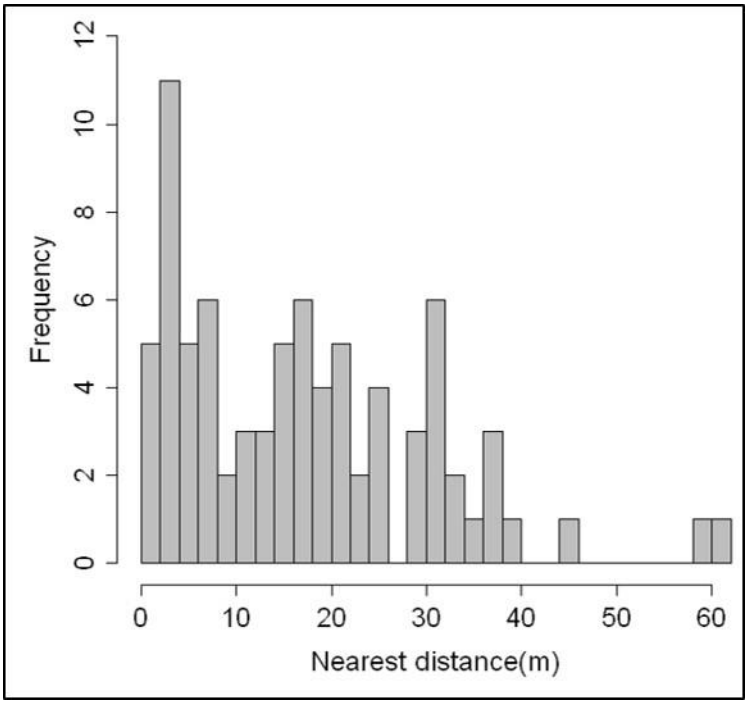

Figure 2.2A. Field validation of remotely sensed Bishop pine mortality. Frequency of remotely sensed dead Bishop pines (n = 80) from 2009 DOQQ to nearest GPS point of dead pine in the field (July 2010).

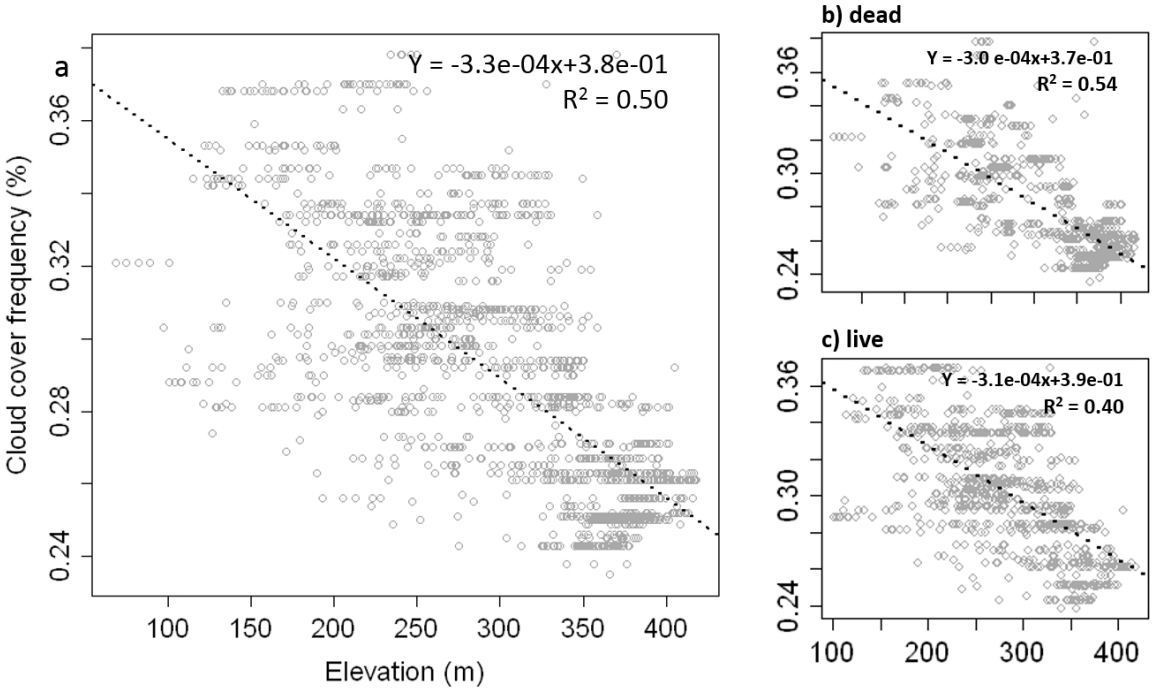

Figure 2.3A. Relationship between elevation and summertime cloud cover frequency . Each data point represents a tree crown or small cluster of trees identified in the 2009 DOQQ. This relationship suggest that: a) Bishop pines tend to grow along a coastal inland gradient along which elevation increases and summertime cloud cover frequency decreases; b) dead trees (n=871) occurred at high elevation and low cloud frequency ; c) live trees (n=869) spanned this gradient.

Table 2.1A. Data sources used for tree mortality map.

Data type	Date acquired	Spatial resolution	Spectral resolution
DOQQ	December 2005 & June 2009	1 m	RGB
AVIRIS	August 2007	2.3 m	224 bands
Airborne LiDAR DEM	January 2012	1 m	1 band

Table 2.2A. Correlation coefficients between variables included in the RF analysis. See Table 1.2 in text for list of variables and data sources.

	clouds	elevation	veg. height	solar insolation	aspect	slope	curvature	twi	prediction
clouds	1	-0.55	0.09	-0.23	-0.04	0.19	-0.12	-0.05	0.54
elevation	-0.55	1	0.19	0.33	0.00	-0.22	-0.01	-0.23	-0.10
veg. height	0.09	0.19	1	-0.14	-0.06	0.16	0.02	-0.05	0.48
solar insolation	-0.23	0.33	-0.14	1	-0.03	-0.80	0.33	-0.01	-0.11
aspect	-0.04	0.00	-0.06	-0.03	1	0.03	0.07	-0.01	-0.03
slope	0.19	-0.22	0.16	-0.80	0.03	1	0.01	-0.10	0.10
curvature	-0.12	-0.01	0.02	0.33	0.07	0.01	1	0.00	-0.08
twi	-0.05	-0.23	-0.05	-0.01	-0.01	-0.10	0.00	1	-0.13
prediction	0.54	-0.10	0.48	-0.11	-0.03	0.10	-0.08	-0.13	1

References

Adams, H.D., Guardiola-Claramonte, M., Barron-Gafford, G. A., Villegas, J.C., Breshears, D.D., Zou, C.B., Troch, P. A, Huxman, T.E., 2009. Temperature sensitivity of drought-induced tree mortality portends increased regional die-off under global-change-type drought. Proceedings of the National Academy of Sciences 106, 7063–6.

Ali, G. A., Roy, A.G., 2010. Shopping for hydrologically representative connectivity metrics in a humid temperate forested catchment. Water Resources Research 46, W12544.

Allen, C.D., Breshears, D.D., 1998. Drought-induced shift of a forest-woodland ecotone: rapid landscape response to climate variation. Proceedings of the National Academy of Sciences 95, 14839–42.

Allen, C.D., Macalady, A.K., Chenchouni, H., Bachelet, D., McDowell, N., Vennetier, M., Kitzberger, T., Rigling, A., Breshears, D.D., Hogg, E.H. (Ted), Gonzalez, P., Fensham, R., Zhang, Z., Castro, J., Demidova, N., Lim, J.H., Allard, G., Running, S.W., Semerei, A., Cobb, N., 2010. A global overview of drought and heat-induced tree mortality reveals emerging climate change risks for forests. Forest Ecology and Management 259, 660–684.

Anderegg, W.R.L., Berry, J. A, Smith, D.D., Sperry, J.S., Anderegg, L.D.L., Field, C.B., 2012. The roles of hydraulic and carbon stress in a widespread climate-induced forest die-off. Proceedings of the National Academy of Sciences 109, 233–7.

Anderson, L. O., Malhi, Y., Aragão, L. E., Ladle, R., Arai, E., Barbier, N., Phillips, O., 2010. Remote sensing detection of droughts in Amazonian forest canopies. New Phytologist, 187, 733-750.

Azevedo, J., Morgan, D.L., 1974. Fog precipitation in coastal California forests. Ecology, 1135-1141.

Barbosa, O., Marquet, P. A., Bacigalupe, L. D., Christie, D. A., Del-Val, E., Gutierrez, A. G., Jones, C.G., Weathers, K.C., Armesto, J. J., 2010. Interactions among patch area, forest structure and water fluxes in a fog-inundated forest ecosystem in semi-arid Chile. Functional Ecology 24, 909-917.

Bi, J., Chung, J., 2011. Identification of drivers of overall liking–determination of relative importances of regressor variables. Journal of Sensory Studies 26, 245-254.

Breiman, L., 2001. Random forests. Machine learning 45, 5-32.

Breshears, D.D., Cobb, N.S., Rich, P.M., Price, K.P., Allen, C.D., Balice, R.G., Romme, W.H., Kastens, J.H., Floyd, M.L., Belnap, J., Anderson, J.J., Myers, O.B., Meyer, C.W., 2005. Regional vegetation die-off in response to global-change-type drought. Proceedings of the National Academy of Sciences 102, 15144–8.

Carbone, M.S., Williams, A.P., Ambrose, A.R., Boot, C.M., Bradley, E.S., Dawson, T.E., Schaeffer, S.M., Schimel, J.P., Still, C.J., 2012. Cloud shading and fog drip influence the metabolism of a coastal pine ecosystem. Global Change Biology 19, 484-497.

Cavender-Bares, J., Bazzaz, F.A., 2000. Changes in drought response strategies with ontogeny in *Quercus rubra*: implications for scaling from seedings to mature trees. Oecologia 124, 8-18.

Cavelier, J., Solis, D., Jaramillo, M. A., 1996. Fog interception in montane forests across the Central Cordillera of Panama. Journal of Tropical Ecology 12, 357-369.

Chambers, J.Q., Asner, G.P., Morton, D.C., Anderson, L.O., Saatchi, S.S., Espírito-Santo, F.D.B., Palace, M., Souza, C., 2007. Regional ecosystem structure and function:

ecological insights from remote sensing of tropical forests. Trends in Ecology & Evolution 22, 414–23.
Clark, D.B., Castro, C.S., Alvarado, L.D.A., Read, J.M., 2004. Quantifying mortality of tropical rain forest trees using high-spatial-resolution satellite data. Ecology Letters 52–59.
Congalton, R.G., 1991. A Review of Assessing the Accuracy of Classifications of Remotely Sensed Data. Remote Sensing of Environment 46, 35–46.
Coops, N.C., Johnson, M., Wulder, M. A., White, J.C., 2006. Assessment of QuickBird high spatial resolution imagery to detect red attack damage due to mountain pine beetle infestation. Remote Sensing of Environment 103, 67–80.
Corbin, J.D., Thomsen, M. A, Dawson, T.E., D'Antonio, C.M., 2005. Summer water use by California coastal prairie grasses: fog, drought, and community composition. Oecologia 145, 511–21.
Cregg, B.M. 1994. Carbon allocation, gas exchange, and needle morphology of *Pinus ponderosa* genotypes known to differ in growth and survival under imposed drought. Tree Physiology 14, 883-898.
Dawson, T.E., 1996. Determining water use by trees and forests from isotopic, energy balance and transpiration analyses: the roles of tree size and hydraulic lift. Tree Physiology 16: 263-272.
Dawson, T.E., 1998. Fog in the California redwood forest: ecosystem inputs and use by plants. Oecologia 117, 476–485.
Dennison, P.E., Brunelle, A.R., Carter, V. A., 2010. Assessing canopy mortality during a mountain pine beetle outbreak using GeoEye-1 high spatial resolution satellite data. Remote Sensing of Environment 114, 2431–2435.
del-Val, E., Armesto, J. J., Barbosa, O., Christie, D. A., Gutiérrez, A. G., Jones, C. G., Marquet, P.A., Weathers, K. C., 2006. Rain forest islands in the Chilean semiarid region: fog-dependency, ecosystem persistence and tree regeneration. Ecosystems 9, 598-608.
Donovan, L.A., Ehleringer, J.R., 1994. Water stress and use of summer precipitation in a Great Basin shrub community. Functional Ecology 8, 289–297.
Dubayah, R.C., 1994. Modeling a Solar Radiation Topoclimatology for the Rio Grande River Basin. Journal of Vegetation Science 5, 627–640.
Edburg, S.L., Hicke, J.A., Brooks, P.D., Pendall, E.G., Ewers, B.E., Norton, U., Gochis, D., Gutmann, E.D., Meddens, A.J., 2012. Cascading impacts of bark beetle-caused tree mortality on coupled biogeophysical and biogeochemical processes. Frontiers in Ecology and the Environment 10, 416–424.
Ewing, H. A., Weathers, K. C., Templer, P. H., Dawson, T. E., Firestone, M. K., Elliott, A. M., & Boukili, V. K. (2009). Fog water and ecosystem function: heterogeneity in a California redwood forest. Ecosystems 12, 417-433.
Fischer, D.T., 2007. Ecological and biogeographic impacts of fog and stratus clouds on coastal vegetation, Santa Cruz Island, CA (Doctoral disserations). University of California, Santa Barbara, CA.
Fischer, D.T., Still, C.J., Williams, A.P., 2009. Significance of summer fog and overcast for drought stress and ecological functioning of coastal California endemic plant species. Journal of Biogeography 36, 783–799.

Floyd, M. L., Clifford, M., Cobb, N. S., Hanna, D., Delph, R., Ford, P., & Turner, D., 2009. Relationship of stand characteristics to drought-induced mortality in three Southwestern pinon-juniper woodlands. Ecological Applications 19, 1223-1230.

Fraser, R. H., Latifovic, R., 2005. Mapping insect-induced tree defoliation and mortality using coarse spatial resolution satellite imagery. International Journal of Remote Sensing 26, 193-200.

Gessler, P.E., Chadwick, O.A., Chamran, F., Althouse, L., Holmes, K., 2000. Modeling Soil – Landscape and Ecosystem Properties Using Terrain Attributes. Soil Science Society of America 64, 2046–2056.

Gitlin, A.R., Sthultz, C.M., Bowker, M.A., Stumpf, S., Paxton, K.L., Kennedy, K., Muñoz, A., Bailey, J.K., Whitham, T.G., 2006. Mortality gradients within and among dominant plant populations as barometers of ecosystem change during extreme drought. Conservation Biology 20, 1477–86.

Guo, Q., Kelly, M., Gong, P., Liu, D., 2007. An Object-Based Classification Approach in Mapping Tree Mortality Using High Spatial Resolution Imagery. GIScience & Remote Sensing 44, 24–47.

Gutierrez, A. G., Barbosa, O., Christie, D. A., del-Val, E. K., Ewing, H. A., Jones, C. G., Marquet, P.A., Weathers, K.C., Armesto, J. J., 2008. Regeneration patterns and persistence of the fog-dependent Fray Jorge forest in semiarid Chile during the past two centuries. Global Change Biology 14, 161-176.

Hanson, P.J., Weltzin, J.F., 2000. Drought disturbance from climate change: response of United States forests. The Science of the Total Environment 262, 205–20.

Harr, R.D., 1982. Fog drip in the Bull Run municipal watershed, Oregon. Water Resources Bulletin 18, 785-789.

Hetrick, W.A., Rich, M, P., Barnes, F.J., Weiss, S.B., 1993. GIS-based Solar Radiation Flux Models. American Society of Photogrammetry and Remote Sensing Technical Papers 3, 132–143.

Hicke, J. A., Johnson, M.C., Hayes, J.L., Preisler, H.K., 2012. Effects of bark beetle-caused tree mortality on wildfire. Forest Ecology and Management 271, 81–90.

Hicke, J. A., Logan, J., 2009. Mapping whitebark pine mortality caused by a mountain pine beetle outbreak with high spatial resolution satellite imagery. International Journal of Remote Sensing 30, 4427–4441.

Huang, C.-Y., Anderegg, W.R.L., 2012. Large drought-induced aboveground live biomass losses in southern Rocky Mountain aspen forests. Global Change Biology 18, 1016–1027.

Hutley, L. B., Doley, D., Yates, D. J., and A. Boonsaner, 1997. Water balance of an Australian subtropical rainforest at altitude: the ecological and physiological significance of intercepted cloud and fog. Australian Journal of Botany 45, 311-329.

Ingraham, N., Matthews, R., 1995. The importance of fog-drip water to vegetation: Point Reyes Peninsula, California. Journal of Hydrology 164, 269–285.

Iacobellis, S. F., Cayan, D.R., 2013. The variability of California summertime marine stratus: Impacts on surface air temperatures. Journal of Geophysical Research: Atmospheres 118, 1-18.

Johnstone, J. A., Dawson, T.E., 2010. Climatic context and ecological implications of summer fog decline in the coast redwood region. Proceedings of the National Academy of Sciences 107, 4533-4538.

Junak, S., Ayers, T., Scott, R., Wilken, D., Young, D.A., 1995. A flora of Santa Cruz Island. Santa Barbara, Calif.: Santa Barbara Botanical Garden.

Kelly, A.E., Goulden, M.L., 2008. Rapid shifts in plant distribution with recent climate change. Proceedings of the National Academy of Sciences 105, 11823–6.

Koepke, D.F., Kolb, T.E., Adams, H.D., 2010. Variation in woody plant mortality and dieback from severe drought among soils, plant groups, and species within a northern Arizona ecotone. Oecologia 163, 1079–90.

Lanner, R.L., 1999. Conifers of California. Los Olivos, CA*: Cachuma Press*.

Limm, E. B., Simonin, K. A., Bothman, A. G., & Dawson, T. E. (2009). Foliar water uptake: a common water acquisition strategy for plants of the redwood forest. *Oecologia*, *161*(3), 449-459.

Limm, E. B., & Dawson, T. E. (2010). Polystichum munitum (Dryopteridaceae) varies geographically in its capacity to absorb fog water by foliar uptake within the redwood forest ecosystem. *American Journal of Botany*, *97*(7), 1121-1128.

McDowell, N., Pockman, W.T., Allen, C.D., Breshears, D.D., Cobb, N., Kolb, T., Plaut, J., Sperry, J., West, A., Williams, D.G., Yepez, E.A., 2008. Mechanisms of plant survival and mortality during drought: why do some plants survive while others succumb to drought? New Phytologist 178, 719-733.

Macomber, S.A., Woodcock, C.E., 1994. Mapping and Monitoring Conifer Mortality Using Remote Sensing in the Lake Tahoe Basin. Remote Sensing of Environment 266, 255–266.

Maggi, K., Meentemeyer, R.K., 2002. Landscape dynamics of the spread of sudden oak death. *Photogrammetric Engineering & Remote Sensing* 68, 1001-1009.

Meigs, G.W., Kennedy, R.E., Cohen, W.B., 2011. A Landsat time series approach to characterize bark beetle and defoliator impacts on tree mortality and surface fuels in conifer forests. Remote Sensing of Environment 115, 3707–3718.

Meentemeyer, R. K., Rank, N. E., Shoemaker, D. A., Oneal, C. B., Wickland, A. C., Frangioso, K. M., Rizzo, D. M., 2008. Impact of sudden oak death on tree mortality in the Big Sur ecoregion of California. Biological Invasions 10, 1243-1255.

Michaelsen, J., Schimel, D.S., Friedl, M.A., Davis, F.W., Dubayah, Ralph, C., 1994. Regression Tree Analysis of satellite and terrain data to guide vegetation sampling and surveys. Journal of Vegetation Science 5, 673–686.

Monger, H., Bestelmeyer, B., 2006. The soil-geomorphic template and biotic change in arid and semi-arid ecosystems. Journal of Arid Environments 65, 207–218.

Moore, D.M., Lees, B.G., Davey, S.M., 1991. A New Method for Predicting Vegetation Distributions using Decision Tree Analysis in a Geographic Information System. Environmental Management 15, 59–71.

Ogle, K., Whitham, T.G., Cobb, N.S., 2000. Tree-Ring Variation in Pinyon Predicts Likelihood of Death following Severe Drought. Ecology 81, 3237–3243.

Pederson, B.S. 1998. The role of stress in the mortality of Midwestern oaks as indicated by growth prior to death. Ecology 79, 79-93.

Perroy, R.L., Bookhagen, B., Asner, G.A., Chadwick, O.A., 2010. Comparison of gully erosion estimates using airborne and ground-based LiDAR on Santa Cruz Island, California. Geomorphology 118, 288-300.

Perroy, R.L., Bookhagen, B., Chadwick, O.A., Howarth, J.T., 2012. Holocene and Anthropocene Landscape Change: Arroyo formation on Santa Cruz Island, California. Annals of the Association of American Geographers 102, 1229-1250.

Peterson, S. H., Franklin, J., Roberts, D. A., van Wagtendonk, J. W., (2012). Mapping fuels in Yosemite National Park. Canadian Journal of Forest Research 43, 7-17.

Ponette-Gonzalez, A.G., Weathers, K. C., Curran, L. M., 2010. Water inputs across a tropical montane landscape in Veracruz, Mexico: synergistic effects of land cover, rain and fog seasonality, and interannual precipitation variability. Global Change Biology 16, 946-963.

Raven, P.H., Axelrod, D.I., 1978. Origin and relationships of the California flora. University of California Press: Berkeley, CA.

Sørensen, R., Zinko, U., Seibert, J., 2006. On the calculation of the topographic wetness index: evaluation of different methods based on field observations. Hydrology and Earth System Sciences 10, 101–112.

Stone, C., Penman, T., Turner, R., 2012. Managing drought-induced mortality in *Pinus radiata* plantations under climate change conditions: A local approach using digital camera data. Forest Ecology and Management 265, 94-101.

Suarez, M.L., Ghermandi, L, Kitzberger, T. 2004. Factors predisposing episodic drought-induced mortality in *Nothofagus*- site, climatic sensitivity and growth trends. Journal of Ecology 92, 954-966.

Uehara, Y., Kume, A., 2012. Canopy Rainfall Interception and Fog Capture by Pinus pumila Regal at Mt. Tateyama in the Northern Japan Alps, Japan. Arctic, Antarctic, and Alpine Research 44, 143-150.

van Mantgem, P.J., Stephenson, N.L., Byrne, J.C., Daniels, L.D., Franklin, J.F., Fulé, P.Z., Harmon, M.E., Larson, A.J., Smith, J.M., Taylor, A.H., Veblen, T.T., 2009. Widespread increase of tree mortality rates in the western United States. Science 323, 521–524.

Vogelmann, H.W.,1973. Fog precipitation in the cloud forests of eastern Mexico. Bioscience 23(2), 96-100.

Walter, H.S., Taha, L.A. 2000. Regeneration of Bishop pine (*Pinus muricata*) in the absence and presence of fire: a case study from Santa Cruz Island, California. In: Browne, D.R., Mitchell, K.L, Chaney, H.W., Eds. Proceedings of the fifth California Islands symposium, 1999 March 29 to April 1; Santa Barbara, California. San Diego, CA: U.S. Department of the Interior, Mineral Management Service (OCS Study MMS 99-0038): 172-181.

Weathers, K. C., Lovett, G. M., Likens, G. E., 1995. Cloud deposition to a spruce forest edge. Atmospheric Environment 29, 665-672.

Williams, A P., Still, C.J., Fischer, D.T., Leavitt, S.W., 2008. The influence of summertime fog and overcast clouds on the growth of a coastal Californian pine: a tree-ring study. Oecologia 156, 601–11.

Williams, A P., 2009. Teasing foggy memories out of Pines on the California Channel Islands using tree-ring width and Stable Isotope approaches (Doctoral disserations). University of California, Santa Barbara, CA.

Williams, A., P., Allen, C.D., Millar, C.I., Swetnam, T.W., Michaelsen, J., Still, C.J., Leavitt, S.W., 2010. Forest responses to increasing aridity and warmth in the

southwestern United States. Proceedings of the National Academy of Sciences 107, 21289–21294.
Wulder, M. A., Dymond, C.C., White, J.C., Leckie, D.G., Carroll, A.L., 2006. Surveying mountain pine beetle damage of forests: A review of remote sensing opportunities. Forest Ecology and Management 221, 27–41.
Wycoff, P.H., Clark, J.S. 2002. The relationship between growth and mortality for seven co-occurring tree species in the southern Appalachian Mountains. Journal of Ecology 90, 604-615.

Chapter III. Coastal fog during seasonal drought: Impact on the water relations of adult and sapling trees in a California pine forest

1. Introduction

Physiological responses and tolerances of plants to changes in seasonal water availability vary across life stages (Yoder et al. 1994; Donovan and Ehleringer 1991; Phillips et al. 2002; Mahall et al. 2009), and understanding this variation is critical for making mechanistically based predictions of how plant species distributions may be affected by climate change in the future. Physiological characteristics, such as gas exchange rates, can vary with tree age (Ryan et al. 1996, Bond 2000, Cavender-Bares and Bazzaz 2000); however, differences in rooting distribution alone can have significant consequences for how trees withstand periods of water stress (Weltzin and McPherson 1997, Cavender-Bares and Bazzaz 2000). The rooting distribution of trees generally becomes more extensive as they grow, allowing greater access to stable water resources at depth (Mahall et al. 2009; Kolb and Stone, 2000), whereas younger, smaller trees tend to have a shallow rooting distribution, are more susceptible to drought (Mahall et al. 2009), and rely on soil moisture that is more ephemeral in space and time (Weltzin and McPherson 1997, Cavender-Bares and Bazzaz 2000).

The difference in the water relations between age classes may also be a function of how closely transpiration rates are controlled by stomatal regulation. The hydraulic limitation hypothesis proposed by Yoder and Ryan (1997) states that tall, and generally old, trees will close stomata more readily than sapling trees to reduce xylem tension (and avoid

excessive embolisms), yet the tradeoff is that taller trees will also experience lower gas-exchange rates and potential growth than shorter trees. In accordance with this hypothesis, it has been demonstrated that leaf hydraulic and stomatal conductance are inversely related to tree age/size (Hubbard et al. 1999), and carbon assimilation rates are reduced in older, taller trees compared to saplings and seedlings (Yoder et al. 1994). However, Donovan and Ehleringer (1992) found that reproductive desert shrub species had higher rates of stomatal conductance than juveniles. The most parsimonious explanation for this pattern is that reproductive plants have greater access to soil moisture and, therefore, can maintain adequate leaf hydration to support transpiration (Passioura 1982, Cavender-Bares and Bazzaz 2000).

In regions with Mediterranean climates, such as coastal California, rainfall typically occurs in the winter months (November-February), while summer months (June-September) are relatively warm and dry; yet summer is also when coastal fog most frequently occurs. Coastal fog, a low-stratus cloud at ground level, is considered a critical factor to the growth and persistence of numerous plant species because it can offset water stress in several ways: 1) direct water inputs via fog-drip from the canopy augment the water budget of the ecosystem (Dawson 1998; Fischer et al. 2009; Carbone et al. 2012; Sawaske and Freyberg 2014), 2) shading by cloud cover reduces heat loading and evapotranspiration losses (Burgess and Dawson 2004; Fischer et al. 2009), and 3) potential foliar absorption of fog water decouples plant water use from the soil (Simonin et al. 2009; Limm et al. 2009; Goldsmith et al. 2013). During the rainless, but foggy, months in Mediterranean climates, it is reasonable to expect that the water relations of smaller, younger trees (saplings) would be disproportionately affected both by drying soil conditions and fog-drip compared to larger,

older trees (adults) (Dawson 1998). Dawson (1998) provides convincing evidence that smaller coast redwood trees obtain a greater fraction of their annual water from summertime fog than do larger trees. The most plausible mechanism by which these small trees access fog water is after it drips from plant canopies (fog-drip) and penetrates shallow soil depths where small trees also have the greatest proportion of their roots (Dawson 1998). A number of studies have shown that fog water can infiltrate soil to reach the rooting zone of several conifer tree species other than coast redwood (Ingraham and Matthews 1995; Scholl et al. 2010), and that these trees use fog water to grow (Williams et al. 2008; Carbone et al. 2012).

The ability of trees to utilize fog water, which is highly variable in space and time, may be important for surviving dry season conditions, and critically important to seedling establishment, sapling survival and overall population dynamics (del-Val et al. 2006). For example, alleviation of water stress through fog-drip from larger tree canopies facilitates tree establishment in California grasslands, which directly impacts plant community composition (Kennedy and Sousa 2006). Gutierrez et al. (2008) demonstrate that tree recruitment within forest patches in a fog-influenced forest has persisted over hundreds of years despite large fluctuations in rainfall patterns, and they strongly suggest that the occurrence of fog-drip buffers tree establishment during drier years. In a related study, del-Val et al. (2006) show that tree regeneration and forest patch structure is strongly influenced by fog-drip from already established trees on the windward (more foggy) side of the forest patch. Coastal fog thus likely plays an important role in plant regeneration rates by enhancing trees water relations through the most vulnerable early life stages. While these and other studies have demonstrated the positive effects of coastal fog on plant water relations in forests during the

summer, our study is one of the few to examine the relative importance of coastal fog on the water relations of trees of different ages.

The objective of our study was to determine how the water relations of adult and sapling trees were affected by changes in moisture during the foggy summer. We conducted our study in the most extensive (3.6 km^2) and westernmost bishop pine (*Pinus muricata* D. Don) stand on Santa Cruz Island (SCI, 34º N, 119º 45' W), which is the largest of the northern islands in Channel Islands National Park (~250 km^2, 38 km E-W extension) located approximately 40 km south of Santa Barbara, California (Fig. 3.3.1a). SCI harbors the southernmost extent of this drought-sensitive and relict tree species in California (Axelrod 1965, Johnson 1977, Raven and Axelrod 1978); a reduction in the population here would impact the distribution of the species as a whole. Furthermore, we know that bishop pines on SCI are vulnerable to drought-induced mortality (Baguskas et al. 2014; Walter and Taha 1999), especially compared to more northern populations that receive almost twice as much rainfall (PRISM Climate Group, Oregon State University). Moreover, the ability for plants to persist through dry periods depends strongly on their access to water resources and physiological mechanisms used to regulate water status, which vary with plant size (Donovan and Ehleringer 1992). In our research we addressed the following questions: 1) How do the water relations and drought tolerance differ between adult and sapling bishop pines during the dry season?; and 2) How does fog affect the water relations of these distinct age classes? We measured predawn and midday water potentials, transpiration rates, and leaf hydraulics (derived from pressure volume curves) to address these questions.

2. Materials and methods

Site description

We compared the water status of adult and sapling trees in a bishop pine forest during the foggy and rain-free summer months (June-September) in coastal, southern California across two years (2010 and 2011). Age class comparisons were stratified between two sites that are part of a coastal-inland moisture gradient (Fig. 3.3.1b, Fischer et al. 2009; Carbone et al. 2012). The site located in Sauces Canyon (Sauces) is closer to the coast and at a lower elevation (296 m) than the more inland but higher elevation site located in Upper Embudo Canyon (Upem – elevation of 427 m). Upem is the more drought-prone site because even though annual rainfall tends to be greater at Upem (e.g., 467 mm vs. 391 mm in 2008), summer daytime cloud cover is less than at Sauces (e.g., 32% vs. 25% in 2008) (Carbone et al. 2012). Therefore, solar radiation, air temperature, and vapor pressure deficits are higher at Upem, which together drive higher potential evaporative losses of water and lead to lower dry season soil water (Carbone et al. 2012).

Microclimate

Microclimate conditions were recorded every 15 minutes at each site. Measured environmental variables included air temperature (T_{air}) and relative humidity (RH) (HMP45C; Vaisala, Helsinki, Finland), from which estimates of saturated vapor pressure deficit (VPD) were calculated. We used T_{air} and RH to calculate the water potential of the atmosphere (Ψ_{atm}) based on software provided by M. Loik (personal communication) and described by Nobel (2005) and Vasey et al. (2012). Fog water inputs were measured with a passive fog-collector connected to an automated tipping-bucket rain gauge (TE 525; Texas

Electronics, Dallas, TX, USA). We converted fog water volumetric inputs (ml) to depth equivalents (mm) using an established relationship between measured fog water input volumes and throughfall from under tree canopies at Sauces (Fischer and Still 2007). Monthly averages were calculated for temperature, relative humidity, and VPD. We calculated total fog water inputs (mm) for each month of our study. We excluded October because we only collected plant measurements on the first two days of the month.

Tree age class

To determine age classes of trees, we use tree size as a proxy (Porté et al. 2002). Tree size was determined by diameter at 1.3 m height (diameter at breast height; DBH) and height of trees (m) (Table 3.3.1). DBH measurements of saplings (height < 3 m) were collected at the base of the tree. Tree height was measured using a laser rangefinder (Opti-logic model 100LHA, Tullahoma, TN). We refer to 'adult' trees as those that have a DBH > 10 cm and height > 5 m, and should be greater than 20 years old based on previous research that developed size-age relationships for the bishop pines on SCI (Hobbs 1979). Sapling trees had DBH < 8 cm measured at the base of the tree and height < 3 m. These trees were likely less than 10 years old (Hobbs 1979).

Plant water status

Between 28-Jun-2011 and 1-Oct-2011, we measured stem water potential from adult and sapling trees (n=6 per age class) at each of the two sites during predawn (0200-0430 hr.) and midday (1200-1400 hr.) periods using a Scholander pressure chamber (Model 1000, PMS Instruments Inc., Corvallis, OR). Predawn stem water potential (Ψ_{pd}, MPa) is an

accepted measure of baseline plant water status on a diurnal timescale (Lambers et al. 2008). Midday stem water potential (Ψ_{md}, MPa) should represent the water status of trees at the time of the day of greatest water stress. We conducted a total of eight sampling periods at each site between June and October. Stem water potential was measured directly in the field. Two stems were clipped from each tree and then placed immediately in a sealed plastic bag (and in the dark during midday) to reduce transpiration of samples prior to determining their water potential. During midday, stems were sampled from the sunlit side of the tree. During predawn, stems were collected from a similar height on the tree to control for variation in gravimetric water potential. Water potential was measured within two minutes from the time of stem collection. Predawn and midday leaf water potential measurements were also collected between June-September in 2010 (n=5 per age class), thus providing an opportunity to examine interannual variation in dry season plant water status.

Fog-drip and soil moisture

To relate fog water inputs measured by the passive fog collector to potential plant available water, we collected fog-drip from beneath tree canopies (throughfall) of adult and sapling trees at each site after nighttime fog events (number of nights: Sauces=12; Upem=11). To do this, we constructed throughfall collectors by placing a 20 cm diameter funnel with a mesh filter on top of a 1 L plastic container. For adult trees at each site, we positioned collectors approximately one and three meters from the trunk along a northwest to southeast axis that paralleled the prevailing wind direction (n=24 collectors, with four collectors per adult tree). We placed fewer throughfall collectors beneath sapling trees at each site because their canopy diameter was smaller (n=12, with two collectors per sapling

tree). We coupled throughfall measurements with instantaneous roving measurements of percent shallow soil moisture (0-10 cm) using a portable Time Domain Reflectometry (TDR) probe (Mini-TRASE, Soil moisture Equipment Corp., Santa Barbara, CA). Due to the limited number of days (12 days total at each site) when we measured both soil moisture and throughfall, we combined age class data across sites to increase our sample size; therefore, we evaluated the correlation between soil moisture and throughfall between age classes, and not between sites.

Stomatal conductance

We related stomatal conductance (g_s) to predawn stem water potential (Ψ_{pd}) and compared the slope of the linear regression (β) to gain insights into plant water regulation for adult and sapling trees at each site. During 2010, we measured midday (1130 – 1430 hr.) g_s using a porometer (SC-1 Leaf Porometer, Decagon Devices Inc., Pullman, WA) from adult and sapling trees over a few days in August ('day of year' [DOY] ~230) and again in September (DOY ~263) at both Sauces and Upem. Ten consecutive porometer measurements were collected per individual tree (n=5 per age class) from randomly selected sunlit needle clusters.

Pressure-volume curves

We generated pressure-volume (PV) curves following the Sack and Pasquet-Kok (2011) "bench dry method". From these curves, we extracted bulk tissue water relation traits (Tyree and Hammel 1972; Sack and Holbrook 2006; Bartlett et al. 2012). In brief, we collected stem samples from six individuals per age class at both sites in December 2012

and July 2013. We transported samples to the laboratory in sealed plastic bags that were kept cool and dark to reduce transpiration. In the laboratory, we excised needles under water from the field collected branch samples and rehydrated them overnight before beginning measurements. Curves were generated by repeatedly measuring needle water potential using a pressure chamber and leaf mass using a 4-digit balance while the needles dried out on a bench top. Measurements were plugged into a spreadsheet constructed to visualize the developing curves and measurements were stopped when a minimum of five data points were observed in the lower (linear) region of the curve. Following these measurements, needles were dried to constant weight in a drying oven and dried samples were used to obtain dry leaf mass (g). PV-curves were constructed by plotting the inverse of water potential ($1/\psi$) versus the relative water content (RWC).

From these PV-curves, we estimated leaf water potential at the turgor loss point (π_{tlp}, MPa), which also defines the soil water potential beyond which a plant theoretically cannot take up water (i.e., the permanent wilting point). Extended periods of turgor loss, i.e., when leaf water potential values are consistently more negative than π_{tlp}, can result in loss of basic plant functions such as photosynthesis (Bartlett et al. 2012). Other leaf traits derived from PV-curves include the following: 1) osmotic potential at full turgor (π_o, MPa) and at π_{tlp}, which can be used to determine the ability of plants to make osmotic adjustments to dry soil conditions; 2) bulk modulus of elasticity at full turgor (ε), which estimates the cell wall rigidity and thus the flexibility of the cell to conform to changes in leaf water content; and 3) relative water content at the turgor loss point (RWC_{tlp}) (Mitchell et al. 2008; Bartlett et al. 2012). We used leaf hydraulic traits from the winter and summer PV-curves to compare π_{tlp} values between age classes and sites to assess drought tolerance and determine if seasonal

adjustments in osmotic potential and/or bulk modulus of elasticity explain shifts in π_{tlp} values.

Data analysis

We calculated the mean and standard deviation for Ψ_{pd} and Ψ_{md} of age classes at each site during each sampling period. A least-squares regression was used to determine the relationship between plant water status (Ψ_{pd} and Ψ_{md}) and DOY for each age class at the two sites between late June and early October. We used DOY to describe time in the dry season and as a proxy for time since the last large rainfall event (> 50 mm), which occurred in February (DOY ~58) in 2010 and in March (DOY ~ 80) in 2011. We also used a least-squares regression to determine the relationship between: 1) g_s and Ψ_{pd}, and 2) Ψ_{pd} and changes in soil moisture (0-10 cm) between age classes. We used ANCOVA to test for differences between the slopes of these regression relationships (β). Least-squares regressions, ANCOVA, and ANOVA were all performed using JMP ver. 10.0.0 software (SAS Institute, Cary, SC).

Following these initial statistical analyses, a linear model was used to predict the water status (Ψ_{pd}) of bishop pines at each site with day of year, age class, and fog water input as predictors in 2011. We did not include 2010 in this analysis because the sample size was much smaller. Other environmental variables (T_{air}, RH, and VPD) were included in the model but they did not enhance the model fit and so were not included in the final model. We evaluated model performance with and without fog water inputs by comparing the difference in model fit to the data. We used cumulative fog water inputs over four days prior to measuring plant water status as our fog water input data because we found the strongest

relationship with this time period compared to cumulative fog over two or even six days, for example. We used a similar approach to predict shallow soil moisture using throughfall (fog-drip), day of year, site, and age class as predictors. All of the model runs were performed using a statistical packages (lm) in R 2.12.2 (R development Core Team 2012).

For leaf hydraulic traits derived from the PV-curve, we used a Wilcoxon Rank Sum to test for statistical differences between age classes both within and between sites. This analysis was appropriate given our small sample size and unequal variances. We also tested for differences between summer and winter π_{tlp} using a Student's t-test. We performed these analyses using JMP ver. 10.0.0 software (SAS Institute, Cary, SC).

3. Results

Microclimate conditions

Average rainfall on SCI was (~500 mm) during the water year from 1-Oct-2009 to 30-Sept-2010 and above average (~740 mm) during the water year from 1-Oct-2010 to 30-Sept-2011, suggesting that the seasonal drought was not as severe during the dry seasons of our sampling periods as it is in some years. Cumulative fog water inputs between June and October in 2011 were 33% greater at Upem than at Sauces (Table 3.3.2; Upem= 403 mm, Sauces= 304 mm), and this difference is consistent with results from previous years (Carbone et al. 2012). In addition, fog events differed in their timing and magnitude between sites (Fig. 3.3.2). At Sauces, measureable fog events arrived earlier in the summer and were generally smaller and less frequent through the dry season. Conversely, Upem experienced

consecutive large fog events between mid-July to mid-August and received almost no measureable fog in June (Fig. 3.3.2).

At Upem, T_{air} was higher, RH was lower, and VPD was much higher compared to Sauces (Table 3.3.2). In addition, average monthly water potential of the atmosphere (Ψ_{atm}) was consistently lower (i.e., more negative) at Upem than at Sauces (Table 3.3.2); however, Ψ_{atm} was much higher (less negative) during foggy than during non-foggy periods at both sites, and this difference was greater at Upem than Sauces sites (Sauces: $\Psi_{atm\ (fog)}$ = -9.4 MPa, $\Psi_{atm\ (no\text{-}fog)}$ = -23.6 MPa; Upem: $\Psi_{atm\ (fog)}$ = -11.5 MPa, $\Psi_{atm\ (no\text{-}fog)}$ = -67.5 MPa). Because solar radiation data were not complete for 2010 or 2011, we refer to values reported by Carbone et al. (2012) who found that annual solar insolation was lower at Sauces than at Upem (~670 W m^{-2} and ~725 W m^{-2}, respectively); this annual difference was due to summertime differences driven by cloud cover gradients. In addition, Carbone et al. (2012) showed ~33% higher annual rainfall totals at Upem than Sauces. Taken together, evaporative effects were stronger at Upem, despite the fact that fog water inputs and rainfall were greater at this site than at Sauces.

Change in bishop pine water status during dry season

In 2011, Ψ_{pd} values declined (i.e., became more negative) during the dry season for adult and sapling trees at both sites, but this change was more rapid for sapling than adult trees as indicated by the steeper negative slopes (β) (Fig. 3.3a and 3b, Table. 3.2A). In addition, the difference in slopes of regression equations were significant between age classes at each site (Table. 3.2A). Unlike changes in Ψ_{pd}'s through the dry season, the slope of the regression line fit to Ψ_{md} values were not significantly different between age classes at

either site (Fig. 3.3a and 3b; Table. 3.2A). Overall, Ψ_{md}'s were consistently lower (more negative) than Ψ_{pd} for adults and saplings at each site, and water status was generally lower for trees at Upem than at Sauces (Fig. 3.3, Table. 3.2A).

In 2010, Ψ_{pd} and Ψ_{md} values declined significantly for adult trees at Sauces between June and September, but the water status of sapling did not change significantly over the same time period (Fig. 3.3c and Table. 3.2A). In addition, there was no significant differences in the slope of regression equations between age classes for either predawn or midday measurements at Sauces (Table. 3.2A). We observed a different pattern at Upem. Ψ_{pd} values of adult and sapling trees tended to increase (i.e., became less negative) between June and September (Fig. 3.3d). The positive change in Ψ_{md} values over time was stronger and steeper for both age classes compared to Ψ_{pd} values (Table. 3.2A). The slope of regression equations did not differ significantly between age classes at Upem for either Ψ_{pd} or Ψ_{md} values (Table. 3.2A). We found that at this site the difference between Ψ_{pd} and Ψ_{md} values (i.e., xylem tension) was greater in July (adult, 0.82 MPa, sapling, 0.68 MPa) than it was following a large, late-season fog event in September (adult, 0.01 MPa, and sapling 0.13 MPa). In sum, the water status of trees at Upem was higher in September than in July during 2010 despite the longer drydown period from lack of rain.

Impact of fog events on the water status of adult and sapling trees

While DOY (a proxy for seasonal variation and time since the last rainfall) explained most of the variance in Ψ_{pd} values at each site, antecedent cumulative fog water inputs had a positive and significant effect on water availability to both adult and sapling trees (Table 3.3). We did not find a significant interaction between fog, DOY and/or age at either site,

suggesting that the effect of fog on plant water status was similar regardless of time or tree age.

During a single fog event at Upem in August 2010, Ψ_{pd} of adult and sapling trees increased as fog water accumulated in the soil (Fig. 3.4); however, the change in water status was greater for saplings (0.33 MPa) than for adults (0.13 MPa). Immediately before the fog event, average Ψ_{pd} was significantly lower in saplings (adult: -0.89 MPa, sapling: -1.24 MPa, P=0.02). By the tail-end of the event (DOY 227), age classes differences were reduced (adult: -0.73 MPa, sapling: -1.02 MPa, P=0.08). Two days after the event, adult and sapling Ψ_{pd} converged on a similarly high, and statistically more similar, value of ~-0.80 MPa (adult: -0.76 MPa, sapling: -0.91 MPa, P=0.11). Relative to the pre-fog event, the peak reduction in water status for adults occurred during the event, while the greatest change for saplings was two days afterward, suggesting a lag time for fog water infiltration into the soil. In addition, the more rapid response of adults to fog events compared to saplings implies potential foliar absorption of fog water by adult trees. Unfortunately, we were not able to capture change in tree water status through a single fog event at Sauces, hence the lack of site comparison.

Fog-drip, soil moisture, and plant water status

Percent shallow soil moisture (0-10 cm) measured with a TDR beneath tree canopies was positively and significantly correlated with Ψ_{pd} values for both adult and sapling trees (Fig. 3.5). In addition, the slope of the linear regression model (β) was significantly steeper for sapling than adult trees (Fig. 3.5), suggesting that sapling trees rely more on shallow soil moisture to maintain their water status compared to adult trees, regardless of site. The most

important explanatory variable of shallow soil moisture was fog-drip from tree canopies (throughfall) (Table 3.4; fog-drip =2.84, t-value=2.55, P<0.01), whereas day of year was not a significant predictor of soil moisture (Table 3.4, DOY=-0.01, t-value=-0.56, P=0.58). We found that soil moisture was significantly lower under sapling trees at Upem compared to all other trees (Upem, saplings*:* 9.9 ± 2.6 %; all other tree groupings: ~13.5%). This could be due to higher insolation and soil evaporation and/or greater drawdown due to root uptake from transpiration. Fog-drip and soil moisture outside tree canopies were negligible compared to beneath tree canopies (data not shown). Throughfall amount was similar per unit area for adult and sapling trees at Sauces (adult=0.23 ± 0.05 cm, sapling=0.20 ± 0.05 cm, P=0.65) likely because sapling trees were in closer proximity to adult trees at this site, and thus received fog-drip from adult trees as well as from their own canopies. At Upem, throughfall was significantly greater under adult trees compared to saplings (adult=0.32 ± 0.05 cm, sapling=0.12 ± 0.06 cm, P=0.01), and the lowest throughfall values beneath Upem saplings agrees with their having the lowest soil moisture values.

Stomatal control on tree water relations

In 2010, we observed a negative relationship between midday stomatal conductance (g_s) and predawn stem water potential (Ψ_{pd}) for both age classes at Sauces, and the slope of the linear regression model (β) tended to be stronger and slightly steeper for adult compared to sapling trees (Fig. 3.6a). At Upem, we observed no relationship between g_s and Ψ_{pd} for either adults or sapling trees (Fig. 3.6b). Even though the relationship between g_s and Ψ_{pd} was variable between sites, adult trees tended to maintain higher conductance rates than saplings (Fig. 3.1A).

Hydraulic leaf traits derived from pressure-volume curves

Average turgor loss point (π_{tlp}) estimates derived from PV-curves ranged from -1.30 MPa to -2.05 MPa with significant variation within and between sites and age classes (Table. 3.3A), where lower (more negative) π_{tlp} values suggest greater drought tolerance. Minimum Ψ_{pd} values observed in the dry season of 2010 or 2011 did not become more negative than π_{tlp} values, except for saplings at Upem in 2011 (Table. 3.3A). To understand potential physiological controls on π_{tlp}, we related π_{tlp} to other hydraulic leaf traits. More negative values of π_o indicate greater solute concentration in plant cells. We found a strong positive relationship between dry season (summer) π_{tlp} and osmotic potential at full turgor (π_o) for adult and sapling trees (Fig. 3.7). The slightly steeper slope for saplings suggests osmotic adjustment by saplings was greater than for adults, but did not differ significantly between age classes (Fig. 3.7). While we tested for relationships between π_{tlp} and other leaf traits, such as elastic modulus, we only found weak correlations with these other variables.

4. **Discussion**

The results of our study contribute novel information about the degree to which fog water inputs affect the water relations of adult versus sapling trees. Specifically, our study provides evidence that fog-drip is a significant contributor to changes in soil water content within the first 10 cm of the soil (Table 3.4), and fluctuations in soil moisture correlate strongly with improved water status of bishop pines, especially sapling trees (Fig. 3.5). Our

results corroborate well with results from a study conducted by Dawson (1998), who evaluated differences in fog water use by different size classes of trees in the fog-influenced northern Californian coast redwood forest and found that smaller trees transpired 40% more fog water than larger trees. Similarly, Cavender-Bares and Bazzaz (2000) found oak seedlings were more responsive to rainfall events during the dry season compared to larger, adult trees, suggesting that these distinct age classes rely on different water resources. In addition, our study shows that a single, large fog event can effectively reverse the dry-down trajectory otherwise experienced by bishop pines during the dry season (Fig. 3.3b vs. 3d); this effect is likely to be especially critical for buffering against water stress in already drought-prone environments.

We observed a smaller difference in Ψ_{pd} between age classes at Sauces in 2011 compared to Upem (Fig. 3.3a and b), indicating that sapling and adult trees at Sauces had similar access to soil water whereas at Upem they did not. Similarly, Vasey et al. (2012) observed that deep and shallow rooted coastal California shrubs had similar access to water at a fog-influenced coastal site compared to a warmer, drier interior site. One explanation for these site differences is that fog-drip supplemented soil water to the shallowly rooted plants such that they had similar access to water as more deeply rooted individuals. We know that fog-drip can contribute a significant amount of water to semi-arid and arid ecosystems (Azevedo and Morgan 1974; Uehara and Kume 2012), and linkages between fog-drip, increased soil moisture, and plant water use have been well established in a variety of coastal ecosystems (Ingraham and Matthews 1995; Burgess & Dawson 2004; Corbin et al. 2005; Scholl et al. 2010). In addition, the structural complexity of the forest canopy is an important component to the hydrology of a foggy forest (Barbosa et al. 2010), thus variation

in canopy architecture and position of saplings versus adult trees on the landscape may help us explain differences in plant water status. A likely explanation for the patterns we observed was that saplings were heavily irrigated by fog-drip as they grew beneath the overlapping canopies of the larger, adult trees, which would homogenize the impact of fog-drip on soil moisture at Sauces. In contrast, sapling and adult trees at Upem grew in greater isolation, thus, the control of canopy size on fog-drip to the soil was stronger at this site.

During a single, large fog event at Upem in 2010, we found that adult tree water status improved during the event while there was a two-day lag in the response by sapling trees (Fig. 3.4). Based on these results, we surmise that foliar absorption of fog-water is likely to occur in bishop pines on SCI and help improve the water status of trees, especially for adult trees at the drier part of the stand. Simonin et al. (2009) found a similar increase in plant water status during a single fog event in the coast redwoods, and provides evidence that foliar absorption of fog water is a viable and important mechanism for foliar hydration during foggy periods. This is a potential mechanism that we did not explicitly test for, but may help explain the late-season increase in plant water status when soil water deficit is usually high.

Do saplings and adults regulate stomatal conductance differently?

When considering differences in stomatal regulation between age classes, Hinckley et al. (1978) notes that thresholds of leaf water potential that induce stomatal closure are higher (less negative) for saplings than for adult trees. In accordance with this pattern, we found that adult trees tended to maintain higher rates of stomatal conductance than sapling trees, and this difference was significant at Upem (Fig. 3.1A). Similarly, Cavender-Bares

and Bazzaz (2000) demonstrate that seedling oak trees close stomata early in the day to avoid water stress while adult trees access deeper water reserves and have higher rates of stomatal conductance. One possible explanation for differences in stomatal conductance between age groups in our study could be that the hydraulic safety margin is narrower for sapling than for adult trees. While we found that stomatal closure was more sensitive to changes in water availability for both age classes at Sauces compared to Upem, it remains unclear from our results if there is a threshold leaf water potential above or below which bishop pines consistently close stomata to preserve their water status.

Hydraulic leaf traits and drought tolerance of bishop pines

One reason for measuring leaf hydraulic traits was to combine them with our estimates of plant water status and attempt to quantify exposure of SCI bishop pines to water stress during the dry season. By comparing π_{tlp} estimates and Ψ_{pd} values from the same plants we can determine if bishop pines on SCI lose turgor during the dry season, an indicator of water stress (Table. 3.3A). These comparisons suggest that, in most cases, bishop pine trees did not experience water stress during the dry-season of 2010 or 2011. The exception is saplings at Upem in 2011, which appear to have lost turgor in late August. In a comparable relict foggy forest in coastal Chile, Negret et al. (2013) found that a variety of dominant plant species did not experience drought stress during the dry season and maintained turgor through various ecological and physiological strategies. However, additional measurements would need to be completed to rule out water stress as a driver of mortality during more severe drought events. It should be noted that our measurements of π_{tlp}, and Ψ_{pd} were completed during different dry seasons. Therefore, any conclusions about

the maintenance of turgor during the 2010 or 2011 dry season should be viewed with caution. For instance, during drier years (e.g., the years preceding the 2009 dieback of bishop pines on SCI, Baguskas et al. 2014), comparisons of π_{tlp} and Ψ_{pd} may tell a different story than the data presented here.

Consistent with the Bartlett et al. (2012) global analysis of drought tolerance across species and biomes, bishop pine across age classes and sites appear to regulate their tolerance to drought (π_{tlp} values) primarily through osmotic adjustment (Fig. 3.7). We did not find a strong relationship between π_{tlp} and any other leaf trait involved with hydraulic regulation; however, we did observed that the elastic modulus (ε) was lower in saplings at Upem relative to other groups (Table. 3.3A). A lower ε corresponds to greater flexibility in cell walls; therefore, this strategy may compensate for a weaker ability of saplings at Upem to adjust to water stress osmotically (Hinckley et al. 1983). Overall, we found that the absolute value of the suite of hydraulic leaf traits from PV-curves agree with global averages determined for coastal, Mediterranean climates (Bartlett et al. 2012).

Influence of coastal fog on population dynamics

Our study implies an important role for fog in enhancing bishop pine seedling survival through the recruitment bottleneck, as has been found to be important in other foggy forests (Gutierrez et al. 2008). Bishop pines become reproductive at an early lifestage (~5 years old) and cone generation continues through adulthood (lifespan is about 100 years). It is possible that generation of a large seed bank is an adaptation to drought-stress because the potential for recruitment is high even if reproductive plants die back during intense drought events. While recruitment is not likely to be high during drought (Lloret et

al. 2004), observations in the field suggest that recruitment is greatest in springtime following winter rainfall events; moreover, seedling survival (and growth) appears to be greatest under the drip-line of canopy trees, where irrigation by fog-drip, as well as exposure to sunlight, are both relatively high during summer. Future research should test the hypothesis that recruitment and establishment is higher in the foggier parts of the stand, and that saplings in foggier areas have greater survival rates than saplings in less foggy areas of the stand.

5. Conclusions

Fog water inputs may only temporarily augment plant-available water, but our study shows that fog-drip that delivers water to the soil clearly has positive effects on the water relations of bishop pines (and especially sapling trees). The effect of fog-drip on bishop pine water relations is especially important for populations, such as our study site, that grow in marginal habitat where individuals are most vulnerable to drought-induced mortality. Studying the response of bishop pines to fog events at the drier site (Upem) was particularly informative as to how important the timing and magnitude of fog events are to the essential physiological function of adult and sapling trees alike. A significant increase in bishop pine water status following a large fog event at the end of summer (when residual soil moisture from winter rains is at its lowest point) provides evidence that fog is important for this species to withstand late-season dry periods, especially in areas where trees are most vulnerable to drought-stress. This is especially true for sapling trees that are more reliant on

fog-drip to maintain water status through the summer than adults. Our results support our primary hypothesis that sapling trees rely on fog water to maintain water status more than adults, which has significant implications for population dynamics in a future climate likely to become both warmer and drier.

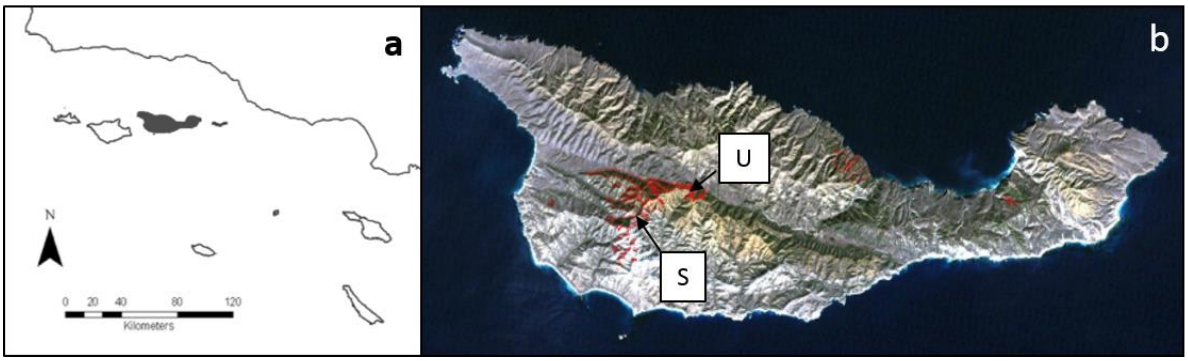

Figure 3.1. (a) Southernmost extent of the bishop pine range in the United States is on Santa Cruz Island (SCI, 34° N, 119° 45' W) (shaded in gray) about 40 km off the coast of Santa Barbara in south-central California. (b) Our study area is the westernmost and largest stand of trees. Within the westernmost Bishop pine stand, we have two sites: Sauces (coastal, mesic) and Upem (Upper Embudo, inland, xeric) indicated by the 'S' and 'U' respectively.

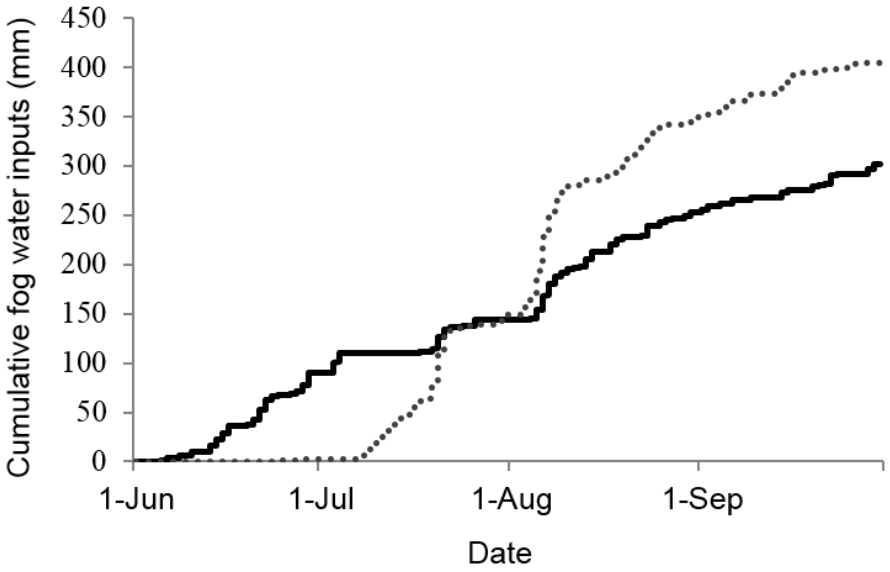

Figure 3.2. Cumulative daily fog water inputs (mm) collected over summer months (June-Sept 2011) by a passive fog collector located at each field site, Sauces (solid line) and Upem (dashed line).

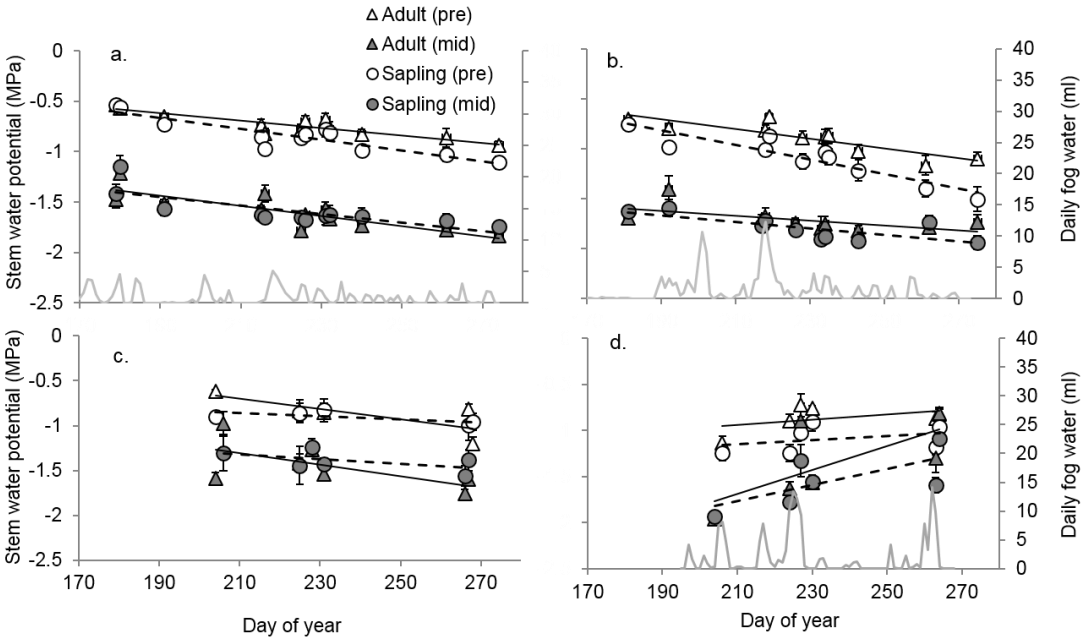

Figure 3.3. Stem water potential of adult (triangles) and sapling (circles) trees during predawn (Ψ_{pd}, open symbols) and midday (Ψ_{md}, filled symbols) in relation to day of year during the dry season (June-September) in 2010 and 2011 at Sauces (a and c) and Upem (b and d), respectfully. Sample size was 5 individuals per age class in 2010 and 6 individuals per age class in 2011. Error bars represent ± SE. Least-squares regression lines were fitted to the non-averaged leaf water potential data. Cumulative daily fog water inputs (ml) are indicated by the gray line. See Table 1S for slope differences between age class at each site across years.

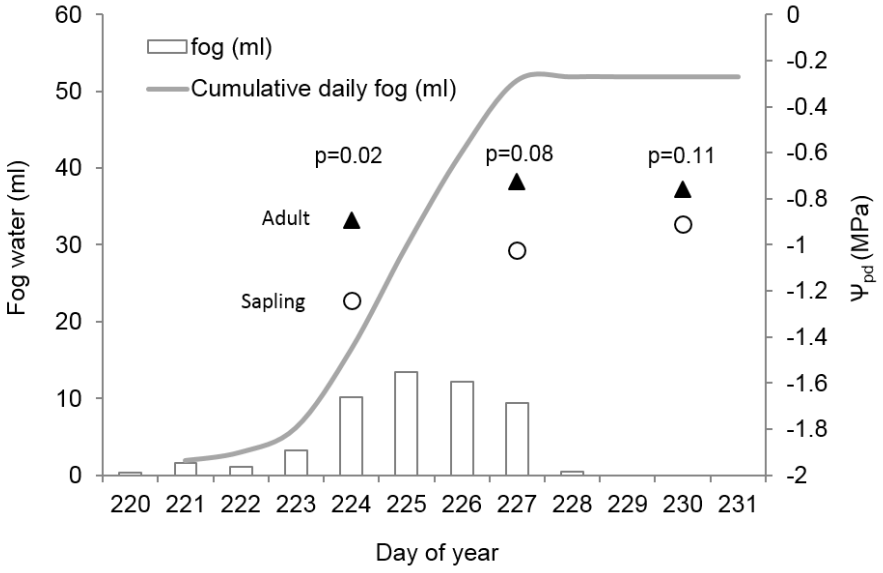

Figure 3.4. Predawn stem water potential (Ψ_{pd}) before, during, and after (DOY 224, 227, 230, respectively) a fog event for adult (filled triangles) and sapling (open circles) trees at Upem in 2010. Degree of statistical difference between age classes at each time point it indicated by p-values above data points ($\alpha = 0.05$).

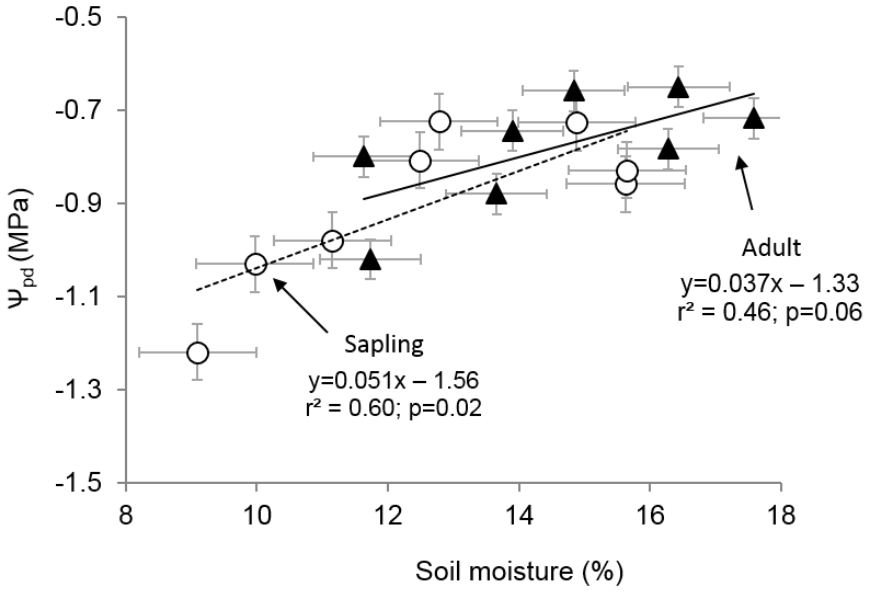

Figure 3.5. Predawn stem water potential (Ψ_{pd}) in relation to percent soil moisture (%) between 0-10 cm for adult and sapling bishop pine trees. Slopes of the least-squares regressions between age classes differ significantly ($F_{(1, 7)}$=0.1, p=0.06). Each data point represents the average of n=8 trees per age class. Data collected during summer 2011 and pooled by site. Error bars represent ± SE.

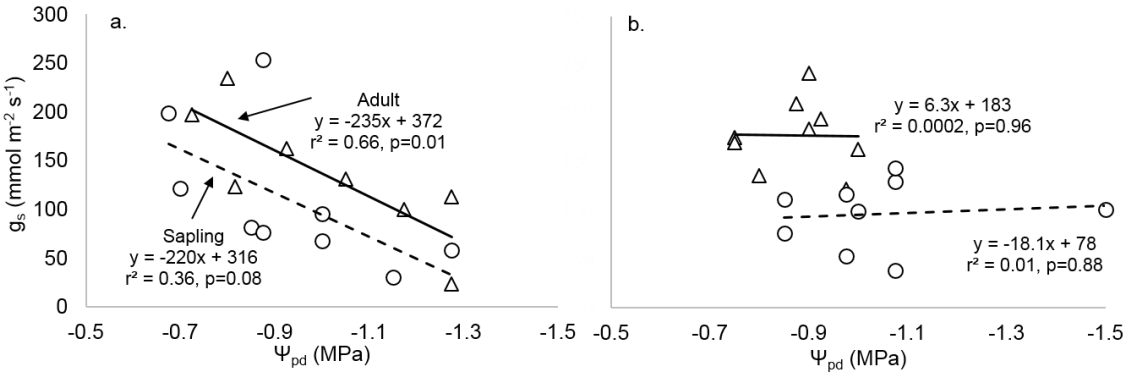

Figure 3.6. Midday stomatal conductance (g_s) in relation to predawn leaf water potential (Ψ_{pd}) for adult (triangles, solid line) and sapling (circles, dashed line) bishop pine trees at Sauces (a) and Upem (b) in August (DOY~223-30) and September (DOY~264-67) in 2010. Each data point represents an individual tree (n=5 per age group) for which we took the average g_s from 10 porometer readings per individual. Least-squares regressions were fitted to these data. Slopes between age classes did not differ from one another at either site (Sauces, p=0.91. Upem, p=0.88).

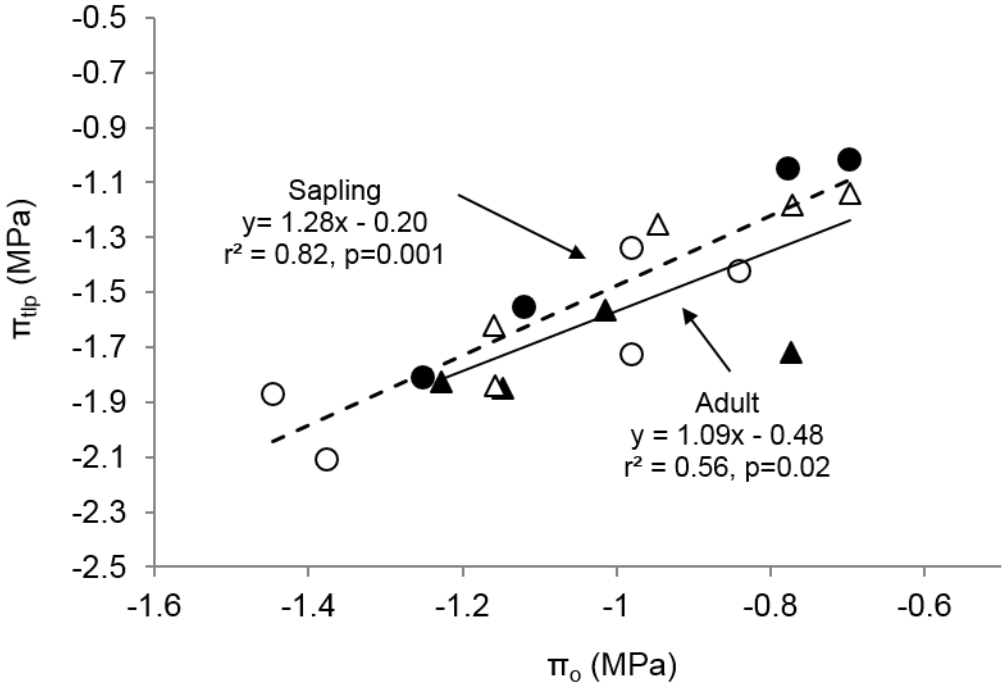

Figure 3.7. Relationship between osmotic potential at full turgor (π_o) and turgor loss point (π_{tlp}) estimates for adult (triangles, solid line) and sapling (circles, dashed line) bishop pines at Sauces (filled symbols) and Upem (open symbols). Slopes between age classes did not differ significantly from one another ($F_{(1, 17)}$=0.19, P=0.66). Leaf hydraulic traits were derived from PV-curve generated from samples in July 2013. More negative values of π_o indicate greater solute concentration in plant cells and more negative values of π_{tlp} indicate greater tolerance to drought stress.

Table 3.1. Tree size estimates based on average diameter at breast height (DBH) and height (m) for each age class at both sites (n=6). Error bars represent ± standard error.

Site	Age	DBH (cm)	Height (m)
Sauces	Adult	25.6 ± 3.9	7.2 ± 0.76
	Sapling	4.2 ± 0.35	2.4 ± 0.18
Upem	Adult	16.5 ± 1.0	6.0 ± 0.42
	Sapling	5.1 ± 0.5	2.7 ± 0.14

Table 3.2. Microclimate variables measured at each site during summer months (June-September) 2011. Monthly average values were calculated for temperature (T_{air}), relative humidity (RH), and vapor pressure deficit (VPD). For fog water inputs, we present the total water (mm) collected by the passive fog collector stationed at each site[a] . Weather station data was incomplete in 2010, so not included.

Site	Month	T_{air} (^{O}C)	RH (%)	VPD	Ψ_{atm}	Total monthly fog water input (mm)	Total fog (mm)
Sauces	**June**	9.0	94.1	0.1	-7.9	91	
	July	12.9	89.8	0.2	-14.2	54	
	Aug.	10.9	95.1	0.1	-6.6	110	
	Sept.	13.5	86.1	0.4	-12.0	49	
	Summer mean	**11.6**	**91.3**	**0.2**	**-10.2**	**76**	**304**
Upem	**June**	10.7	91.9	1.3	-11.0	2	
	July	14.3	85.0	1.7	-21.5	146	
	Aug.	13.7	86.3	1.6	-19.5	201	
	Sept.	16.0	78.3	1.9	-21.0	54	
	Summer mean	**13.7**	**85.4**	**1.7**	**-18.3**	**101**	**403**

[a]The volume of fog water (ml) was converted to a depth equivalent (mm) using an accepted relationship between fog water inputs and throughfall from bishop pine canopies (Fischer and Still 2007).

Table 3.3. Parameter estimates of a linear model that predicts water status (Ψ_{pd}) of Bishop pines at each site (Sauces and Upem) as a function of day of year (DOY), age, and with or without fog water inputs collected by the passive fog collectors in the field. Model improves significantly with addition of cumulative fog water inputs (mm) four days prior to Ψ_{pd} measurement. There was no significant interaction between fog and day of year or age at either site.

Site	Model	Parameters	Estimate	SE	t	P	Adj. R^2
Sauces	No fog	Intercept	0.27	0.10	2.84	0.005	0.48
		DOY	-0.004	0.0004	-10.72	<0.001	
		Age	-0.09	0.024	-3.95	<0.001	
	Fog	Intercept	0.17	0.098	1.73	0.09	0.52
		DOY	-0.004	0.0004	-10.41	<0.001	
		Age	-0.097	0.023	-4.12	<0.001	
		Fog	1.70	0.51	3.33	0.001	
Upem	No fog	Intercept	0.50	0.15	3.45	<0.001	0.53
		DOY	-0.006	0.0006	-9.71	<0.001	
		Age	-0.21	0.03	-6.23	<0.001	
	Fog	Intercept	0.33	0.15	2.22	0.028	0.56
		DOY	-0.005	0.0006	-8.89	<0.001	
		Age	-0.207	0.032	-6.48	<0.001	
		Fog	0.68	0.21	3.19	0.002	

Table 3.4. Parameter estimates of a linear model that predicts percent soil moisture (0-10 cm) beneath bishop pine tree canopies as a function of day of year (DOY), fog-drip (throughfall, cm), age, and site class. We did not find significant interactions between variables in the model.

Parameters	Estimate	SE	t	P-value	R^2
Intercept	17.0	4.5	3.7	<0.001	0.32
DOY	-0.01	0.02	-0.56	0.58	
Throughfall	2.84	1.12	2.55	0.01	
Age	-1.92	0.61	-3.2	<0.01	
Site	-3.13	0.59	-5.3	<0.001	

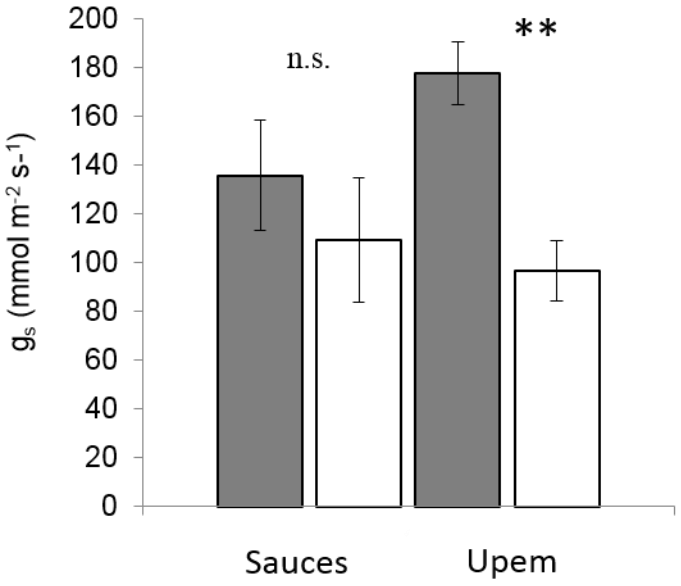

Fig. 3.1A. Average of stomatal conductance (g_s) for adult (filled bars) and sapling (open bars) trees at Sauces and Upem. Each bar represents the average g_s of 5 individual trees per age class pooled by date (DOY~223-30 and DOY~264-67) in 2010. We took the average g_s from 10 porometer readings per individual. Significant difference is indicated by asterisk ($\alpha = 0.05$).

Table 3.2A. Parameters of linear regression functions ($Y=\beta_o + \beta x$) fitted to relationships between predawn leaf water potential (Y) and day of year during dry season (x) for adult and sapling trees at each site in 2010 (n=5/age class) and 2011 (n=6/age class) (also see Fig. 3). P-value indicates if slope if different from zero. In addition, for each year, we tested for slope differences between age classes at each site. Different letters associated with slope values (β) represent statistical differences between age classes within a site (α = 0.05), and associated F-statistics and P-values are in the last two columns of the table.

									Slope differences	
Year	**Time of day**	**Site**	**Age**	***n***	β	β_o	**P-value**	**R^2**	**F-ratio**	**P-value**
2010	**predawn**	Sauces	Adult	6	-0.005 [a]	0.44	0.02	0.36	$F_{(1, 8)}$=0.93	0.34
			Sapling	6	-0.002 [a]	-0.31	0.32	0.08		
		Upem	Adult	6	0.003 [b]	-1.65	0.08	0.16	$F_{(1, 8)}$=0.47	0.49
			Sapling	6	0.001 [c]	-1.43	0.53	0.02		
2010	**midday**	Sauces	Adult	6	-0.007 [a]	0.21	0.004	0.34	$F_{(1, 8)}$=1.9	0.17
			Sapling	6	-0.003 [a]	-0.81	0.33	0.06		
		Upem	Adult	6	0.014 [b]	-4.61	0.0014	0.51	$F_{(1, 8)}$=1.09	0.31
			Sapling	6	0.009 [b]	-3.70	0.004	0.44		
2011	**predawn**	Sauces	Adult	6	-0.0037 [a]	0.08	<0.001	0.37	$F_{(1, 10)}$=4.4	0.037
			Sapling	6	-0.0054 [b]	0.37	<0.001	0.53		
		Upem	Adult	6	-0.005 [a]	0.24	<0.001	0.32	$F_{(1, 10)}$=3.9	0.049
			Sapling	6	-0.0073 [c]	0.57	<0.001	0.50		
2011	**midday**	Sauces	Adult	6	-0.005 [a]	-0.49	<0.001	0.46	$F_{(1, 10)}$=0.40	0.53
			Sapling	6	-0.004 [a]	-0.59	<0.001	0.30		
		Upem	Adult	6	-0.002 [b]	-1.12	0.001	0.13	$F_{(1, 10)}$=0. 42	0.52
			Sapling	6	-0.003 [b]	-1.03	<0.001	0.27		

Table 3.3A. Average hydraulic leaf traits derived from pressure-volume curves generated for sapling and adult trees at each site in December 2012 (Winter) and July 2013 (Summer). Traits include water potential at the turgor loss point (π_{tlp}), osmotic potential at full turgor (π_o), relative water content at the turgor loss point (RWC_{tlp}), and the elastic modulus (ε) (Mean $\pm$ SE). Minimum predawn stem water potential values ($\Psi_{pd\ (min)}$) from 2010 and 2011 are provided for comparison with summer π_{tlp} values. Different letters indicate a significant difference between age classes at each site and between sites for a given parameter based on Wilcoxon-signed rank test, when replicates were 4, and Student t-test when replicates were 5 and above.

		Sauces		Upem	
Leaf trait	**Age class**	**Summer**	**Winter**	**Summer**	**Winter**
n	Adult	4	5	4	6
	Sapling	4	6	5	6
π_{tlp} (MPa)	Adult	-1.30 ± 0.22[a]	-1.20 ± 0.12	-1.76 ± 0.12[b]	-2.05 ± 0.15
	Sapling	-1.78 ± 0.29[b]	-1.22 ± 0.10	-1.35 ± .34[a]	-1.60 ± 0.11
π_o (MPa)	Adult	-0.89 ± 0.21[a]	-0.78± 0.08	-1.06 ± 0.18[a]	-1.25 ± 0.17
	Sapling	-1.16 ± 0.30[a]	-0.76± 0.05	-0.97 ± 0.23[a]	-0.98 ± 0.05
RWC_{tlp} (%)	Adult	89.43 ± 4.39[a]	92.7 ± 1.0	79.38 ± 1.82[b]	86.8 ± 1.5
	Sapling	87.11 ± 2.66[a]	92.9 ± 1.0	89.30 ± 2.84[a]	86.2 ± 1.3
ε (MPa)	Adult	8.50 ± 6.20[ab]	9.38 ± 0.99	4.94 ± 0.37[a]	8.78 ± 1.5
	Sapling	9.28 ± 4.66[b]	9.78 ± 1.2	8.21 ± 1.70[b]	7.14 ± 0.8
$\Psi_{pd\ (min)}$	Adult	-1.20 (‘10) -0.94 (‘11)	--	-1.13 (‘10) -1.16 (‘11)	--
	Sapling	-1.0 (‘10) -1.11 (‘11)	--	-1.25 (‘10) -1.51 (‘11)	--

References

Axelrod, DI (1967). Geologic history of the California insular flora. In R. N. Philbrick (Ed.), Proceedings of the Symposium on the Biology of the California Islands. Santa Barbara Botanical Garden, California, pp 267–315.

Azevedo, J., Morgan, D.L., 1974. Fog Precipitation in Coastal California Forests. Ecology 55, 1135–1141.

Baguskas, S.A., Peterson, S.H., Bookhagen, B., Still, C.J., 2014. Evaluating spatial patterns of drought-induced tree mortality in a coastal California pine forest. For. Ecol. Manage. 315, 43–53.

Barbosa, O., Marquet, P. A., Bacigalupe, L.D., Christie, D. a., Del-Val, E., Gutierrez, A.G., Jones, C.G., Weathers, K.C., Armesto, J.J., 2010. Interactions among patch area, forest structure and water fluxes in a fog-inundated forest ecosystem in semi-arid Chile. Funct. Ecol. 24, 909–917. doi:10.1111/j.1365-2435.2010.01697.x

Bartlett, M.K., Scoffoni, C., Sack, L., 2012. The determinants of leaf turgor loss point and prediction of drought tolerance of species and biomes: a global meta-analysis. Ecol. Lett. 15, 393–405. doi:10.1111/j.1461-0248.2012.01751.x

Bond, B.J., 2000. Age-related changes in photosynthesis of woody plants. Trends Plant Sci. 5, 349–53.

Burgess, S.S.O., Dawson, T.E., 2004. The contribution of fog to the water relations of Sequoia sempervirens (D. Don): foliar uptake and prevention of dehydration. Plant, Cell Environ. 27, 1023–1034. doi:10.1111/j.1365-3040.2004.01207.x

Carbone, M.S., Park Williams, A., Ambrose, A.R., Boot, C.M., Bradley, E.S., Dawson, T.E., Schaeffer, S.M., Schimel, J.P., Still, C.J., 2012. Cloud shading and fog drip influence the metabolism of a coastal pine ecosystem. Glob. Chang. Biol. 19, 484–97. doi:10.1111/gcb.12054

Cavender-Bares J, Bazzaz F. (2000) Changes in drought response strategies with ontogeny in Quercus rubra: implications for scaling from seedlings to mature trees. Oecologia 124:8–18. doi: 10.1007/PL00008865

Corbin, J.D., Thomsen, M. a, Dawson, T.E., D'Antonio, C.M., 2005. Summer water use by California coastal prairie grasses: fog, drought, and community composition. Oecologia 145, 511–21. doi:10.1007/s00442-005-0152-y

Dawson, T.E., 1998. Fog in the California redwood forest: ecosystem inputs and use by plants. Oecologia 117, 476–485. doi:10.1007/s004420050683

del-Val, E., Armesto, J.J., Barbosa, O., Christie, D. a., Gutiérrez, A.G., Jones, C.G., Marquet, P. a., Weathers, K.C., 2006. Rain Forest Islands in the Chilean Semiarid Region: Fog-dependency, Ecosystem Persistence and Tree Regeneration. Ecosystems 9, 598–608. doi:10.1007/s10021-006-0065-6

Donovan, L.A., Ehleringer, J.R., 1991. Ecophysiological differences among juvenile and reproductive plants of several woody species. Oecologia 86, 594–597.

Donovan, L.A., Ehleringer, J.R., 1992. Contrasting patterns among size and life- shrub history classes of a semi-arid shrub. Funct. Ecol. 6, 482–488.

Fischer, D.T., Still, C.J., 2007. Evaluating patterns of fog water deposition and isotopic composition on the California Channel Islands. Water Resour. Res. 43, n/a–n/a. doi:10.1029/2006WR005124

Fischer, D.T., Still, C.J., Williams, A.P., 2009. Significance of summer fog and overcast for drought stress and ecological functioning of coastal California endemic plant species. J. Biogeogr. 36, 783–799. doi:10.1111/j.1365-2699.2008.02025.x

Goldsmith, G.R., Matzke, N.J., Dawson, T.E., 2013. The incidence and implications of clouds for cloud forest plant water relations. Ecol. Lett. 16, 307–14. doi:10.1111/ele.12039

Gutiérrez, A.G., Barbosa, O., Christie, D. a., Del-Val, E., Ewing, H. a., Jones, C.G., Marquet, P. a., Weathers, K.C., Armesto, J.J., 2008. Regeneration patterns and persistence of the fog-dependent Fray Jorge forest in semiarid Chile during the past two centuries. Glob. Chang. Biol. 14, 161–176. doi:10.1111/j.1365-2486.2007.01482.x

Hinckley, T.M., Duhme, F., Hinckley, A.R., Richter, H., 1983. Drought relations of shrub species: assessment of the mechanisms of drought resistance *. Oecologia 59, 344–350.

Hinckley, T.M., Lassoie, J.P., Running, S.W., 1978. Temporal and Spatial Variations in the Water Status of Forest Trees. For. Sci. 20, a0001–z0001.

Hobbs E (1980) Effects of grazing on the northern populations of Pinus muricata on Santa Cruz Island, California. In DM Power (ed.) The California Islands: Proceedings of a multidisciplinary symposium. Santa Barbara Natural History Museum, California, pp 159-166.

Hubbard, R.M., Bond, B.J., Ryan, M.G., 1999. Evidence that hydraulic conductance limits photosynthesis in old Pinus ponderosa trees. Tree Physiol. 19, 165–172.

Ingraham, N.L., Matthews, R. a., 1995. The importance of fog-drip water to vegetation: Point Reyes Peninsula, California. J. Hydrol. 164, 269–285. doi:10.1016/0022-1694(94)02538-M

Johnson, DL (1977) The late Quaternary climate of coastal California : Evidence for an ice age refugium. Quaternary Research 8:154–179.

Kennedy, P.G., Sousa, W.P., 2006. Forest encroachment into a Californian grassland: examining the simultaneous effects of facilitation and competition on tree seedling recruitment. Oecologia 148, 464–74. doi:10.1007/s00442-006-0382-7

Kolb, T.E., Stone, J.E., 2000. Differences in leaf gas exchange and water relations among species and tree sizes in an Arizona pine-oak forest. Tree Physiol. 20, 1–12.

Lambers, H., Chapin, F.S., Pons, T.L. (Eds.), 2008. Plant Physiological Ecology, 2nd ed. Springer New York, New York, NY. doi:10.1007/978-0-387-78341-3

Limm, E.B., Simonin, K. a, Bothman, A.G., Dawson, T.E., 2009. Foliar water uptake: a common water acquisition strategy for plants of the redwood forest. Oecologia 161, 449–59. doi:10.1007/s00442-009-1400-3

Lloret, F., Casanovas, C., Penuelas, J., 1999. Seedling survival of Mediterranean shrubland species in relation to root : shoot ratio , seed size and water and nitrogen use. Funct. Ecol. 13, 210–216.

Mahall, B.E., Tyler, C.M., Cole, S.E., Mata, C., 2009. A comparative study of oak (Quercus, FAGACEAE) seedling physiology during summer drought in southern California. Am. J. Bot. 96, 751–761. doi:10.3732/ajb.0800247

Mitchell, P.J., Veneklaas, E.J., Lambers, H., Burgess, S.S.O., 2008. Leaf water relations during summer water deficit: differential responses in turgor maintenance and variation in leaf structure among different plant communities in south-western Australia. Plant. Cell Environ. 31, 1791–802. doi:10.1111/j.1365-3040.2008.01882.x

Negret, B.S., Pérez, F., Markesteijn, L., Castillo, M.J., Armesto, J.J., 2013. Diverging drought-tolerance strategies explain tree species distribution along a fog-dependent moisture gradient in a temperate rain forest. Oecologia 173, 625–635. doi:10.1007/s00442-013-2650-7

Nobel, PS (2005) Physiochemical and Environmental Plant Physiology, 3rd edn. Elsevier/Academic Press, Burlington.

Passioura, J. B. (1982) Water in the soil-plant-atmosphere continuum. In: Lange OL, Nobel PS, Osmond CB, Ziegler H (eds.) Physiological Plant Ecology II. Springer, Berlin, pp 5-33.

Phillips, N., Bond, B.J., McDowell, N.G., Ryan, M.G., 2002. Canopy and hydraulic conductance in young , mature and old Douglas-fir trees. Tree Physiol. 22, 205–211.

Porte, A., Trichet, P., Didier, B., Loustau, D., 2002. Allometric relationships for branch and tree woody biomass of Maritime pine (Pinus pinaster). For. Ecol. Manage. 158, 71–83.

Raven, PH, Axelrod DI (1978) Origin and relationships of the California flora. Univ of California Press.

Ryan, M., Binkley, D., Fownes, J., 1997. Age-related decline in forest productivity: pattern and process. Adv. Ecol. Res. 213–262.

Ryan, M.G., Yoder, B.J., 1997. Limits to Tree Height Hydraulic and Tree Growth What keeps trees from growing beyond a certain height ? Bioscience 47, 235–242.

Sack, L., Holbrook, N.M., 2006. Leaf hydraulics. Annu. Rev. Plant Biol. 57, 361–81. doi:10.1146/annurev.arplant.56.032604.144141

Sack L, Pasquet-Kok J. Leaf pressure-volume curve parameters. 2011, Apr 05. In *PrometheusWiki*.

Sawaske SR, Freyberg DL (2014) Fog, fog drip, and streamflow in the Santa Cruz Mountains of the California Coast Range. Ecohydrology n/a–n/a. doi: 10.1002/eco.1537

Scholl, M., Eugster, W., Burkard, R., 2010. Understanding the role of fog in forest hydrology: stable isotopes as tools for determining input and partitioning of cloud water in montane forests. Hydrol. Process. 25, 353–366. doi:10.1002/hyp.7762

Simonin, K. a, Santiago, L.S., Dawson, T.E., 2009. Fog interception by Sequoia sempervirens (D. Don) crowns decouples physiology from soil water deficit. Plant. Cell Environ. 32, 882–92. doi:10.1111/j.1365-3040.2009.01967.x

Tyree, M.T., Hammel, H.T., 1972. The Measurement of the Turgor Pressure and the Water Relations of Plants by the Pressure-bomb Technique. J. Exp. Bot. 23, 267–282. doi:10.1093/jxb/23.1.267

Uehara, Y., Kume, A., 2012. Canopy Rainfall Interception and Fog Capture by Pinus pumila Regal at Mt. Tateyama in the Northern Japan Alps, Japan. Arctic, Antarct. Alp. Res. 44, 143–150. doi:10.1657/1938-4246-44.1.143

Vasey MC, Loik ME, Parker VT (2012) Influence of summer marine fog and low cloud stratus on water relations of evergreen woody shrubs (Arctostaphylos: Ericaceae) in the chaparral of central California. Oecologia 170:325–37. doi: 10.1007/s00442-012-2321-0

Walter, H.S., Taha, L.A., 1999. Regeneration of bishop pine (Pinus muricata) in the absence and presence of fire: a case study from Santa Cruz Island, California. Proc. fifth Calif. Islands Symp.

Weltzin, J.F., McPherson, G.R., 1997. Spatial and temporal soil moisture resource partitioning by trees and grasses in a temperate savanna, Arizona, USA. Oecologia 112, 156–164. doi:10.1007/s004420050295

Williams, A.P., Still, C.J., Fischer, D.T., Leavitt, S.W., 2008. The influence of summertime fog and overcast clouds on the growth of a coastal Californian pine: a tree-ring study. Oecologia 156, 601–11. doi:10.1007/s00442-008-1025-y

Yoder, B.J., Ryan, M.G., Waring, R.H., Schoettle, A.W., Kaufmann, M.R., 1994. Evidence of Reduced Photosynthetic Rates in Old Trees. For. Sci. 40, 513–527.

Yoder BJ, Ryan MG (1997) Limits to tree height hydraulic and tree growth. What keeps trees from growing beyond a certain height ? Bioscience 47:235–242.

Chapter VI. Impact of fog-drip versus fog immersion on the physiology of Bishop pine saplings

1. Introduction

Coastal fog is a common phenomenon during the dry season climate in a variety of Mediterranean ecosystems. In these areas, warm descending air over cool ocean surfaces traps a layer of cool, moist air at the surface. Moisture in this marine boundary layer condenses forming low-stratus clouds that are pushed inland by onshore winds and intercepted by land. The occurrence of coastal fog can offset dry season drought conditions in a number of ways: 1) shading by low stratus clouds can reduce potential evapotranspiration and suppress transpiration (Bruijnzeel & Veneklaas 1998, Williams et al. 2008, Berry & Smith 2012, Alvarado-Barrientos et al. 2013), 2) fog droplets drip to the ground increasing soil moisture (occult precipitation) (Azevedo & Morgan 1974, Harr 1982, Ingraham & Matthews 1995, Carbone et al. 2012) , and 3) foliar uptake of fog water can reduce leaf water deficit (Burgess & Dawson 2004, Simonin et al. 2009, Limm et al. 2009, Goldsmith et al. 2013) and contribute to whole-plant rehydration (Eller et al. 2013, Laur & Hacke, 2014). Coastal fog events have been shown to significantly dampen the effects of water stress for many plant species in a variety of coastal ecosystems (Corbin et al. 2005, del-Val et al. 2006, Ewing et al. 2009, Carbone et al. 2012, Vasey et al. 2012) as well as agroecosystems (Moratiel et al. 2013). While coastal fog may have a narrow spatial footprint, foggy areas support a disproportionate number of rare, endemic species as well as economically vital industries (e.g. agriculture). As drought conditions become more frequent in highly productive, yet water-limited, ecosystems, such as in coastal California,

understanding the mechanisms by which coastal fog ameliorates water stress is of increasing social, economic, and ecological importance.

The most obvious contribution of fog water to plants is through fog-drip to the soil; however, foliar uptake of fog water has received increased attention by researchers as a significant, yet largely overlooked, mechanism of plant water use. Studies have demonstrated that foliar water uptake occurs in a wide array of plant species in different ecosystems, ranging from coastal forests to high elevation deserts (Boucher et al. 1995, Burgess & Dawson, 2004, Breshears et al. 2008, Simonin et al. 2009, Limm et al. 2010, Goldsmith 2013, Eller et al. 2013). Our ability to distinguish the relative effects of fog-drip and fog immersion (that can result in foliar absorption of water) on water and carbon relations of plants is important for making accurate predictions of how potential changes in the fog regime may impact hydrologic and ecologic function of fog-influenced ecosystems in the future.

Water typically moves along a water potential gradient from the soil through a plant out to the atmosphere from high to low potential. Under certain conditions, however, this direction of flow is reversed. In order for leaves to absorb water from the atmosphere (rain and fog droplets), relative humidity must be high, leaf surfaces must be wet, and leaf water deficit must be high (Goldsmith et al. 2013, Laur & Hacke 2014). However, leaf cuticles are generally hydrophobic. Hydrophobicity is evolutionarily favored because it reduces water loss from leaves and prevents stomata from becoming clogged with liquid water, which would limit CO_2 uptake (Ishibashi & Terashima 1995); therefore, shedding water is important. Despite cuticle hydrophobicity, numerous studies have shown that liquid water can enter leaves. Munne-Bosch (1999) successfully tracked dew into mesophyll cells using

fluorescent stains and microscopy and suggested that trichomes facilitated foliar uptake. Burgess and Dawson (2004) illustrate that fungal hyphae can penetrate stomata and potentially facilitate water entry into the leaf tissue of coast redwoods. In a cloud forest in Mexico, Eller et al. (2013) demonstrate that 42 % of total foliar water content in pine trees was derived from diffusion of water through leaf cuticles and that cuticles were less hydrophobic than predicted. Moreover, reverse sapflow and elevated soil moisture were tightly correlated with foliar uptake events. In a recent study, Laur and Hacke (2014) provide evidence that once water is absorbed by conifer needles, aquaporins (water channel proteins) can facilitate radial water movement from leaves to the vascular tissue. These studies not only identify the importance of leaf anatomy, biochemistry, and symbiotic relationships in understanding foliar water uptake, but they also highlight this alternative path of plant water use that has significant implications for carbon and water balance of plants in fog-influenced ecosystems.

The objective of our study was to distinguish the effects of fog immersion (i.e., leaf-wetting events) versus fog-drip to the soil on the physiological function of a fog-dependent pine species, Bishop pine (*Pinus muricata* D.Don). Bishop pine is one of many rare and endemic plant species restricted to the fog belt of coastal California. Recent studies show that the water relations, growth rates, and survival during drought are all improved by persistent coastal fog that occurs during the dry season (summer, June-September) (Williams et al. 2008, Fischer et al. 2009, Carbone et al. 2012, Baguskas et al. *in review*). At the southern extent of the species range on Santa Cruz Island, CA, Carbone et al. (2012) report that cumulative summertime fog-drip can contribute as much as 30-40% to total annual precipitation, which is especially important during below average rainfall years

(<500 mm). Field observations support the hypothesis that increases in shallow soil moisture driven by fog-drip is the leading mechanism by which fog water becomes available to Bishop pines (Carbone et al. 2012, Baguskas et al. *in review*). To date, no study has tested whether foliar absorption of water occurs in this species and how important this mechanism of water use may be to the carbon balance of Bishop pines relative to fog-drip. In this study, we investigated mechanisms of Bishop pine fog water use and consequences on carbon assimilation and photochemical potential by addressing the following question: Is fog immersion important to maintaining the physiological function of Bishop pine saplings relative to trees that also receive fog-drip or no fog at all?

A widely accepted and commonly used approach to quantify plant stress in response to some environmental stressor, such as decline in soil moisture, is to measure the degree of chlorophyll fluorescence (Genty et al. 1989, Maxwell & Johnson 2000). Light energy absorbed by plants not used for photochemistry is either re-emitted as long-wave radiation from the leaf (chlorophyll fluorescence) or dissipated as heat. Unlike leaf gas-exchange rates, which are controlled by a variety of environmental factors, chlorophyll fluorescence is a metric of the performance of photochemical machinery. Quantum yield of CO_2 assimilation is positively related to the quantum efficiency of photosystem II (ΦPSII) (Genty et al. 1989, Epron et al. 1995, Valentini et al. 1995). Furthermore, many studies have demonstrated that quantum efficiency of photosystem II (ΦPSII) diminishes as water stress increases in a variety of ecosystems (Flexas et al. 1999, Mahall et al. 2009). Based on these established relationships, we expected chlorophyll fluorescence in Bishop pine saplings to increase with varying degrees of water stress as affected by our watering regimes. Specifically, we expected saplings in the fog-drip and immersion (FDI) group to have the

highest electron transport rates and highest ΦPSII values through the dry-down period compared to the group that only experienced fog immersion (FI). We hypothesized that control plants (C), which received no fog at all, would experience the greatest water stress, which would induce greater damage to photochemical machinery.

2. Methods

Experimental design

To test for the physiological mechanisms underlying fog water use by Bishop pine during the dry (yet foggy) season in southern California, we manipulated fog water inputs to potted Bishop pine saplings during a three week dry-down period (29 August – 14 September 2012). In 2010, two-year old saplings were purchased from a native plant nursery that sourced seeds from a mainland population about 30 miles north of Santa Barbara, CA. Saplings were transplanted to 20 L well-drained black plastic pots using a cactus soil mix (Uni-Gro Premium Cactus Mix). Since the cactus soil mix had no additional nutrients, we added diluted organic liquid kelp fertilizer (1 ml fertilizer: 250 water ml) to the soil to prevent nutrient deficiency. Saplings were 3-4 years old at the time of the experiment.

We artificially generated nine nighttime (2100 – 0600 hours local time) fog events over the three-week dry-down period. We constructed an enclosed 'fog chamber' with a PVC frame and plastic sheets (~1.2 x 1.5 x 1.2 m) within which fog events were generated using an ultrasonic device (model MHS10, Mainland Mart Corp., El Monte, CA), which produced fog droplets (droplet size ~10 microns in diameter). The timing and duration of our simulated late-season fog events corresponded to typical diurnal patterns of fog events in the area, which tend to occur at night and dissipate during early morning (Fischer et al.

2009, Carbone et al. 2012). To simulate the dry-down period, all potted plants were watered to field capacity at the beginning of the experiment, but not provided additional water (other than from the fog treatments) over the three-week period. Fifteen saplings were randomly assigned one of three treatments: 1) fog-drip and fog-immersion (FDI), 2) fog immersion alone (FI), and 3) no fog water inputs (control, C). In effect, the control (C) group provided a baseline for how Bishop pine saplings responded physiologically to soil dry-down. We should note that this experiment did not take place within a controlled greenhouse setting, thus all plants were exposed to ambient conditions during the day, which were mostly clear, sunny days, but sometimes overcast. In addition, C group plants were kept outside of the fog chamber at night while plants in the FI and FDI groups were fogged inside the chamber.

Fog treatment

In the FI treatment group, plant canopies were wet by fog droplets but fog-drip was excluded from the soil surface (details below). In the FDI treatment group, plant canopies experienced foliar wetting as well as fog-drip to the soil. We excluded drip to the soil from the canopy then manually added the same amount of 'fog-drip' to each FDI pot to control for differences in canopy architecture and harvesting efficiencies. The volume of 'fog-drip' added was the average fog-drip generated from all five FDI plant canopies after a simulated nighttime fog event (450 ml). In the field, average wetting depth ranges from 0.02 to 1.4 cm from fog-drip after a fog event. In the greenhouse, adding 450 ml of water resulted in a wetting depth of 0.8cm –mid-range of these field observations. 'Fog-drip' water was poured into a plastic container that had holes punctured in the bottom allowing water to drip into the soil. Containers were removed from the soil surface once empty (~10-15 minutes).

To exclude fog-drip from the soil surface of FI and FDI plants, we placed plastic "skirts" over the pots that extended from the base of the main trunk over the edge of the pot. These "skirts" were kept elevated ~ 8 cm above the rim of the pot to allow air flow and prevent condensation. In addition, "skirts" were sealed to the trunk with duct seal to prevent fog water entering the soil via stemflow. To control for any treatment effect of the plastic "skirts," such as reduced evaporative loss or increased soil temperature, "skirts" were also placed on C plants whenever they were placed on FI and FDI plants. Lastly, all plants that received fog treatments were placed in the fog chamber at the same time. To standardize the effect of fog exposure across fog treatment groups, we rotated the position of plants in the chamber between fog events.

Microclimate observations

To monitor changes in microclimate conditions, we installed temperature and relative humidity sensors (model VP-3, Decagon Devices, Inc., Pullman, WA) inside and outside the fog chamber. To determine the degree of leaf-wetting during fog events, we installed a leaf wetness sensor (model LWS, Decagon Devices, Inc., Pullman, WA) inside the fog chamber as well as outside, for comparison. LWS stay wet until humidity drops to sufficiently low levels to evaporate off the saturated layer. In the fog chamber, leaf wetness measurements after 0800 hr in the morning are irrelevant to our analyses because plants were removed from the fog chamber after fog events by 0730 hr. To detect changes in soil moisture across treatment and control groups, we installed volumetric soil moisture probes (model EC-5 Decagon Devices, Inc.) at 2 and 10 cm depth in each potted plant. In the field, soil water potential within the first 15 cm of the soil is positively affected by fog events

(Fischer et al. 2007, 2009), hence we monitored soil moisture at 2 and 10 cm depth to capture the effect of fog-drip on potential plant-available water. Soil probes were calibrated for the soil substrate used in the pots in this experiment. The probes are relatively insensitive to temperature variation in the soil, i.e., volumetric soil water content changes by 0.01 cm^3 cm^{-3} with a change in temperature of about 10 °C. Observations from all sensors were recorded every 15 minutes.

Leaf gas exchange measurements

We measured maximum leaf-level gas exchange rates using a portable photosynthesis system (model LI-COR 6400XT, LI-COR Bioscience, Lincoln, NE) from all plants on a total of eleven days of the dry-down period. Specifically, leaf gas-exchange rates measurements were collected from three randomly selected needles (~6 needles per sample) located on sunlit branches on each of the five plants per group. Measurements were collected on in the morning (between 0800-1130 hr.) following simulated fog events. The light condition in the leaf chamber was set to 1800 μmol m^{-2} s^{-1}, and CO_2 reference concentration was 400 ppm. Leaf temperature (T_{leaf}) and relative humidity (RH) inside the leaf chamber were allowed to vary naturally. On average, T_{leaf} was 25 ± 2.1 °C, and RH was 41 ± 3.14 %. Water-use efficiency for each treatment and control group was calculated as A_{max}/g_s (Field et al. 1983).

Chlorophyll fluorescence measurements

Concurrent with leaf gas exchange rates, we quantified the photochemical efficiency of photosystem II (ΦPSII) (defined as $\Delta F/F_m'$) and electron transport rates (ETR), i.e., the

overall photosynthetic capacity of PSII (Maxwell & Johnson, 2000), from three light-adapted leaves on each plant in the treatment and control groups using a portable fluorometer (MINI-PAM, Heinz Walz GmbH, Germany). Specifically, we extracted maximum rates of response variables ($\Phi PSII_{max}$ and ETR_{max}) from light-response curves on light-adapted leaves (see equation for curves in Table 1). Light levels (photosynthetic photon flux density, PPFD µmol photons m^{-2} s^{-1}) were established using the Light-Curve program with eight consecutive saturating light bursts ranging in intensity (200, 600, 1000, 1200, 1600, 2200, 3200, 4200 PPFD µmol photons m^{-2} s^{-1}). In addition to sampling light-adapted leaves, we quantified maximum chlorophyll fluorescence from dark-adapted leaves at the beginning of the experiment. For all measurements, we used a distance clip to maintain an exact distance between the leaf surface and fiber-optic cables.

Statistical analysis

Repeated measures analysis of variance was performed to test for within-subject (time since beginning of dry-down) and between-subject (treatment) effects on leaf gas-exchange rates for all plant groups. A Bonferroni *post-hoc* test was conducted to test for differences between treatment and control groups during the dry-down. We performed a Mauchly's test of sphericity to test for equal variances. Repeated measures and the post-hoc test were performed using SPSS (version 18.0, SAS Institute, Cary, NC) statistical software package. Pairwise comparisons were performed using a Student's t-test to assess differences between leaf-level responses between fog treatment and control groups at each sampling time point. Both of these analyses were performed using the JMP Pro (version 10.0.0, SAS Institute, Cary, NC, USA) statistical software package.

Non-linear regressions were used to test for correlation between fluorescence response variables (ETR and ΦPSII) and light (PPFD). Curve-fitting was performed using MATLAB (version R2014a, Mathworks, Natick, MA, USA). Coefficients of the light curve equations were generated for each plant on each day of the dry-down. Using the coefficient values, maximum ETR values (ETR_{max}) were extracted at 2000 µmol m^{-2} s^{-1} (the light level at which the curve began to plateau), and pairwise comparisons were performed to test for statistical differences between treatment and control groups.

Linear regressions were used to test for correlation between leaf physiological response variables and volumetric soil water content (VSWC, cm^3 cm^{-3}) within each fog treatment and control group. Statistical differences between regression lines were tested using JMP Pro (version 10.0.0, SAS Institute, Cary, NC, USA) statistical software package.

3. Results

Microclimate observations

All plants were kept outside of the fog chamber on each day of the experiment between 0700-2000 hr. Only FI and FDI plants experienced nighttime fog events between 2100-0600 h. Leaf wetness increased during simulated nighttime fog events inside the fog chamber (Fig. 4.1), indicating that sapling needles were wetted by these events. During fog events, average relative humidity (RH %) inside the fog chamber (mean ± SD) was 95 ± 0.03% and average ambient temperature ($T_{air,}$ C°) was 20.5 ± 2.15 C° (Fig. 4.1A). At night outside the fog chamber, average RH was 90 ± 0.03% and average T_{air} was 17.6 ± 1.1 C°. While T_{air} generally decreases during natural fog events, it appears that the chamber itself

had insulating effects, despite the fact that air was mixed with a fan and the water feeding the chamber was cool.

Outside of the fog chamber, average daily T_{air} was 21.5 ± 1.1 C° and RH was 75 ± 0.4% (Fig. 4.1A). Small rain events affected the study area in the evening of day 9 (0.5 mm) and day 10 (1.0 mm) of the dry-down (Sept. 6th and 7th, 2012, respectively) (data available on Santa Barbara county website: http://www.countyofsb.org/pwd/water/downloads/hydro/200dailys.pdf). All plants were left outside the fog chamber during the rain events. While these rain events were registered by the LWS (Fig. 4.1), indicating that sapling canopies got wet, the total amount of rainfall (1.5 mm) over both nights was minimal (recorded by a local meteorological station) and barely wet the soil surface of plotted saplings.

Effect of dry-down and simulated fog events on soil moisture

Average volumetric soil water content (VSWC, $cm^3\ cm^{-3}$) at 2 and 10 cm depth was significantly higher in the FDI group (2 cm: 0.34 ± 0.03; 10 cm, 0.32 ± 0.03) compared to FI (2 cm: 0.21 ± 0.05; 10 cm: 0.18 ± 0.05) and C (2 cm: 0.16 ± 0.05; 10 cm: 0.13 ± 0.06) groups through the dry-down period (Fig. 4.2). We compared VSWC between FI and C groups and found that the relative difference in VSWC (at both soil depths) was 15 % higher in FI than C saplings at the beginning of the experiment and 90 % higher by the end of the dry-down (Fig. 4.2). The relative difference in VSWC between FI and FDI was only 1.5 % higher in FDI than FI saplings at the beginning of the dry-down, but 150 and 200% higher at 2 and10 cm, respectively, in FDI by the end of the experiment (Fig. 4.2). During fog events, VSWC increased by 30% at 2 cm and by 10% at 10 cm in the FDI group while soil moisture

did not change in response to fog events in the FI group. There was no change in VSWC in the C group during fog events because these plants were kept outside the fog chamber.

Leaf gas-exchange

We observed a significant effect of both the drydown (time since water was withheld) ($P<0.0001$) and the interaction between treatment and time ($P=0.003$) on the maximum photosynthetic rates (A_{max}) of plants (Fig. 4.3a, Table 4.1A). Fog immersion alone had a positive effect on A_{max} of saplings relative to the C group; however, FDI saplings had much higher photosynthetic rates than FI or C saplings (Fig. 4.3a). At the beginning of the experiment (day 1), average A_{max} of the C group (4.50 ± 0.46 µmol m^{-2} s^{-1}) was not significantly different from the FI (4.02 ± 0.26 µmol m^{-2} s^{-1}) and FDI groups (5.01 ± 0.45 µmol m^{-2} s^{-1}) (C-FI, $P=0.16$ and C-FDI, $P=0.11$, respectively); however, the FI group was significantly lower than the FDI group ($P=0.004$). Differences in A_{max} among C and fog treatment groups did not occur until midway through the dry-down period. On day 8, average A_{max} of FI plants (3.39 ± 0.50 µmol m^{-2} s^{-1}) fell in-between the FDI (4.57 ± 0.35 µmol m^{-2} s^{-1}) and the C plants (2.33 ± 0.32 µmol m^{-2} s^{-1}). Differences among groups were statistically significant ($F_{(2, 13)} =23.5$, $p<0.001$). Separation of average A_{max} values among plant groups was maintained through the final day of the dry down, when we observed the greatest divergence (Fig. 4.3, FDI=4.37 ± 0.31, FI=2.37 ± 0.42, C=1.14 ± 0.22 µmol m^{-2} s^{-1}, $F_{(2,13)} =74.4$, $p<0.001$).

Maximum stomatal conductance (g_s, mol m^{-2} s^{-1}) showed similar variation between fog treatment and control groups through the dry-down period as compared to A_{max} (Fig. 4.3b). On day 1, g_s of FI plants was slightly lower than FDI plants (Fig. 3b, FDI= $0.10 \pm$

0.01, FI= 0.07 ± 0.01 mol m^{-2} s^{-1}, P=0.06), but neither fog treatment group differed significantly from the C group (0.09 ± 0.02 mol m^{-2} s^{-1}, P=0.13). FDI plants diverged significantly from C and FI plants on day 3 and maintained higher stomatal conductance rates for the duration of the dry-down (Fig. 4.3b).

Maximum electron transport rate (ETR_{max}, µmol photons m^{-2} s^{-1}) over the dry-down varied similarly to leaf gas exchange rates (Fig. 4.3c). ETR_{max} values were the same across plant groups during the first several days of the experiment; however, by day 8, ETR_{max} of the FDI group (157 ± 6 µmol photons m^{-2} s^{-1}) increased significantly compared to C plants (135 ± 14 µmol photons m^{-2} s^{-1}) and FI plants (144 ± 21 µmol photons m^{-2} s^{-1}). The range of ETR_{max} values in the FI group was 120-213 µmol photons m^{-2} s^{-1}, which generally fell within the bounds of FDI and C group values.

Water use efficiency (WUE) increased for all plants during the dry-down period (Fig. 4.4). WUE increased earlier during the dry-down period in the control group than either fog-treatment groups, suggesting closer regulation of water loss via stomatal closure in plants experiencing higher water stress. For the C group, WUE increased significantly by 27% between the beginning (avg. day 1 & 2) and middle (avg. day 8 & 9) of the dry-down, then stabilized thereafter. For FI and FDI plants, average WUE did not change between the beginning and middle of the dry-down, but then increased significantly by 40% and 18%, respectively, at the end of the dry-down (Fig. 4.4., $P<0.01$).

Chlorophyll fluorescence

Average maximum quantum efficiency of PS II (F_v/F_m) (from dark-adapted needles) was similar across fog treatment and control groups at the beginning of the dry-down

(C=0.81 ± 0.03, FI=0.80 ± 0.02, FDI=0.82 ± 0.04, $F_{(2,13)}$=0.65, P=0.52). The light-response curves illustrate that the effect of water availability had a greater impact on the electron transport rate (ETR) than quantum efficiency of PSII in light-adapted leaves (ΦPSII) across all treatment and control groups (Fig. 4.5 a-f and see Table 4.2A for fit of non-linear regression lines). In response to changes in PPFD, ETR, or overall photosynthetic capacity, was greatly diminished in the control group by the end of the dry-down period compared to plants in the fog treatment groups (Fig. 4.5a, b, and c). Between the beginning and the end of the dry-down, the ETR_{max} was 70 µmol photons m^{-2} s^{-1} lower in the control group compared to 40 and 10 µmol photons m^{-2} s^{-1} lower in the FI and FDI fog treatment groups, respectively. ΦPSII was less responsive to changes in PPFD across treatment and control groups and between the beginning and end of the dry-down (Fig. 4.5d, e, and f).

Relationship between soil moisture and leaf physiology

The relationship (β) between leaf response variables (A_{max}, g_s, and ETR_{max}) and changes in soil moisture were all positive and significant in the control group (Fig. 4.6, A_{max}: r^2=0.70; β= 14.0 ± 3.08, P=0.0014; g_s: r^2=0.83; β= 0.35, P<0.001; ETR_{max}: r^2=0.78; β= 408.9 ± 76.3, P=0.0007). For FI plants, the correlation between leaf-level physiology and soil moisture was also positive, yet weaker compared to the control group (Fig. 4.6, A_{max}: r^2=0.62; β= 7.13 ± 1.86, P=0.0041; g_s: r^2=0.73; β= 0.24, P=0.0009; ETR_{max}: r^2=0.55; β= 340.5 ± 108.2, P=0.0137), suggesting plants that experienced fog immersion may have relied less on soil moisture to support leaf function compared to plants that received no fog at all. The slopes of the regression lines fitted to the relationship between A_{max} and soil moisture were marginally significantly different between FI and C groups (Fig. 4.6, $F_{(1,8)}$

=3.5 p=0.08). Slopes between these two groups did not differ significantly with respect to other leaf responses and soil moisture. In the FDI group, leaf physiology was not significantly correlated to changes in soil moisture because variation in soil moisture was minimal (Fig. 4.6., A_{max}: r^2=0.005; β= -1.73 ± 7.82, P=0.83; g_s: r^2=0.28; β= -0.23, P=0.09; ETR_{max}: r^2=0.14; β= -329.6 ± 278, P=0.26).

Relationship between leaf-gas exchange rates and chlorophyll fluorescence

A_{max} was strongly correlated with g_s across treatment and control groups (Fig. 4.7a; FDI: r^2=0.51; β= 39.4 ± 12.7; FI: r^2=0.81; β= 29.2 ± 4.7; C: r^2=0.91; β= 41.3 ± 4.14). Conversely, A_{max} was weakly correlated with ETR_{max} (Fig. 4.7b. FDI: r^2=0.13; β= -0.01 ± 0.009; FI: r^2=0.039; β= 0.0042 ± 0.007; C: r^2=0.38; β= 0.019 ± 0.008). Only in the C group did the relationship between A_{max} and ETR_{max} differ significantly from zero (t-ratio=2.22, P=0.05). These relationships suggest that stomatal regulation of leaf gas-exchange rates is more important to leaf carbon-balance of Bishop pines over a short-term dry down than is the efficiency of the photochemical system.

4. Discussion

Our results show that fog-immersion alone provides sufficient moisture to Bishop pine saplings to maintain carbon assimilation rates even as soil moisture declines (Fig. 3). Relative to the control group, FI plants maintained higher carbon assimilation rates but had a weaker relationship between leaf gas-exchange rates and soil moisture (Fig. 6a & b). These results suggest that FI saplings had access to water sources other than soil moisture in order to support photosynthesis. It is probable that foliar absorption of fog water is a mechanism

by which saplings immersed in fog maintained higher gas exchange rates compared to saplings that received no fog at all. Yet, the primary mechanism by which this coastal forest tree species benefits from nighttime fog events is through fog-drip, which increases soil moisture (Fig. 2).

The results of our study corroborate with other studies that investigated foliar water uptake (Limm et al. 2009, Simonin et al. 2009, Eller et al. 2013, Laur & Hacke 2014). In particular, Simonin et al. (2009) provide convincing evidence from both field observations and a greenhouse study that foliar water uptake significantly improves the water and carbon relations of coast redwoods (*Sequoia sempervirens* D.Don). They found that leaf-wetting events from nighttime fog immersion alone maintained A_{max} values similar to fully irrigated plants (~ 4 μmol m^{-2} s^{-1}). Similarly, in our study, Bishop pines that were effectively irrigated by fog-drip also maintained A_{max} values between 4-5 μmol m^{-2} s^{-1}; however, saplings only immersed in fog exhibited lower A_{max} values (~ 3 μmol m^{-2} s^{-1}) than observed by Simonin et al. (2009). In addition, both our study and Simonin et al. show that saplings immersed in fog were less sensitive to changes in soil water content compared to plants that receive no fog at all (Fig. 6a).

Cloud immersion has been shown to suppress of transpiration rates and reduce demand for soil water in montane cloud forests in Mexico (Berry et al. 2012, Alvarado-Barrientos et al. 2014), southern Appalachian mountains in the United States (Berry et al. 2012), and even agricultural systems in China (Mortiel et al. 2013). It is possible that nighttime transpiration, which has been observed in Bishop pines in the field (unpublished data), was suppressed, which would result in greater efficiency of nighttime re-equilibration and reduce demand for

soil water (Limm et al. 2009). Another explanation for this pattern is that direct foliar absorption of fog water reduces the demand for soil water during the day.

Fog-drip was mainly responsible for higher rates of leaf gas-exchange rates and photosynthetic capacity of this species; however, foliar wetting from nighttime fog events augments water availability to Bishop pines, regardless of the specific mechanism. By increasing shallow soil moisture, fog water that drips beneath plant canopies effectively mitigates against soil water deficit during the dry season (Dawson 1998, Corbin et al. 2005, Scholl et al. 2010). In support of this primary mechanism of fog water use, we show that physiological performance of sapling trees that received both fog-drip and fog-immersion was significantly greater than saplings that only experienced fog immersion and drastically greater than the plants that did not receive fog at all (Fig. 3a and b, Fig. 4).

Effects of soil dry-down and fog treatments on carbon assimilation and photochemistry

By quantifying the degree of chlorophyll fluorescence together with instantaneous leaf gas-exchange rates, we were able to report on performance of the photochemical system in relationship to overall carbon assimilation rates. We found that A_{max} was strongly correlated with stomatal conductance (g_s) while weakly correlated with ETR (Fig. 7a and b). The relationship between A_{max} and g_s is consistent with results from numerous plant physiological studies that show photosynthesis is limited by diffusion of CO_2 into the leaf when stomata are closed (Wong et al. 1979, Farquhar and Sharkey 1982, Ball et al. 1987, Collatz et al. 1991). The potential mechanistic linkages between carbon assimilation and ETR are better elucidated by results from the light-response curves.

The decline of ETR in the control group between the beginning and end of the dry-down was greater than in either fog-treatment group (Fig. 4.3 a-c), which supports our hypothesis that availability of fog water alleviates leaf-level water stress and improves photosynthetic capacity of plants. While ETR appears to be a good indicator of relative plant stress between Bishop pines under different water regimes, this was not the case for quantum yield of PSII photochemistry (ΦPSII) (Fig. 4.3 d-f). Overall, soil water depletion and fog water inputs did not affect the ΦPSII in Bishop pine saplings as much as the overall photosynthetic capacity (ETR) of saplings *in vivo*. The insensitivity of ΦPSII to effects of water-stress indicates that damage of PSII was not induced by dehydration, and it further suggests that Bishop pine saplings are effective at dissipating excess energy that protects the PSII reaction center (Epron et al. 1992).

All plants increased in their water-use efficiency (WUE) between the beginning and end of the dry-down period (Fig. 4.4). Higher WUE occurred earlier for control plants than plants in either fog treatment group. Between fog treatment groups, the increase in WUE was significantly greater in the FI group compared to the FDI group which supports the idea that fog immersion is only secondary to fog-drip in offsetting water stress of Bishop pines.

Fog effects on soil water supply vs. demand

An interesting pattern emerged in the immersion-only group that elucidates potential mechanistic interactions between foliar absorption and soil moisture dynamics. From day 3 through the end of the dry-down period, we found that soil moisture in the immersion-only group was consistently greater at both 2 and 10 cm depth, compared to the control group (Fig. 2). This observation, in conjunction with the weaker correlation between A_{max} and soil

moisture for immersion-only plants (Fig. 4.6), suggests that soil water uptake was reduced in plants only immersed in fog compared to plants in the control group. Possible mechanisms that may explain why FI plants had higher soil moisture than control plants include: 1) reduced nighttime transpiration during fog events, or 2) foliar absorption of fog water. Because relative humidity was similar inside (95%) and outside (90%) the fog chamber during fog events (Fig. 4.1A), it is unlikely that there were large differences in evapotranspiration rates between FI and C plant groups. The more probable mechanism is that daily leaf water deficit was sufficiently quenched by foliar absorption of water, which reduced plant demand for soil moisture. This explanation is consistent with other studies that demonstrate reduced demand for soil water in plants that exhibited signs of foliar absorption (Dawson 1998).

5. Conclusion

By distinguishing the effects of fog-drip and fog-immersion on plant physiology, this study contributes to our mechanistic understanding of how coastal fog influences plant ecophysiology. In particular, our study contributes to a growing list of species for which foliar uptake has been shown to be a viable mechanism of plant water use. We demonstrate that fog immersion alone significantly buffers sapling trees from experiencing the negative effects of soil water deficit on leaf gas-exchange rates. While leaf-wetting from fog immersion during soil dry-down augments plant water relations, the effect is secondary to the influence of direct fog-drip to the soil. We also show fog-immersion alone can reduce plant demand for soil moisture, which has implications for the water balance in fog-influenced forests. For example, increased soil moisture during the seasonal dry season

could change competitive interactions between species and have indirect effects on plant species composition in a warmer, drier future.

Future changes in the fog regime of coastal California (and other foggy places) could have detrimental effects on the persistence of many species that distinguish the area as a hotspot of biodiversity. Interdisciplinary research efforts are underway to improve our predictive power of how increases or decreases in the frequency and extent of coastal fog will impact the ecohydrology of natural and managed ecosystems (Williams et al. *in press*). A recent study that examined sources of variability in coastal cloud frequency from southern California to the Alaskan Islands shows promise of generating more accurate predictions of fog climatologies in the future (Schwartz et al. 2014). Identifying local and regional scale fluctuations of fogginess (e.g., the elevation at which the marine layer intercepts land, the duration of fog events, and the liquid water content in low-stratus clouds) is critical for assessing the vulnerability of many species to drought stress that are already restricted to the fog belt of California, such as Bishop pine. At the southern extent of the species range, Bishop pine populations are highly susceptible to drought-induced mortality (Baguskas et al. 2014) and rely on coastal fog to persist through the dry season; therefore, the outcome of our study is important for making mechanistically-based predictions of the distribution of Bishop pine in the future.

The findings from the present study are important for informing how changes in the fog regime may impact plant performance, and potentially survival, in fog-influenced ecosystems. We demonstrate that fog-drip plays a critical role in the ability for the dominant tree species in a coastal forest ecosystem to photosynthesize during a period of time when they are most vulnerable to drought stress. Furthermore, our findings contribute to a growing

body of literature that supports the hypothesis that foliar absorption of fog is possible, and that it positively affects the carbon and water relations of fog-dependent plant species. We advocate future research to investigate the answers to unresolved questions as to how the influence of fog events on plant physiology in the short-term (hours to days) may impact plant productivity and hydrologic cycling on longer timescales (months to years).

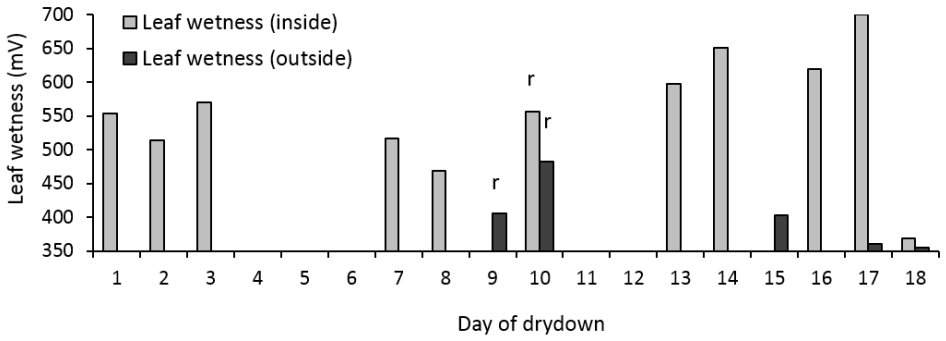

Figure 4.1. Average daily leaf wetness observations inside and outside the fog chamber. Height of bars is proportional to the wetness of leaves. Natural rain events ('r') occurred in the evening of the 9th (0.5 mm) and 10th (1.0 mm) day of the dry-down. Rain events affected the Santa Barbara area.

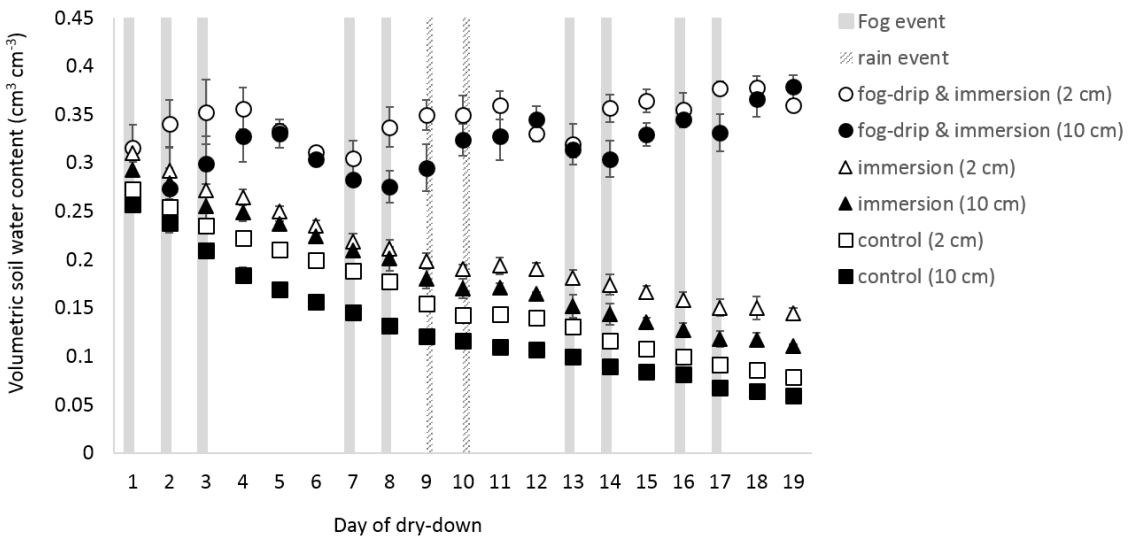

Figure 4.2. Average volumetric soil water content at 2 and 10 cm depth (n=5 and 3, respectively) for each treatment group during the dry-down period (circles, fog-drip & immersion; triangles, fog immersion; squares, control)**.** Grey bars represent simulated nighttime fog events. Average soil moisture among treatment groups and control were significantly different from each other at each time point based on pairwise comparisons ($p<0.001$). Within each group, soil moisture at 2 and 10 cm was significantly different from day 1 through the dry-down period ($p<0.001$). Error bars represent standard error of the mean.

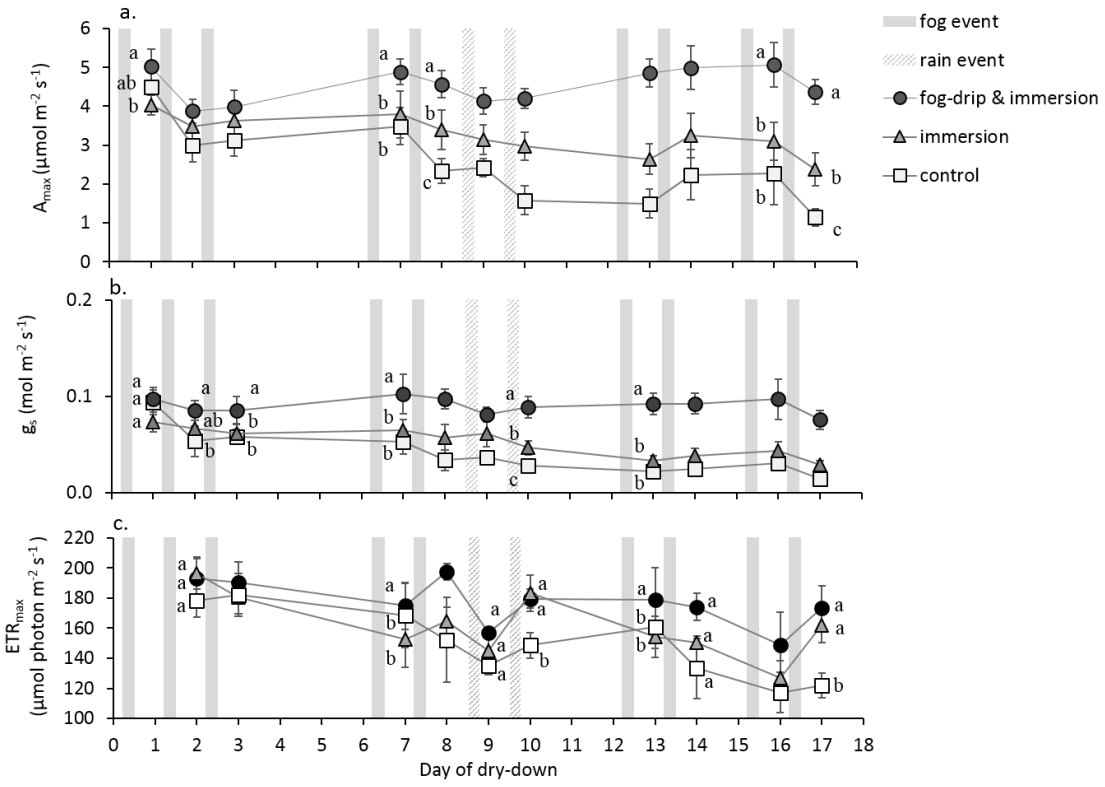

Figure 4.3. (a) Maximum photosynthetic rate (A_{max}), (b) stomatal conductance (g_s), and (c) maximum electron transport rate (ETR_{max}) of sapling Bishop pines in fog treatment and control groups during the dry-down period. Each point represents the average response value for all plants within each group (n=5). Error bars represent standard error of the mean. Different letters within the plot indicate significant differences among groups on a given day of the experiment based on pairwise comparisons (α =0.05), and is only indicated when there is a change in significance among groups.

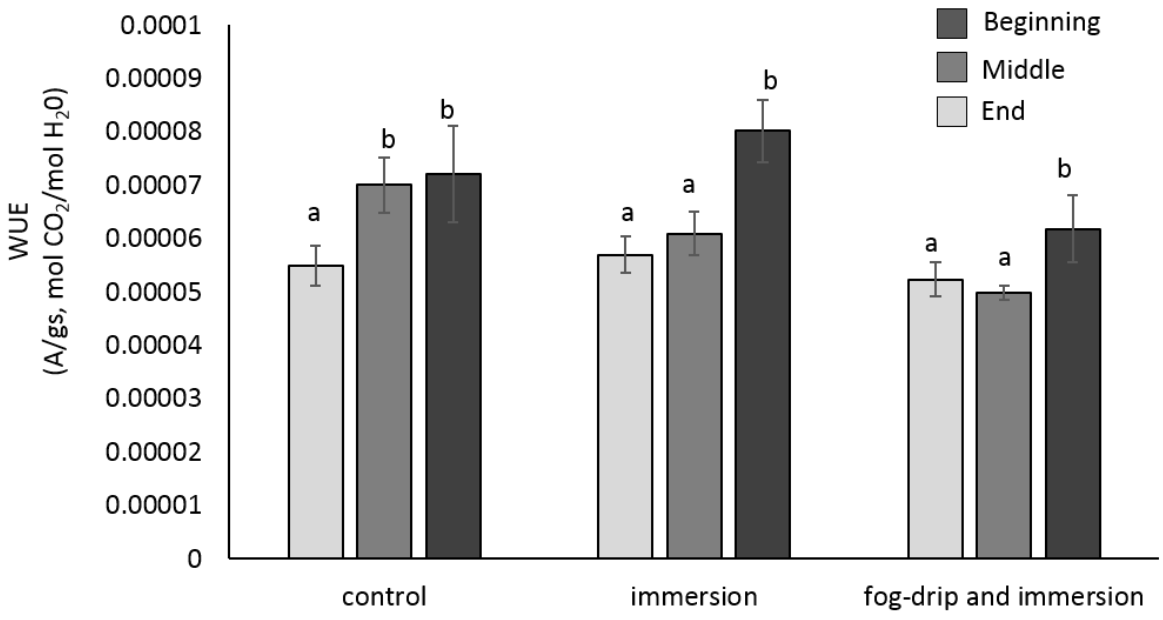

Figure 4.4. Average water use efficiency (calculated as maximum photosynthesis rate (A_{max}) divided by stomatal conductance (g_s) of sapling Bishop pines at the beginning (day 1 & 2), middle (day 8 & 9), end (day 16 & 17) of the dry down. The average of all five plants per treatment and control groups were taken over two days. Error bars represent standard error of the mean. Within groups, different letters indicate significant differences between the beginning, middle, and end of the experiment based on pairwise comparisons (α =0.05).

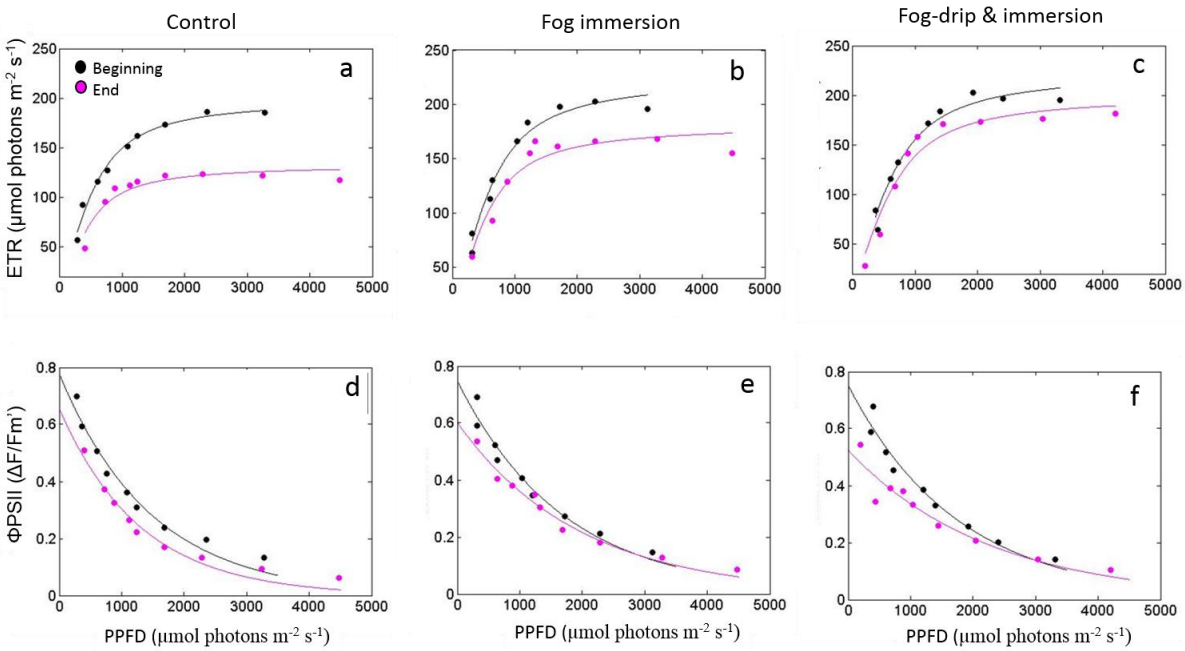

Figure 4.5. Average electron transport rate (ETR, µmol photons m^{-2} s^{-1}) (upper) and the quantum efficiency of PSII photochemistry (ΦPSII) defined as $\Delta F/F_m'$ (lower) in response to changes in photosynthetic photon flux density (PPFD, µmol photons m^{-2} s^{-1}) between the beginning (day 1) and end (day 17) of the dry-down across treatment and control groups. Light-response curves were performed on three light-adapted leaves per plant, and there were 5 plants per treatment or control group. Error bars represent standard error. See Table 4.2A for model fit parameters (equations, coefficients, and model fit results).

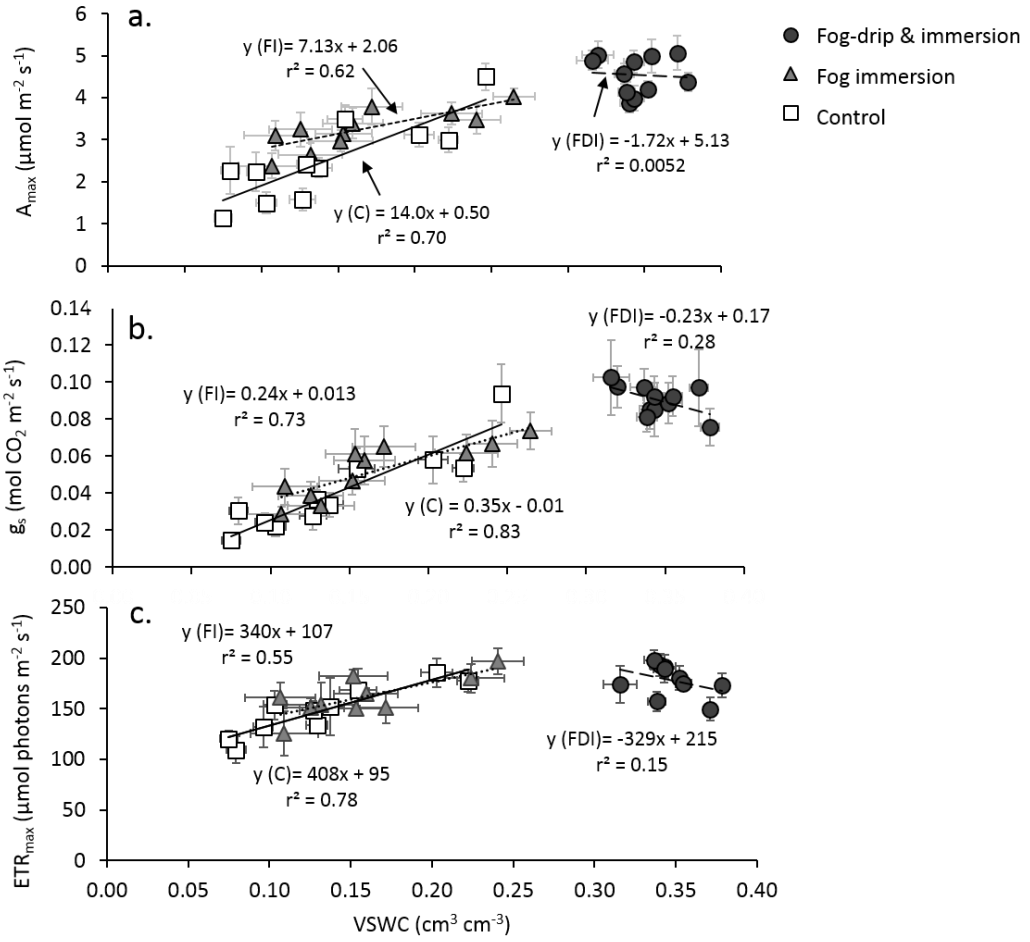

Figure 4.6. Correlation between average volumetric soil water content (VSWC) at 2 & 10 cm depths and (a) maximum photosynthetic rate (A_{max}), (b) stomatal conductance (g_s), and (c) electron transport rate (ETR) of sapling Bishop pines in fog treatment and control groups during the dry down period. Each point represents the average value of A_{max} for all plants within each group (n=5) on each day of measurement (total =11 days). Soil depths were pooled when calculating average VSWC. Error bars represent standard error. A linear regression relationship was fitted to non-pooled depth data.

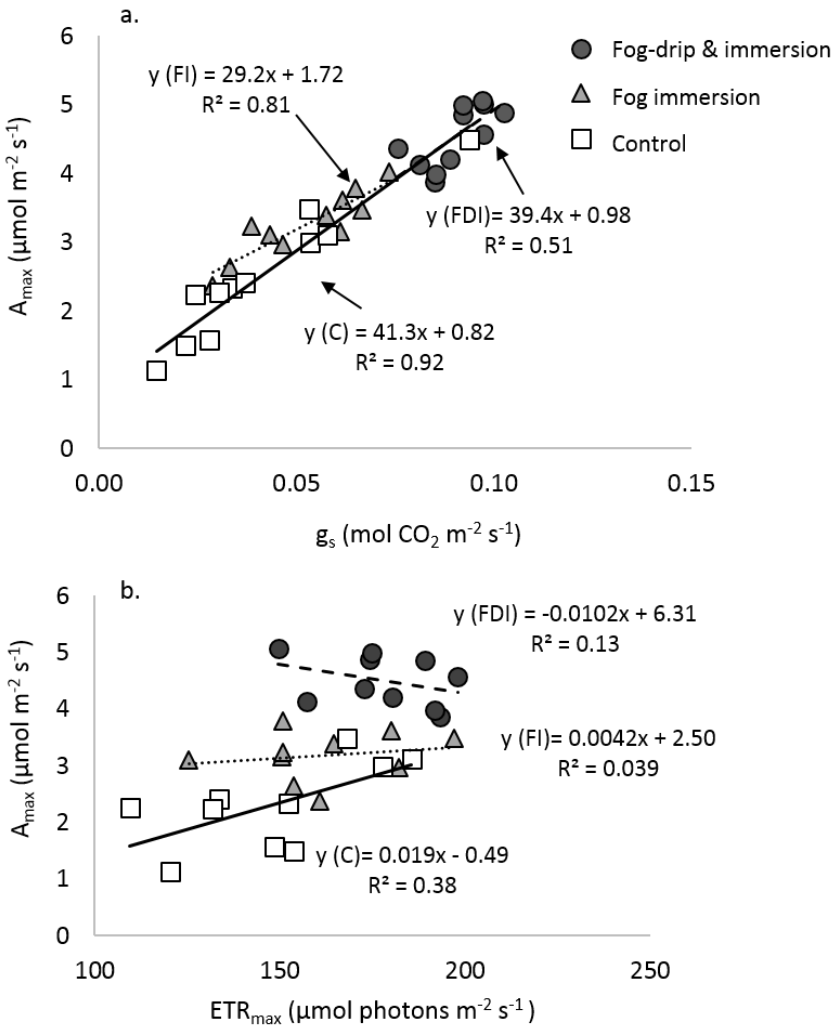

Figure 4.7. Relationship between maximum photosynthesis (A_{max}) and a) stomatal conductance (g_s) rate and b) maximum electron transport rates (ETR_{max}) for Bishop pine saplings in fog treatment (FDI and FI) and control (no water) groups.

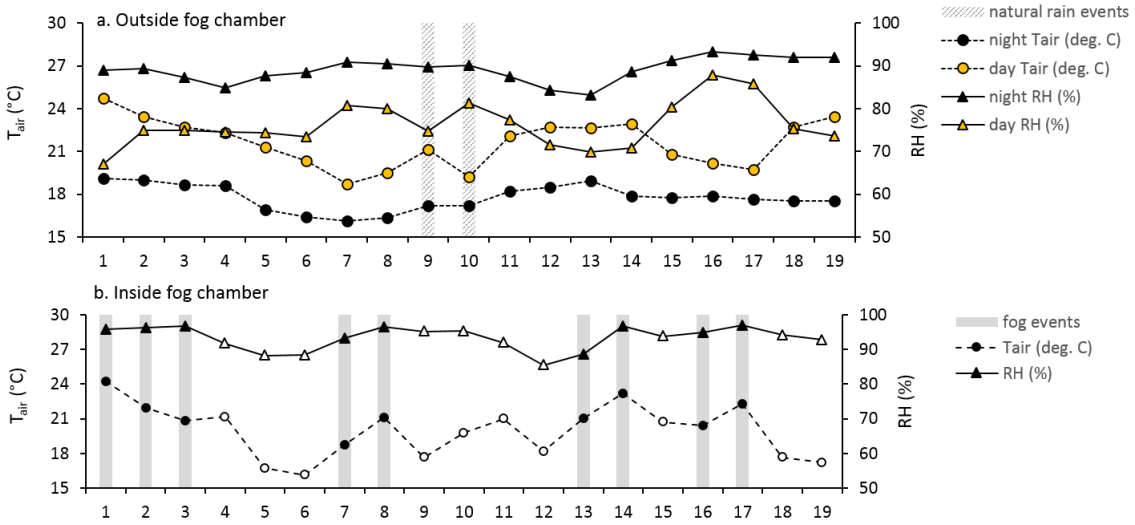

Figure 4.1A. a) Average daytime and nighttime ambient temperature (T_{air}, C°) (range: 19.7-22.6 C°) and relative humidity (RH, %) ((range: 70-82%) outside the fog chamber; b) Average nighttime T_{air} and RH (range: 87-97%) inside the fog chamber. FI and FDI plants were only in the fog chamber at night during fog events and were otherwise kept outside with the C plants; therefore, open symbols indicate points in time irrelevant to plant physiology.

Table 4.1A. Repeated measures analysis for the effects of the dry-down (time, within-subject variation) and treatment (between-subject variation) through time on maximum photosynthetic rates (Amax) of Bishop pine saplings.

Source	Response variable	F-value	df (numerator)	df (denominator)	P-value
Time	Amax	5.88	1	11	<0.0001
Treatment * Time	Amax	2.30	2	11	0.003

Mauchly's test of Sphericity was not significant (P=0.24), thus assumption of sphericity was not violated.

Table 4.2A. Fit of non-linear regressions to light-response curve data (see Fig. 5 a-f) including 95% confidence intervals (n=5). Model fit adopted from Thronley (2002) to fit a non-linear regression to the relationship between ETR and PPFD as seen in Fig. 5 a-c (y = (a*x + b - sqrt((a*x + b)^2 - 4*a*b*0.75*x))/2*0.75). A negative exponential equation was used to fit a non-linear regression to the relationship between ΦPSII and PPFD as seen in Fig. 4.5d-f (y=a*exp(b*x)).

		ETR vs. PPFD			ΦPSII vs. PPFD		
Group	Day of dry-down	a	b	r2	a	b	r2
Control	Beginning	0.46 (0.40, 0.51)	357.1 (336.7, 377.5)	0.98	0.73 (0.68, 0.79)	-0.00062 (-0.00071, -0.00053)	0.88
	End	0.35 (0.24, 0.46)	237.4 (212.9, 261.9)	0.87	0.63 (0.59, 0.68)	-0.00078 (-0.00087, -0.00069)	0.93
FI	Beginning	0.47 (0.40, 0.53)	402.8 (371, 434.6)	0.97	0.73 (0.69, 0.78)	-0.00057 (-0.00064, -0.0005)	0.91
	End	0.41 (0.29, 0.53)	324.2 (288.6, 359.8)	0.91	0.58 (0.52, 0.64)	-0.00049 (-0.0006, -0.0004)	0.82
FDI	Beginning	0.43 (0.35, 0.51)	400.7 (363.9, 437.5)	0.96	0.73 (0.69, 0.78)	-0.00057 (-0.00064, -0.0005)	0.91
	End	0.38 (0.29, 0.48)	359.2 (314.8, 403.5)	0.94	0.58 (0.52, 0.64)	-0.00049 (-0.00059, -0.0004)	0.82

References

Alvarado-Barrientos, M.S., Holwerda, F., Asbjornsen, H., Dawson, T.E., Bruijnzeel, L. A., 2014. Suppression of transpiration due to cloud immersion in a seasonally dry Mexican weeping pine plantation. Agric. For. Meteorol. 186, 12–25. doi:10.1016/j.agrformet.2013.11.002

Azevedo J., Morgan D.L.. 1974. Fog Precipitation in Coastal California Forests. *Ecology* 55: 1135–1141.

Baguskas, S.A., Peterson, S.H., Bookhagen, B., Still, C.J., 2014. Evaluating spatial patterns of drought-induced tree mortality in a coastal California pine forest. For. Ecol. Manage. 315, 43–53.

Berry, Z.C., Smith, W.K., 2012. Cloud pattern and water relations in Picea rubens and Abies fraseri, southern Appalachian Mountains, USA. Agric. For. Meteorol. 162-163, 27–34. doi:10.1016/j.agrformet.2012.04.005

Breshears, D.D., McDowell, N.G., Goddard, K.L., Dayem, K.E., Martens, S.N., Meyer, C.W., Brown, K.M., 2008. Foliar absorption of intercepted rainfall improves woody plant water status most during drought. Ecology 89, 41–47.

Burgess, S.S.O., Dawson, T.E., 2004. The contribution of fog to the water relations of Sequoia sempervirens (D. Don): foliar uptake and prevention of dehydration. Plant, Cell Environ. 27, 1023–1034. doi:10.1111/j.1365-3040.2004.01207.x

Carbone, M.S., Williams, A.P., Ambrose, A.R., Boot, C.M., Bradley, E.S., Dawson, T.E., Schaeffer, S.M., Schimel, J.P., Still, C.J., 2012. Cloud shading and fog drip influence the metabolism of a coastal pine ecosystem. Glob. Chang. Biol. 19, 484–97. doi:10.1111/gcb.12054

Corbin, J.D., Thomsen, M. A, Dawson, T.E., D'Antonio, C.M., 2005. Summer water use by California coastal prairie grasses: fog, drought, and community composition. Oecologia 145, 511–21. doi:10.1007/s00442-005-0152-y

Dawson, T.E., 1998. Fog in the California redwood forest: ecosystem inputs and use by plants. Oecologia 117, 476–485. doi:10.1007/s004420050683

del-Val, E., Armesto, J.J., Barbosa, O., Christie, D. a., Gutiérrez, A.G., Jones, C.G., Marquet, P. a., Weathers, K.C., 2006. Rain Forest Islands in the Chilean Semiarid Region: Fog-dependency, Ecosystem Persistence and Tree Regeneration. Ecosystems 9, 598–608. doi:10.1007/s10021-006-0065-6

Eller, C.B., Lima, A.L., Oliveira, R.S., 2013. Foliar uptake of fog water and transport belowground alleviates drought effects in the cloud forest tree species, Drimys brasiliensis (Winteraceae). New Phytol. 199, 151–62. doi:10.1111/nph.12248

Epron, D., Dreyer, E., Breda, N., 1992. Photosynthesis of oak trees [Quercus petraea (Matt .) Liebl .] during drought under field conditions : diurnal course of net CO2 assimilation and photochemical efficiency of photosystem II. Plant, Cell Environ. 15, 809–820.

Ewing, H. a., Weathers, K.C., Templer, P.H., Dawson, T.E., Firestone, M.K., Elliott, A.M., Boukili, V.K.S., 2009. Fog Water and Ecosystem Function: Heterogeneity in a California Redwood Forest. Ecosystems 12, 417–433. doi:10.1007/s10021-009-9232-x

Fischer, D.T., Still, C.J., 2007. Evaluating patterns of fog water deposition and isotopic composition on the California Channel Islands. Water Resour. Res. 43, n/a–n/a. doi:10.1029/2006WR005124

Fischer, D.T., Still, C.J., Williams, A.P., 2009. Significance of summer fog and overcast for drought stress and ecological functioning of coastal California endemic plant species. J. Biogeogr. 36, 783–799. doi:10.1111/j.1365-2699.2008.02025.x

Flexas, J., Escalona, J.M., Medrano, H., 1999. Water stress induces different levels of photosynthesis and electron transport rate regulation in grapevines. Plant, Cell Environ. 22, 39–48. doi:10.1046/j.1365-3040.1999.00371.x

Genty, B., Briantais, J.-M., Baker, N.R., 1989. The relationship between the quantum yield of photosynthetic electron transport and quenching of chlorophyll fluorescence. Biochim. Biophys. Acta - Gen. Subj. 990, 87–92. doi:10.1016/S0304-4165(89)80016-9

Harr, D.R., 1982. Fog drip in the bull run municipal watershed, Oregon. Water Resour. Bull. 18.

Ingraham, N.L., Matthews, R. A., 1995. The importance of fog-drip water to vegetation: Point Reyes Peninsula, California. J. Hydrol. 164, 269–285. doi:10.1016/0022-1694(94)02538-M

Ishibashi, M., Terashima, I., 1995. Effects of continuous leaf wetness on photosynthesis: adverse aspects of rainfall. Plant, Cell Environ. 18, 431–438. doi:10.1111/j.1365-3040.1995.tb00377.x

Laur, J., Hacke, U.G., 2014. Exploring Picea glauca aquaporins in the context of needle water uptake and xylem refilling. New Phytol. 203, 388–400. doi:10.1111/nph.12806

Limm, E.B., Dawson, T.E., 2010. Polystichum munitum (Dryopteridaceae) varies geographically in its capacity to absorb fog water by foliar uptake within the redwood forest ecosystem. Am. J. Bot. 97, 1121–1128. doi:10.3732/ajb.1000081

Limm, E.B., Simonin, K. a, Bothman, A.G., Dawson, T.E., 2009. Foliar water uptake: a common water acquisition strategy for plants of the redwood forest. Oecologia 161, 449–59. doi:10.1007/s00442-009-1400-3

Mahall, B.E., Tyler, C.M., Cole, S.E., Mata, C., 2009. A comparative study of oak (Quercus, FAGACEAE) seedling physiology during summer drought in southern California. Am. J. Bot. 96, 751–761. doi:10.3732/ajb.0800247

Maxwell, K., Johnson, G.N., 2000. Chlorophyll fluorescence--a practical guide. J. Exp. Bot. 51, 659–68.

Moratiel, R., Spano, D., Nicolosi, P., Snyder, R.L., 2013. Correcting soil water balance calculations for dew, fog, and light rainfall. Irrig. Sci. 31, 423–429. doi:10.1007/s00271-011-0320-2

Munne-Bosch, S., Nogue, S., Alegre, L., 1999. Diurnal variations of photosynthesis and dew absorption by leaves in two evergreen shrubs growing in Mediterranean field conditions. New Phytol. 144, 109–119.

Scholl, M., Eugster, W., Burkard, R., 2010. Understanding the role of fog in forest hydrology: stable isotopes as tools for determining input and partitioning of cloud water in montane forests. Hydrol. Process. 25, 353–366. doi:10.1002/hyp.7762

Schwartz, R., Gershunov, A., Iacobellis, S.F., Cayan, D.R., 2014. North American west coast summer low cloudiness: Broadscale variability associated with sea surface temperature. Geophys. Res. Lett. 41, 1–8. doi:10.1002/2014GL059825.Received

Simonin, K. A, Santiago, L.S., Dawson, T.E., 2009. Fog interception by Sequoia sempervirens (D. Don) crowns decouples physiology from soil water deficit. Plant. Cell Environ. 32, 882–92. doi:10.1111/j.1365-3040.2009.01967.x

Valentini, R., Epron, D., Angelis, P.D.E., Matteucci, G., Dreyer, E., 1995. In s / fci estimation of net CO2 assimilation , photosynthetic electron flow and photorespiration in Turkey oak (Q

. cerris L .) leaves : diurnal cycles under different levels of water supply. Plant, Cell Environ. 18, 631–640.
Vasey, M.C., Loik, M.E., Parker, V.T., 2012. Influence of summer marine fog and low cloud stratus on water relations of evergreen woody shrubs (Arctostaphylos: Ericaceae) in the chaparral of central California. Oecologia 170, 325–37. doi:10.1007/s00442-012-2321-0
Williams, A.P., Still, C.J., Fischer, D.T., Leavitt, S.W., 2008. The influence of summertime fog and overcast clouds on the growth of a coastal Californian pine: a tree-ring study. Oecologia 156, 601–11. doi:10.1007/s00442-008-1025-y

Chapter V. Conclusions

5.1. Summary

The primary goal of this research was to elucidate how and why coastal fog is important to the distribution and ecophysiology of a coastal forest in a Mediterranean climate. While this work focused on the water relations and mortality risk of Bishop pine trees that grow on Santa Cruz Island (SCI), the lessons learned extend beyond the scope of this study to other fog-influenced coastal ecosystems.

Overall, at a broader spatial (1-10 km) and temporal scale (months to years), I have demonstrated that the frequency of coastal fog is a significant environmental control on the local distribution of Bishop pines on SCI because it buffers the effects of drought stress. At the scale of individual trees, my results supports the hypothesis that sapling Bishop pines are more vulnerable to experiencing water stress during the dry season compared to adult trees;

however, the water status of saplings is also more strongly affected by fog water inputs provided by fog-drip to the soil. Implicit from these findings is that fog water inputs are important for survival of Bishop pines at early life stages. Meanwhile, my controlled experiments provide evidence that increasing soil moisture through fog-drip is not the only way Bishop pines use fog water, but foliar uptake is also possible. This is important when considering that sapling trees have smaller canopies and are more limited in 'harvesting' fog water. This research generates many new questions that are important for increasing our understanding of the importance of fog to population dynamics: 1) To what extent do fog water inputs affect seedling germination and recruitment? and 2) How important is the contribution of fog versus rain in advancing Bishop pines though the population bottleneck?

5.2. Main Conclusions

I used remote sensing techniques to explore the spatial pattern and underlying drivers of drought-induced tree mortality in the largest and westernmost Bishop pine forest on SCI. Following a two-year drought period, tree mortality was found to be highest in the drier, more inland margins of the forest stand. This area of highest mortality is also where modeled soil water deficit was greatest based on previous research (Fischer et al. 2009). The spatial pattern of dead trees was best explained by the frequency of summertime clouds, elevation, and tree height. Specifically, mortality was lowest for larger trees (~8-10 m tall) in more foggy parts of the stand located at moderate elevations. Based on a Random Forest analysis that evaluated the hierarchical relationships between environmental predictor variables, the probability of mortality was also found to be highest at the inland extent of the

stand where trees occur at the upper limit of their elevation range (~400 m). The coexistence of these main factors with other landscape variables helps identify areas of suitable habitat for Bishop pines across the stand and extends our understanding of what limits the local distribution of the species. This part of my dissertation was published in 2014 in the journal, *Forest Ecology & Management*.

Next, I investigated the influence of coastal fog events on the water relations of adult and sapling Bishop pines at two sites that differed in their moisture regime on SCI. The results of this study showed that sapling trees are more vulnerable to water stress during the dry season than adult trees, likely attributed to differences in rooting distribution and access to deep soil water resources. Furthermore, the water status of sapling trees was more strongly affected by changes in shallow soil moisture driven by fog-drip. By assessing the physiological response of multiple life stages of Bishop pine to the dual effects of seasonal dry-down and intermittent fog events, this study can contribute to mechanistically based predictions of how the distribution of Bishop pines, and other coastal tree species, may be affected by changes in available moisture in the future. This work has been submitted for publication to the journal, *Oecologia*, in early September 2014.

My greenhouse study examined in greater detail the mechanisms by which fog water affects the leaf-level physiology of Bishop pines. This study demonstrated that the combined effect of fog-drip and fog-immersion effectively maintained carbon assimilation rates through a dry-down period. As soil moisture declined, fog immersion alone maintained higher carbon assimilation rates and photosystem function than in saplings that received no fog at all. The results of this study support the idea that foliar absorption of fog water is a viable mechanism of fog water use by Bishop pines, and that such water absorption can

moderate the effects of seasonal dry-downs even if the amount of absorbed water is small. The outcome of this study elucidates the specific mechanisms of how coastal fog events can impact the carbon and water balance of fog-influenced ecosystems. This work will be submitted for publication in the journal, *New Phytologist*, in October 2014.

5.3. Recommendations for Future Work

Several technical issues that would refine the research presented herein have been identified and are discussed below to aid in future work.

In the remote sensing of tree mortality study (Chapter 2), automating the process of identifying dead tree canopies would allow a user to easily and efficiently update the coverage of Bishop pine mortality, as was observed following the extreme drought in 2014. The 2014 drought was more severe than the 2007-2009 drought and appears to have induced Bishop pine mortality in areas that were hypothesized to be buffered from drought stress, including cooler, foggier portions of the westernmost Bishop pine stand (Chapter 2, Fig. 5). Hence, updating the map of Bishop pine mortality for the 2014 drought event has important implications for predicting the effects of intense drought on population dynamics. This could be achieved by repeating the classification techniques described in Chapter 2, using a post-drought image from a 2014 aerial photograph at 1m spatial resolution. However, it would be more time efficient to identify dead tree canopies through a change in greenness between pre and post-drought imagery. The VARI vegetation index is sensitive to plant water stress and can be calculated using color DOQQs, so would be ideal for identifying trees that died.

Validating the map of tree mortality generated in Chapter 2 could have been improved if field-based validation points had been collected closer to the time that the image

of red tree canopies was acquired. For researchers interested in quantifying the spatial extent of drought-induced tree mortality, I recommend performing the following four steps: 1) collect sub-meter accuracy GPS points of dead and live trees in the field as soon as signs of mortality become apparent; 2) associate with those points observations of the condition of the tree, e.g., % red foliage in the canopy, evidence of bark beetle infestation, and size parameters; 3) establish photo points from multiple perspectives to document the process of plant degradation following drought; 4) monitor in the field any other plant species that may exhibit similar signs of mortality, i.e., are drought-tolerant species also experiencing mortality?; 5) contract remote sensing of the study area to overall temporally with field work.

The physical processes that result in coastal fog are complex, and fog events themselves are inherently ephemeral in space and time, making generation of fog climatologies challenging over multiple spatial and temporal scales. However, using remote sensing techniques in conjunction with conducting field-based research on the ecohydrologic impacts of coastal fog are both necessary steps to modeling current and future dynamics of the fog regime (Rastogi et al. 2013). Generating finer resolution fog maps that account for the intersection between the low-stratus clouds and topography has immense ecological significance because it will determine where on the landscape there may be direct water inputs via fog-drip versus just shading effects, or no effect at all. Applying a finer spatio-temporal map of coastal fog frequency that accounts for topographic variation would greatly improve the ability to assess the influence of coastal fog on water deficit risk in general.

In the field-based study (Chapter 3), coupling measurements of plant water status to leaf level gas exchange rates would have greatly improved the analysis of the physiological response of Bishop pines to changes in seasonal moisture availability (e.g., drying soil versus fog-water inputs). The technical challenge in doing this, however, is that wet leaves cannot be sampled for leaf gas-exchange rates. Leaves were wet from fog water deposition through the hours of the day when it would have been optimal to measure photosynthetic rates (0800-1100 hr). While some argue that leaves could be dried off before sampling, the risk of contaminating the instrument (model LiCOR 6400 XT, LiCOR Inc., Lincoln, NE) with water would be high and the measurements potentially not useful as CO_2 diffusion into leaves is reduced when they are wet. On the other hand, restricting measurements to midday when stomata tend to close in response to high vapor pressure deficits would also bias the dataset. Resolving this conundrum would have greatly improved my ability to assess the mechanistic responses of plants to fog water inputs, i.e., does fog influence the threshold of water potential above which trees shut down? Alternatively, installing sapflow probes would have provided continuous measurements of water movement through the plants, which correlates well to transpiration rates and possibly foliar absorption of fog water. A challenge using this technique is installing probes into smaller trees.

Collecting integrated measurements of plant productivity and fitness would have complemented the physiological datasets very well. For example, measuring growth of adult and sapling trees at monthly increments using dendrometer bands could have provided insight into the influence of local environmental conditions on net carbon gain of adult versus sapling trees. Recording changes in tree diameter at high frequency (e.g., hourly on a

foggy vs. non-foggy day) using dendrometer bands would be an interesting approach to quantify water use of trees in response to fog events. In addition to growth, quantifying reproductive output is useful for evaluating fitness consequences of trees living in more or less stressful environments. One approach could be to establish transects and measure seedling recruitment and mortality. In addition, cone production is a measure of potential reproductive success; however, germination and establishment of seedlings is a more useful fitness metric.

Selecting multiple sites that stratified the marine layer was an initial goal of this project, but was not feasible logistically. Future studies should strongly consider selecting sites that consistently fall below, within, and above the marine layer in order to evaluate the multiple effects coastal fog has on the water, energy, and carbon budget of the ecosystem. Specifically, the relative importance of cloud-shading and fog-drip in a field setting could be assessed more rigorously using this approach.

In the greenhouse study (Chapter 4), to fully assess the lasting effects of fog immersion and fog-drip on plant physiology, it would have been advantageous to measure leaf physiology in-between fog events as opposed to only immediately after these events. To this end, it would have been interesting to continue collecting measurements several consecutive days after the fog treatment to assess how long the positive effect of fog immersion alone on leaf gas exchange rates lasted.

Collecting plant water relations data (i.e., predawn and midday xylem pressure potential) in addition to leaf-level function would have improved our analysis of the effects of fog-drip versus fog immersion on whole-plant water relations. There were two reasons why this did not occur. First, Bishop pine saplings had a limited amount of stem and leaf

material, thus we did not want to induce a treatment effect by removing too much plant material as the experiment progressed. Second, sampling predawn and midday xylem pressure potential using the Scholander pressure chamber on single needles was not feasible because the rubber gasket fittings in the instrument were too large.

Including additional depth increments over which soil moisture was measured (e.g., 2, 5, 10, 15, and 20 cm) would have allowed us to evaluate the degree to which fog water percolates into the soil and the importance of deeper water resources on plant function. Also, by keeping plants in a more controlled environment, we could have eliminated external variables that may have affected plant responses. Though, extending greenhouse results to field scenarios would remain a challenge even if these improvements were made.

5.4. Implications

5.4.1. Linking plant ecophysiology to biogeography

Correlations between the occurrence of species and present-day climate are a first order principle in most species distribution models, e.g.,'bioclimate envelope' or 'environmental niche' models. The outcome of this dissertation supports the idea that it is necessary to include spatial and temporal variability of coastal fog into climate models to accurately project the distribution of Bishop pines, and other fog-dependent species, in the future. A shortcoming of this correlative framework for modeling species distribution is that the underlying mechanism of species boundaries is based on the vulnerability of different life states to mortality and the probability of reproductive success. Additionally, a limitation of plant ecophysiological studies is that most do not test for the heritability of physiological characteristics (Mooney, 1976). Linking plant ecophysiology to range dynamics requires

that physiological mechanisms be connected to fitness consequences of populations (Sexton et al, 2009). Recent studies have made salient efforts to combine ecophysiological and environmental data with population dynamics to increase the predictive power of species distribution models (Angert and Schemske 2005; Sexton et al. 2009; Holt 2005; Eckhart et al. 2010). While it was not the explicit goal of this dissertation to parameterize species distribution models, the data collected herein can be used to support such efforts.

5.4.2. Past and future patterns of fog, rain, and the distribution of Bishop pine

Decades of research show that plant species distributions are sensitive to changes in climate (Walther et al. 2002, Parmesean and Yohe, 2003). Projecting how species ranges will likely shift under different climate change scenarios has important ecological and evolutionary implications that can inform conservation efforts to preserve biodiversity. On geologic timescales in California, major shifts in species composition along the coast (and across the state) coincide with the transition between cooler, wetter conditions of the late-Quaternary to warmer, drier conditions in the early Holocene (Johnson 1977, Raven and Axelrod, 1978). Specifically, greater effective precipitation and cooler temperatures during the late-Pleistocene supported continuous stands of coniferous forests from as far south as Carpenteria through the northern part of the state in Mendocino county (Johnson 1977, Raven and Axelrod 1978, Anderson et al. 2008). The onset of a dry spell (Xerothermic) between 8,000 and 3,000 years ago caused a fragmentation of these forests into disjunct populations, which occupied cooler, wetter microhabitats along the coast (Axelrod 1967, Johnson 1976, Anderson et al. 2010). If climate change projections for California are accurate, we can expect conditions to become warmer and drier than they are today (Cayan

et al. 2008). With these predictions alone, it is reasonable to expect that populations of drought-sensitive plant species restricted to mesic habitats may diminish in the future. This outcome is more probable for populations at the southern extent of the species range, such as Bishop pines on SCI -- a species which has already exhibited vulnerability to widespread mortality following brief, yet intense, droughts in 1989-1990 and 1997-1999.

In 2014, California experienced the most extreme drought of the past 100 years, and the negative impacts across ecological, social, and economic realms have been severe. Annual precipitation over three consecutive rainfall seasons (2012, 2013, and 2014) in Santa Barbara county has been 66%, 46%, and 41% of the long-term average (~45 cm), respectively. Reservoirs in central and southwest California have dropped to 30% of storage capacity. Limited water availability to some of the most productive agricultural systems in the world has resulted in farmers abandoning thousands of acres of cropland in 2014 (Howitt et al. 2014). In natural ecosystems, even drought-tolerant species have exhibited signs of mortality. In the Bishop pine populations on SCI, anecdotal evidence and personal observation suggest that the extent of tree mortality in response to the 2012-14 drought is significantly greater than the area affected by the 2007-09 drought. We learned from the spatial analysis of Bishop pine mortality following the 2007-2009 drought that Bishop pines were most susceptible to mortality at the margins of the stand and at higher, inland locations on SCI (Chapter 2, Fig. 3d). The most recent mortality event is consistent with these patterns; however, tree mortality has also occurred in the foggier, cooler, and wetter areas of the stand where trees were predicted to be more buffered from drought stress (Chapter 2, Fig. 5). These observations raise an interesting point about the role of fog versus rain in the water budget of this ecosystem. While the amount of fog water trees receive may allow

Bishop pines to persist through the dry season in an average rainfall year, it does not seem to be enough to mitigate the effects of drought-induced mortality after consecutive years of below average rainfall.

5.4.3. Predicting changes to the coastal fog regime in California.

It remains highly uncertain how the magnitude, seasonality, and/or spatial extent of the fog regime may change in the future. However, several studies over the past five years have advanced our understanding of the controls on fog formation and how the fog regime may be affected by climate change. Johnstone and Dawson (2010) showed that fog frequency in northern California was 33% lower between 1951-2008 than the period between 1901 and 1925. They suggest that this trajectory is likely to continue into the future with projected increases in sea surface temperature (SST) driven by a weakening of upwelling winds associated with a weaker gradient between coastal and inland temperatures. Improving our ability to predict how coastal fog patterns may change in the future hinges on reducing the uncertainty associated with projections of fog climatologies in present day. Recent studies have contributed significantly to this goal. At synoptic and regional scales, Iacobellis and Cayan (2013) investigated the variability of summer (June-September) marine stratus clouds and how they are associated with surface temperature anomalies along the entire California coastline and offshore islands. They report that summer cloud cover is correlated strongly with the strength and height of the thermal inversion that caps the atmospheric marine layer; moreover, patterns of summer marine stratus formation differ between northern and southern California. In both regions, the inland extent of the marine layer is limited by coastal topography (Iacobellis and Cayan 2013). Swartz et al. (2014)

show similar patterns. At a local scale, Rastogi (2013) combined multiple datasets (remote sensing products, digital elevation models, airport observations, and radiosonde data) to generate a fog climatology for the northern Channel Islands, which were downscaled to biologically meaningful spatial (100 m) and temporal (hourly to monthly) resolutions. The map of fog frequency used in the Random Forest analysis in Chapter 2 was 250 m spatial resolution. Rastogi's map of fog inundation was not available at the time of our Random Forest analysis of environmental drivers underlying drought induced tree mortality in Chapter 2; however, it is clear that using a more finely resolved map of fog inundation in this analysis would have resulted in a more accurate projection of where Bishop pine would be more or less vulnerable to drought-induced mortality. For example, was the probability of surviving drought greater if trees were growing where low-stratus clouds intercepted land versus where they were shaded by the cloud cover?

5.4.4. Feedbacks between tree mortality and the water budget in a foggy forest

Fog is different from rain. Rainfall deposits water more uniformly over the land whereas fog water inputs are much more spatially heterogeneous and fog-drip is constrained to below the canopy (or intercepting surface). Yet, the total amount of fog water that enters the ecosystem from fog-drip can equal or even exceed winter precipitation during a low rainfall year (Carbone et al. 2012, e.g., rain=188 mm, fog-drip=326 mm in 2009). Because amount of direct water inputs from fog-drip is a function of interception area, i.e., leaf area, canopy height, leaf morphology, I suspect that there could be interesting effects of tree mortality on the water budget of fog-influenced forests. The high surface area to volume ratio of conifer needles makes pines efficient 'fog harvesters;' furthermore, the larger the

tree, the more fog intercepted and thus fog-drip to the ground. By reducing the number of conifer canopies in the forest, drought-induced tree mortality will effectively reduce water inputs during the dry season. Though, if the forest was only thinned by drought events, the remaining trees would also have less competition for water. Nonetheless, fewer tree would also result in reduced shading effects by the canopy and result in greater evaporative losses of water during the dry season. We learned from the field work conducted on SCI that sapling Bishop pines are also more susceptible to experiencing water stress during the dry season, but their water status is more strongly affected by fog water inputs. Changes in environmental conditions associated with tree mortality events would leave sapling trees most vulnerable to mortality, i.e., with less fog interception by the adults and lower direct summer water inputs, will the population be able to persist? Moreover, I do not think that the shading effects of fog alone would be able to dampen water stress enough to mitigate the effects of drought, even though the marine layer can significantly reduce heat loading (Williams et al. 2008, Johnstone et al. 2013). Instead, I speculate that if the Bishop pine population were to experience another intense drought (without relief of an above average rainfall year), that the local distribution will contract considerably, and areas once dominated by Bishop pines will transition to drought-tolerant shrubs. To assess the impact of drought on species composition and hydrologic function in this, and other, foggy forests, a broader question worthy of future research is: *What is the impact of drought-induced tree mortality on the water balance of fog-influenced ecosystems?*

5.5. Future Directions

I believe there are two important priorities that future fog research should address to improve our understanding of the complex relationships between fog events and the ecohydrologic function of ecosystems. First, develop finer scale spatial (≤ 30 m pixel) and temporal (hourly or daily daytime and nighttime events) fog climatologies that are linked to cloud properties (liquid water content, height of cloud base), topographic variation (i.e., where do clouds intercept land?), and ground-based measurements of energy and water budgets of ecosystems (e.g., fog water inputs, streamflow, surface temperature, soil moisture). There are a number of studies that are moving the science in this direction (Williams et al. *in prep*, Baldocchi and Waller 2014, Rastogi 2013), but resources and collaborations should converge to continue the support of these efforts. Second, expand the temporal extent of plant ecophysiological studies to the whole water year rather than just focus on the impact of fog during the dry season. By doing this, we could better answer the question, *To what extent does fog extend the rainy season?* This is an especially important question to be able to answer because even if precipitation does not change much, temperature is projected to increase up to 4.5 °C (Cayan et al. 2008), which will increase evaporative loss of water. By accounting for fog water inputs in addition to rain, we will gain an improved understanding of how changes in fog will impact the ecohydrology of managed and natural ecosystems.

References

Anderson, R.L., Byrne, R., Dawson, T.E., 2008. Stable isotope evidence for a foggy climate on Santa Cruz Island, California at ~16,600 cal. yr. B.P. Palaeogeogr. Palaeoclimatol. Palaeoecol. 262, 176–181. doi:10.1016/j.palaeo.2008.03.004

Anderson, R.S., Starratt, S., Jass, R.M.B., Pinter, N., 2009. Fire and vegetation history on Santa Rosa Island, Channel Islands, and long-term environmental change in southern California. J. Quat. Sci. 25, 782–797. doi:10.1002/jqs.1358

Angert, A.L., Schemske, D.W., 2005. The evolution of species' distributions: reciprocal transplants across the elevation ranges of Mimulus cardinalis and M. lewisii. Evolution 59, 1671–84.

Axelrod, D.I., 1967. Geologic history of the California insular flora, in: Philbrick, R.N. (Ed.), Proceedings of the Symposium on the Biology of the California Islands. Santa Barbara Botanical Garden, pp. 267–315.

Carbone, M.S., Park Williams, A., Ambrose, A.R., Boot, C.M., Bradley, E.S., Dawson, T.E., Schaeffer, S.M., Schimel, J.P., Still, C.J., 2012. Cloud shading and fog drip influence the metabolism of a coastal pine ecosystem. Glob. Chang. Biol. 19, 484–97. doi:10.1111/gcb.12054

Cayan, D.R., Maurer, E.P., Dettinger, M.D., Tyree, M., Hayhoe, K., 2008. Climate change scenarios for the California region. Clim. Change 87, 21–42. doi:10.1007/s10584-007-9377-6

Eckhart, V.M., Singh, I., Louthan, A.M., Keledjian, A.J., Chu, A., Moeller, D.A., Geber, M.A., 2010. Plant-Soil Water Relations and Species Border of Clarkia xantiana ssp. xantiana (Onagraceae). Int. J. Plant Sci. 171, 749–760. doi:10.1086/654845

Howitt, R.E., Medellin-Azuara, J., MacEwan, D., Lund, J.R. and Sumner, D.A. (2014). Economic Analysis of the 2014 Drought for California Agriculture. Center for Watershed Sciences, University of California, Davis, California. 20p. Available at <http://watershed.ucdavis.edu>.

Iacobellis, S.F., Cayan, D.R., 2013. The variability of California summertime marine stratus: Impacts on surface air temperatures. J. Geophys. Res. Atmos. 118, 9105–9122. doi:10.1002/jgrd.50652

Johnson, D.L., 1977. The Late Quaternary Climate of Coastal California : Evidence for an Ice Age Refugium. Quat. Res. 8, 154–179.

Johnstone, J. A, Dawson, T.E., 2010. Climatic context and ecological implications of summer fog decline in the coast redwood region. Proc. Natl. Acad. Sci. U. S. A. 107, 4533–8. doi:10.1073/pnas.0915062107

Johnstone, J.A., Roden, J.S., Dawson, T.E., 2013. Oxygen and carbon stable isotopes in coast redwood tree rings respond to spring and summer climate signals 118, 1438–1450. doi:10.1002/jgrg.20111

Mooney, 1976. Some contributions of physiological ecology to plant population biology. Syst. Bot. 1, 269–283.

Parmesan, C., Yohe, G., 2003. A globally coherent fingerprint of climate change impacts across natural systems. Nature 421, 37–42. doi:10.1038/nature01286

Rastogi, B. 2013. Characterizing spatial and temporal patterns of cloud cover and fog inundation for the Northern Channel Islands of California. University of California, Santa Barbara. Electronic Dissertations G76.5.U5 S25 RASB 2013 [Online]

Raven, P.H., Axelrod, D.I., 1978. Origin and relationships of the California flora. University of California Press: Berkeley, CA.

Schwartz, R., Gershunov, A., Iacobellis, S.F., Cayan, D.R., 2014. North American west coast summer low cloudiness: Broadscale variability associated with sea surface temperature. Geophys. Res. Lett. 41, 1–8. doi:10.1002/2014GL059825.Received

Sexton, J.P., McIntyre, P.J., Angert, A.L., Rice, K.J., 2009. Evolution and Ecology of Species Range Limits. Annu. Rev. Ecol. Evol. Syst. 40, 415–436. doi:10.1146/annurev.ecolsys.110308.120317

Walther, G., Post, E., Convey, P., Menzel, A., Parmesank, C., Beebee, T.J.C., Fromentin, J., Ove, H., Bairlein, F., 2002. Ecological responses to recent climate change. Nature 416, 389–395.

Williams, A.P., Still, C.J., Fischer, D.T., Leavitt, S.W., 2008. The influence of summertime fog and overcast clouds on the growth of a coastal Californian pine: a tree-ring study. Oecologia 156, 601–11. doi:10.1007/s00442-008-1025-y